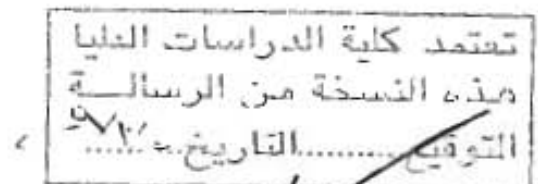# EFFECT OF LINK LOCATION ON BEHAVIOR OF ECCENTRICALLY BRACED FRAMES

By
**Amir Sahip Irhium**

Supervisor
**Dr. Nazzal S. Armouti**

**This Thesis was submitted in Partial Fulfillment of the Requirements for the Master's Degree of Science in Civil Engineering/Structures.**

**Faculty of Graduate Studies**
**The University of Jordan**

تعتمد كلية الدراسات العليا
هذه النسخة من الرسالة
التوقيع.........التاريخ........

**October, 2009**

## Committee Decision

This thesis (Effect of Link Location on Behavior of Eccentrically Braced Frames) was successfully defended and approved on **30/9/2009.**

**Examination Committee**                    **Signature**

Dr. Nazzal S. Armouti, (Supervisor)
Assoc. Prof. of Civil Engineering

Dr. Abdelqader S. Najmi, ( Member)
Prof. of Civil Engineering

Dr. Yasser M. Hunaiti, ( Member)
Prof. of Civil Engineering

Dr. Yahia A. Abdel-Jawad, (Member)
Prof. of Civil Engineering
(Jordan University of Science and Technology)

# DEDICATION

*To my father, mother, wife, my family, and friends who were a big*

*inspiration to my achievement.*

*To all who supported, and encouraged me to make my dreams true*

*specially Eng. Abullah A. AL-Jiburi.*

*I love you all.*

<div align="right">

*Amir*

*September, 2009*

</div>

# ACKNOWLEDGMENT

I would like to thank first of all almighty God for supporting me with strength, and patience to fulfill this study. I would like to express my deep appreciation to my supervisor, Dr. Nazzal Armouti, for his endless assistance and support in carrying out this study, taking to heart the responsibility of keeping the flow of research, and presentation, avoiding obscurity, and strengthening consistency in the best way possible, I would also like to thank the Civil Engineering Department and members of the examining committee for their suggestions.

I extend my gratitude to Dr. Hassoun Hadid who has supported me all through the period of my study.

Finally, I would like to give thanks to all who supported me.

**Table of Contents**

1. **INTRODUCTION**

2. **LINK BEHAVIOUR OF ECCENTRICALLY BRACED FRAMES**

## 3. MODELS ANALYSIS AND PROCEDURES

## List of Tables

**List of Figures**

# List of Abbreviations

| | |
|---|---|
| BF | Braced Frame |
| BOL | Beam Outside the Link |
| CBF | Concentrically Braced Frame |
| CP | Collapse Prevention |
| d | Overall Beam Depth |
| e | Link Length |
| EBF | Eccentrically Braced Frame |
| $E_s$ | Steel Modules of Elasticity |
| F | Force |
| FR | Fully Restrained |
| $F_y$ | Specified Minimum Yield Stress |
| IMF | Intermediate Moment Frame |
| IO | Immediate Occupancy |
| k | Stiffness |
| L | Span Length |
| LS | Life Safety |
| M | Moment |
| $M_{ce}$ | Expected Moment Strength |
| MF | Moment Frame |
| $M_p$ | Fully Plastic Moment Capacity |
| NSPA | Nonlinear Static Procedure Analysis |
| OCBF | Ordinary Concentrically Braced Frame |
| OMF | Ordinary Moment Frame |
| P | Axial Load |
| Q | Generalized Component Load |
| $Q_{ce}$ | Generalized Component Expected Strength |
| RC | Reinforced Concrete |
| SCBF | Special Concentrically Braced Frame |
| SMF | Special Moment Frame |
| T | Tension Force |

| | |
|---|---|
| $t_f$ | Thickness of the Flange |
| TMF | Truss Moment Frame |
| $t_w$ | Thickness of the Web |
| V | Shear |
| $V_{ce}$ | Expected Shear Strength |
| $V_n$ | Link Nominal Shear Strength |
| $V_p$ | Fully Plastic Shear Capacity |
| $V_{ult}$ | Ultimate Shear Force |
| Z | Plastic Section Modulus |
| $\gamma$ | Link Rotation Angle |
| $\gamma_p$ | Link Plastic Rotation Angle |
| $\Delta$ | Link Deformation |
| $\Delta_y$ | Yield Deformation |
| $\Delta_{pl}$ | Plastic Deformation |
| $\varepsilon$ | Strain |
| $\varepsilon_u$ | Ultimate Strain |
| $\varepsilon_S$ | Steel strain |
| $\varepsilon_y$ | Yield Strain |
| $\theta$ | Chord Rotation |
| $\theta_p$ | Plastic Story Drift Angle |
| $\theta_y$ | Yield Rotation |
| $\kappa_u$ | Curvature at Ultimate state |
| $\mu_c$ | Cyclic Ductility Ratio |
| $\mu_\Delta$ | Displacement Ductility Ratio |
| $\mu_\varepsilon$ | Strain Ductility Ratio |
| $\mu_\theta$ | Rotational Ductility Ratio |
| $\mu_\Phi$ | Curvature Ductility Ratio |
| $\Phi$ | Strength Reduction Factor |
| $\Phi_u$ | Ultimate Curvature |
| $\Phi_y$ | Yield Curvature |
| $\sigma$ | Stress |
| $\sigma_y$ | Yield Stress |

# EFFECT OF LINK LOCATION ON BEHAVIOR OF ECCENTRICALLY BRACED FRAMES

By
**Amir Sahip Irhium**

Supervisor
**Dr. Nazzal S. Armouti**

## ABSTRACT

The main objective of this study is to contribute a better understanding of the effect of link location on behavior of eccentrically braced frames (EBFs).

This study aims to help the structural engineers in order to design seismic resisting steel structures that have large inelastic deformation due to earthquake. As will be shown the study concerns about Eccentrically Braced Frames (EBFs) which can be described as a combination of moment resisting frame which gives good ductility, and concentrically braced frame which gives strength, and stiffness. Researches and studies of EBFs started at 1970s, up to date with the new architectural requirement.

The EBF configurations covered in this study are the common types which are: K-Braced EBF, D-Braced EBF, and V-Braced EBF. Each EBF configuration is studied according to the description of link's length: short link (shear yielding), long link (flexural yielding), and intermediate link (combined shear and flexural yielding).

Analysis has been performed using SAP2000 software (static and dynamic finite element analysis of structure, version 12), by modeling 2D frames with different type of braces. Each model has been subjected to gravity load and seismic load (lateral displacement). The analysis used is nonlinear static procedure analysis (pushover analysis) which is a popular tool for seismic performance evaluation of existing and new buildings.

It will be noted that shear yielding link is the best type resisting lateral force (seismic load) because a large portion of the link yield in a relatively uniform manner. On the other hand, in the flexural yield link type, yielding occurs only at the link ends.

This study shows that K-Braced short link configuration offers good stiffness, and strength characteristics, the link in this configuration is located at mid-span of the beam.

This study also demonstrates that K-Braced and V-Braced with short link type are the superior types due to ductility and link deformation.

Finally, the results of the study obtained from SAP2000 compared well with the experimental results by (Michael D. Engelhardt, 2005).

# CHAPTER ONE

# INTRODUCTION

## 1.1. General

The use of steel structures is common and widely applied, because the characteristic and properties of steel sections used in terms of feasibility, availability, as well as other terms relevant to speed erection and flexibility of maneuvering in terms of integrating the structural-architectural-building services systems.

Steel structures have historically performed well at earthquakes, and little loss of life can be attributed to collapse of steel buildings. This good track record can likely be attributed to several reasons:

a. Steel structures are generally lighter than masonry or reinforced concrete (RC). Lower weight translates to lower seismic forces.

b. Steel structures typically show good ductility, even when they are not specifically designed or detailed for seismic resistance.

c. Many of the highly destructive earthquakes around the world have occurred in areas where there are very few steel structures. Thus, the exposure of steel structures to strong earthquakes has been perhaps somewhat less than other types of construction.

Steel frame systems are usually used to resist lateral forces (wind and seismic effect). There are three main types for such structures which are shown in Figure (1.1); Moment Frames (MF), Truss Moment Frames (TMF), and Braced Frames (BF). Moment Frames (MF) has three types of seismic steel moment-resisting frames which are; Ordinary Moment Frames (OMF), Intermediate Moment Frames (IMF), and Special Moment Frames (SMF). All the three framing systems are designed assuming ductile behavior of varying degrees. SMF are considered the most ductile of the three types of moment frames.

Truss Moment Frames (TMF) dissipates energy by flexure and axial yielding of the top and bottom chords and diagonals sequentially. Braced Frames (BF) includes; Concentrically Braced Frames (CBF) and Eccentrically Braced Frame (EBF).

The design CBF is performed by ensuring that plastic deformations only occur in the braces and this type usually possess greater lateral stiffness which can limit the damage due to drift.

CBF can be divided into two types which are; Special Concentrically Braced Frames (SBFs) and Ordinary Concentrically Braced Frames (OCBFs).

EBF combines both steel moment frame and braced frame. In moment frames, the connection is capable of resisting a story drift angle, Figure (1.3) shows typical EBF geometries. Concentrically Braced Frames is stiff since the intersection beam-brace connection is continuous. In addition to the main building elements floors, roofs, and walls, the structural system must include bracing members that provide lateral support for main members, resistance lateral loads on the building, redundant load path, and stiffness to the structure limit deflections. An economical and safe design properly integrates these systems into a completed structure.

The EBF has been used for more than two decades as a seismic load resisting system primarily in buildings for flexibility of maneuvering in terms of integrating the structural-architectural-building service systems.
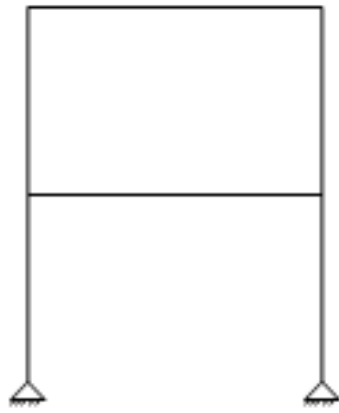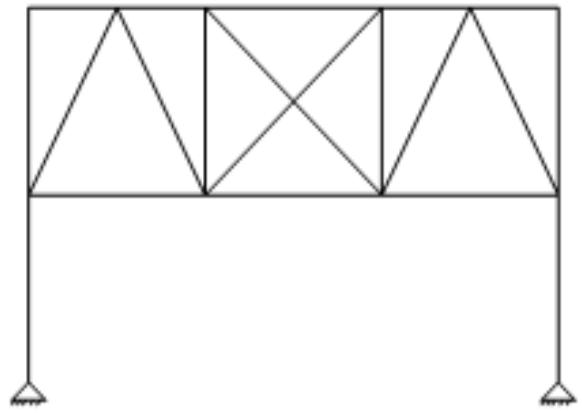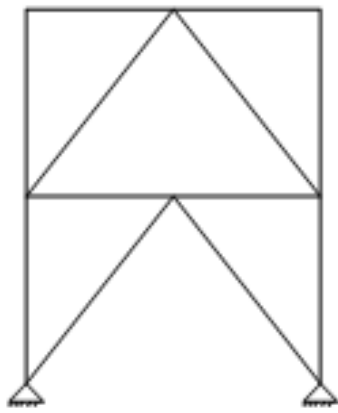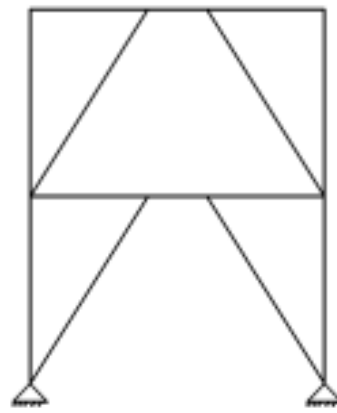
Figure (1.1): Types of Frame

Eccentrically Braced Frames (EBF) are braced frames in which at least one end of every brace is connected so that the brace force is transmitted through shear and bending of a short isolated beam segment called "link". The "link" which characterizes the (EBF) can be between the brace connection and the column or between two braces connections. The diagonal brace, at least at one end, is connected to the end of the link rather than the beam-column joint. Link beam can be located adjacent to a column or at the center of a beam. Eccentrically Braced Frames are very special as the detailing issues associated with link mechanism require special consideration such as adding stiffeners and lateral member to resist lateral torsional buckling.

The eccentric segment of the beam, the link, undergoes flexural or shear yielding prior to deformations of the other members. Energy is dissipated through shear and/or flexural yielding in this link. The braces, columns, portions of the beam outside the link, and all related connections are designed to remain nominally elastic as the link deforms and reaches its expected strength. During extreme loading, it is anticipated that the link will deform plastically with significant ductility and energy dissipation.

The Eccentrically Braced Frame (EBF) is essentially a hybrid, offering lateral stiffness approaching that of Concentrically Braced Frame (CBF) and ductility approaching that of a Special Moment Frame (SMF) system. The plastic design has several advantages over the elastic design since it fully uses the property of steel, namely ductility, which may be defined as the ability of material to undergo large deformation without much loss in its strength. The redistribution of forces/moments utilizes the important benefit of the ductile behavior of steel. There are three major variables in the design of an EBF:

- The bracing configuration.

- The link length.

- The link section properties.

The design of the link portion of the beam is the most critical element of an EBF. The design of an EBF is usually based on both stress and drift control including rotation angle, which both are equally significant. This differs from the design of a Moment Frames where usually drift controls the design, or a Concentrically Braced Frames where stress controls the design. An EBF generally possesses excellent ductility, efficient limits of building drift and exhibit excellent seismic performance.

Eccentric Bracing System is a unique structural system that attempts to combine the strength and stiffness of a braced frame with the inelastic behavior and energy dissipation characteristic of a moment frame. The eccentric beam element (link) acts as a "fuse" by limiting large forces from entering and causing buckling of braces. The benefits of structural "Fuse" concept:

- Seismically induced damage is concentrated in the fuses.

- Following a damaging earthquake only the fuses would need to be replaced, the elastic structure returns to its original position (self-recenterting capacity).

EBF systems have two important specifications, ductility and stiffness (Engelhardt et al., 1989). EBFs are expected to withstand significant inelastic deformations in the link-beams when subjected to the forces resulting from the motions of the design earthquake. The diagonal braces, and beam segments outside of the links should be designed to remain essentially elastic under the maximum forces that can be generated by the fully-yielding and strain-hardened links (AISC, 2005). The design principals of EBF can be understood more effectively by investigating the tensile strength of string of chain as illustrated in Figure (1.2).
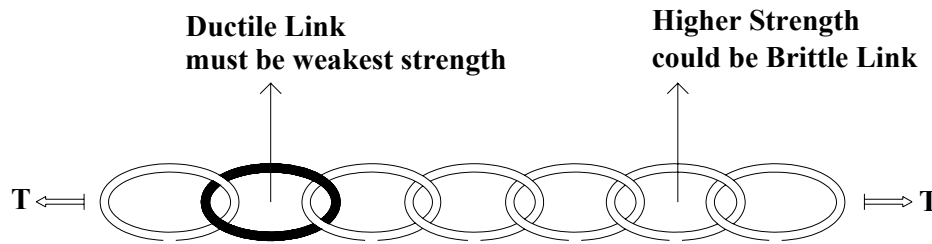
Figure (1.2): Representing EBF Systems as String of Chain

It can be concluded that the ductility of whole chain could be controlled by the ductility of one of its segments. The nominal tensile strength of this segment is supposed to be controlled by its ductility. Whereas other segments of the chain could be brittle and should be designed so that they have strength higher than the maximum strength of the lean segment. In EBF systems the link beam should be considered as a lean segment of the chain and other parts of system like columns and beams out of the link should be considered as brittle parts of chain (Bruneau et al., 1998). This concept is called Capacity Design, the maximum force take to the maximum capacity for weakest link (ductile link); the basic strategy is to proportion the component to fail in a ductile manner by making the capacity in other modes greater.

The system (EBF) maintains stability even under large inelastic deformations. Essential features of the link are length and shear yielding. Whether the link develops plastic hinges or yield in shear is a function of its length. If the link length is more than twice the beam depth, link will yield in flexure. If the link length is less than twice the beam depth, link will yield in shear. By changing the link lengths, the stiffness of an (EBF) can be modified.

Shear yielding is an excellent energy dissipation mechanism since large deflections can take place without failure or deterioration. However, moment frames are relatively flexible and their design is usually governed by the drift limitations in order to control the damage, the ductility and energy dissipation capacity of concentrically braced frames can significantly deteriorate if braces buckle under seismic loading. Eccentrically Braced Frames (EBFs) successfully combine the advantages of the moment frames and concentrically braced frames, namely high ductility and lateral stiffness, while eliminating the shortcomings of those frames by limiting the inelastic activity to ductile shear links and keeping braces essentially elastic without buckling, thus maintaining high lateral stiffness during earthquake events.

All inelastic activity is intended to be confined to properly detailed links. Links act as structural fuses that can dissipate seismic input energy without degradation of strength and stiffness, thus limiting the force transferred to the adjacent column, braces and beam segments.

The critical beam segment is a "link" and is designated by its length, links in EBF act as structural fuses to dissipate the earthquake induced energy in a building in a stable manner. To serve its intended purpose, a link needs to be properly detailed to have adequate strength and stable energy dissipation. Typical EBF geometries are shown in Figure (1.3).

EBF advantages will achieve high elastic stiffness, excellent ductility, and energy dissipation, EBF is to dissipate energy in the shear or moment links and protect the remained frame from inelastic action, including the braces.

The concept of capacity design can also be understood through an analogy to electrical wiring in a building. Electrical wiring is protected by a fuse, so that in case of an electrical overload, the fuse burns out before the wiring is damaged, thereby protecting the wiring. This protection can only be achieved if the fuse is weaker than the wiring. In a seismic-resistant steel frame, the plastic hinge locations serve as a fuse to protect against overload. In an earthquake, the plastic hinge "fuses" (beams in moment frames, links in EBFs, etc.) limit the forces that can be transferred to the remainder of the frame, thereby protecting the remainder of the frame. However, this can only be achieved if the plastic hinge locations are the weakest elements of the frame, to assure ductile yielding occurs in the beam ends, before fracture of a connection or buckling of a column.

(A) Split K-Braced EBF

(B) D-Braced EBF

(C) V-Braced EBF

(D) Split V-Braced EBF

(E) Inverted Y Braced EBF

(F) Opposite Y Braced EBF

(a=column, b=brace, c=link, d=beam outside link)
Some possible bracing arranement for EBFs
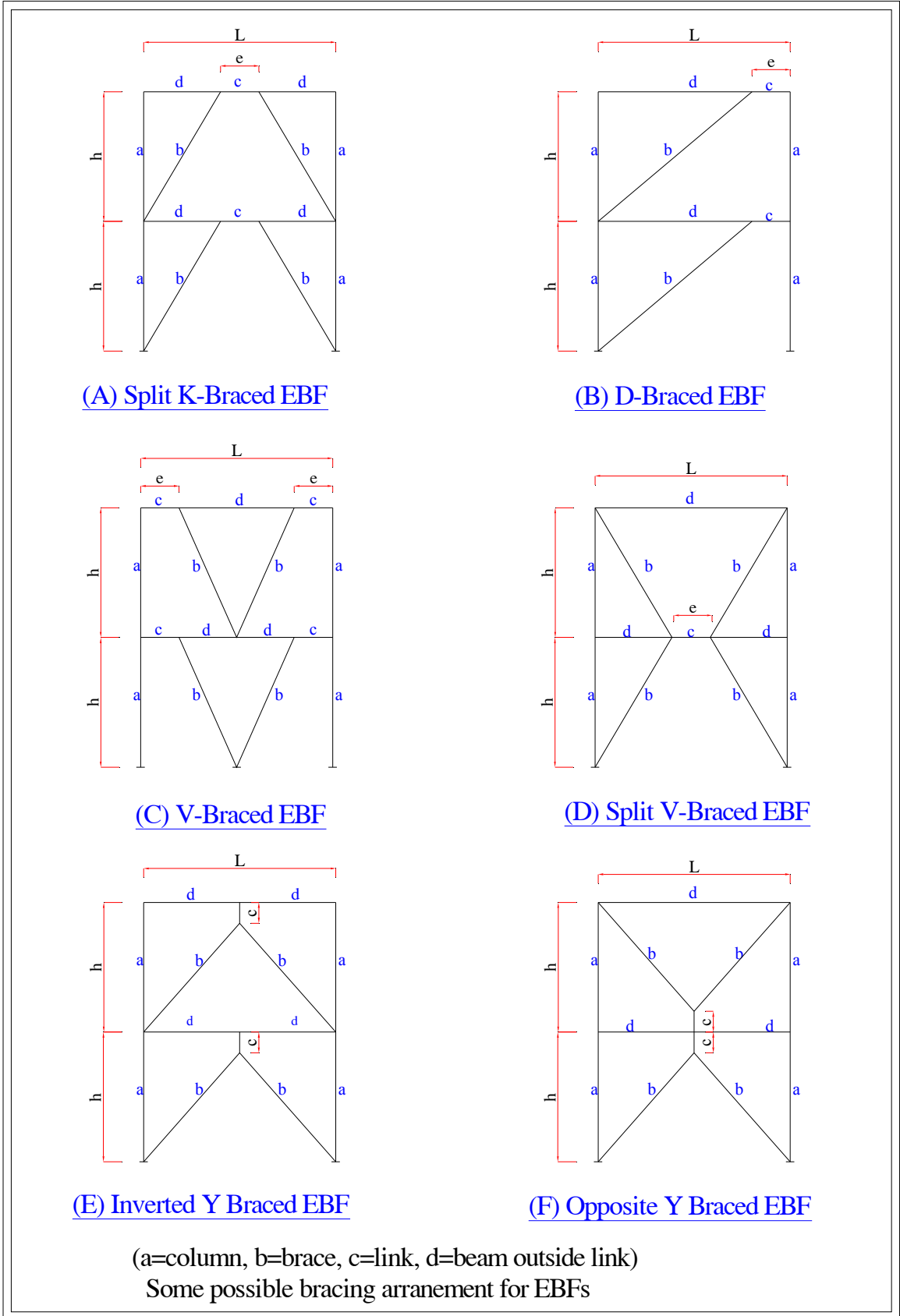
Figure (1.3): Typical EBF Configurations

## 1.2. Research Objectives

The main objectives of this study are:

1- Define type of links as:

- Short links [Link length is less than $(1.6M_p/ V_p)$] according to AISC Seismic Provisions for EBF (2005).

- Long links also known as flexural yielding links [Link length (e) is more than $(2.6M_p/V_p)$] according to AISC Seismic Provisions for EBF (2005).

- Intermediate links, shear and flexural links [Link length (e) more than $(1.6M_p/ V_p)$ and less than $(2.6M_p/V_p)$] according to AISC Seismic Provisions for EBF (2005).

   Link length "e" is key parameter that controls inelastic behavior. Longer links provide less strength, stiffness and ductility than shorter links.

2- Comparison of link location on the behavior of EBF using three types of EBF systems (split K- type braced EBF, D – braced EBF and V – braced EBF) in the shear or moment links. In addition to the comparison of the kinematics of the EBF.

3- Comparison of link length on the behavior of EBF by selecting different types of short and long links.

## 1.3. Methodology

In general, buildings may be modeled as plane frames. Due to the effort that is involved in static nonlinear analysis, experience skills in modeling are important aspects of such analysis.

Throughout this study SAP2000 (V12.0.0 Advanced) is used. For the last three decades, SAP has been recognized as the industry standard for building analysis and design software. SAP has evolved into a complicatedly integrated building analysis and design environment.

The Force-Displacement (Moment-Rotation) curve shown in Figure (1.4) is suggested by National Earthquake Hazard Reduction Program (NEHRP) to define the yield value and the plastic deformation following yielding to be used in performance-based design.

This curve defines values at six points, A-B-C-D-E-F, as shown in Figure (1.4). The plot may specify a symmetric curve, or a one that differs in the positive and negative direction.

The shape of this curve as shown is intended for nonlinear static analysis. The following points should be noted:

- Point A is the origin.
- Point B represents yielding no plastic deformation occurs in the hinge up to point B, regardless of the deformation value specified for point B. The displacement (rotation) at point B will be subtracted from the deformations at points C, D, and E. Only the plastic deformation beyond point B will be exhibited by the hinge.

- Point C represents the ultimate capacity for nonlinear static analysis. However, the curve may specify a positive slope from C to D for other purposes.

- Point D represents a residual strength for nonlinear static analysis. However, the curve may specify a positive slope from C to D or D to E for other purposes.

- Point E represents total failure. Beyond point E the hinge will drop load down to point F directly below point E on the horizontal axis. One can specify a large value for the deformation at Point E in order to make sure that no failure will occur in this way.

The curve may specify additional deformation measures at points IO (Immediate Occupancy), LS (Life Safety) and CP (Collapse Prevention). These are informational measures that are reported in the analysis results and used for performance-based design. They do not have any effect on the behavior of the structure.

Prior to reaching point B, all deformations are linear and occur in the Frame Element itself, not in the hinge. Plastic deformation beyond point B occurs in the hinge in addition to any elastic deformation that may occur in the element.
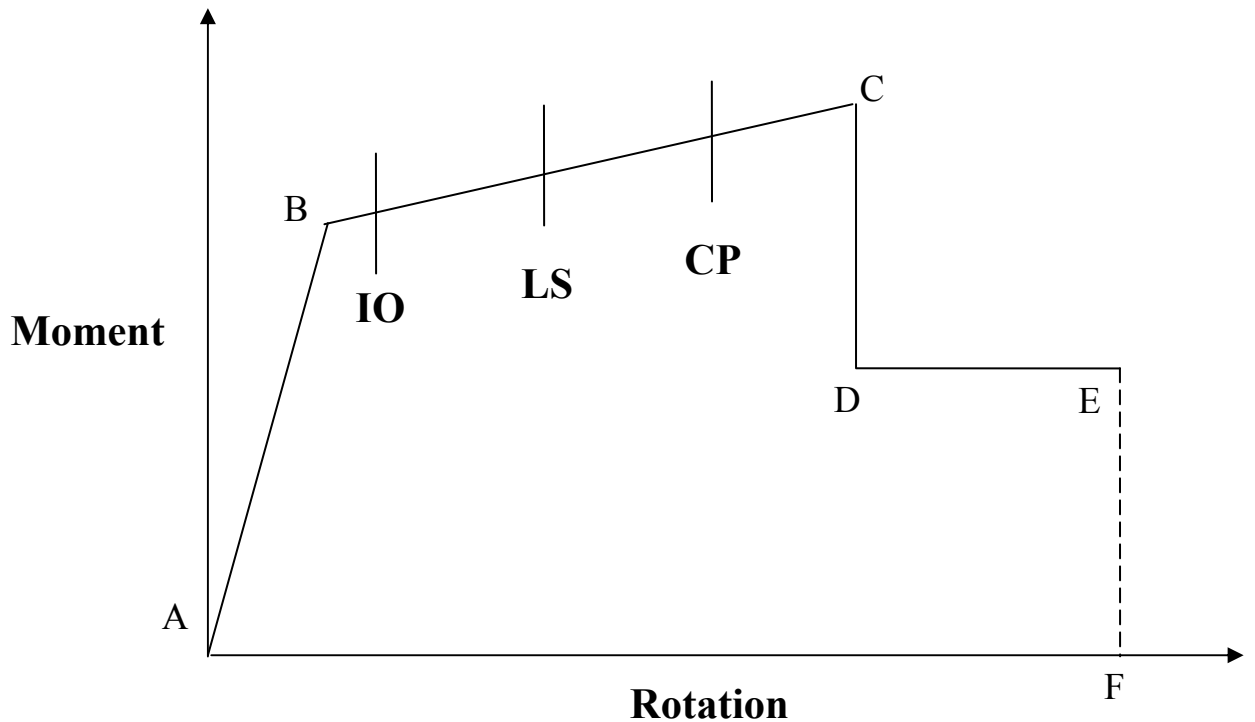
Figure (1.4): A-B-C-D-E-F Curve for Moment vs. Rotation and the Same Type of
Curve is Used for Force vs. Displacement

Building performance levels or limit states are chosen discrete levels of building
damage under earthquake excitation. Seismic performance of a building is determined
by obtaining story-based structural member damage ratios under a linear or non-linear
analysis. According to Federal Emergency Management Agency (FEMA 356) the
building performances are as in the following:

Immediate Occupancy (IO) no damage to structural or non-structural components.
For each main direction that seismic loads affect, at any story at most 10% of beams
can be at moderate damage level; however, the rest of the structural elements should be
at slight damage level.

Life Safety (LS) Limited damage to structural components; building can be
maintained; no substantial loss of life: For each main direction that seismic loads affect,
at any story at most 30% of beams and some of columns can be at heavy damage level;
however, shear contributions of overall columns at heavy damage must be lower than

20%. The rest of the structural elements should be at slight or moderate damage levels, buildings at this state are assumed to be at Life Safety Performance Level.

Collapse Prevention (CP) No global collapse of building frame; partial collapses acceptable: For each main direction that seismic loads affect, at any story at most 20% of beams can collapse. Rest of the structural elements should be at slight damage, moderate damage, or heavy damage levels, the buildings at this state are assumed to be at Collapse Prevention Performance Level. Functionality of a building at this performance level has risks for life safety and building should be strengthened.
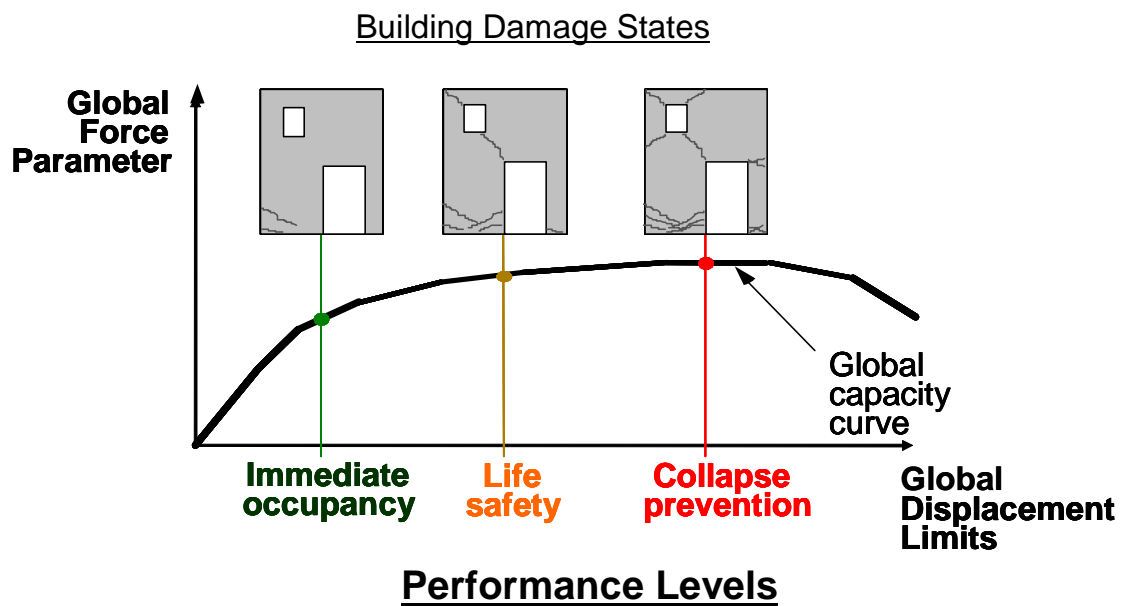


Figure (1.5): Building Performance Levels

## 1.4. Thesis Layout

The influence of link location and length on behavior of EBF was studied in details in the following chapters:

Chapter Two introduces the links behavior for eccentrically braced frames and it includes link plastic rotation angle, links forces, link nominal shear strength, link rotation angle, shear yielding links, flexural yielding link, and EBF rigid-plastic kinematics.

Chapter Three is the analysis work by computer. It provides and outlines examples (model work), and a full description of the study cases, modeling procedures, geometric and material assumption. In addition, length definition, type brace definition, displacement control definition and analysis criteria have been clarified.

Based on the results of this study, the last chapter draws conclusions and recommendations that have been derived during the course of this research.

## 1.5. Review of Literature

Few researches are carried out in studying the influence of seismic design for EBFs. Some of the researches which are related to our study are cited below.

1. "Seismic Design Practice For Eccentrically Braced Frames Base On The 1994 UBC", By Roy Becker & Michael Ishler, Steel Tips, Structural Steel Educational Council, Technical Information & Product Service, December 1996, pp. 1-27 . This study presents the design of the link portion of the beam as the most critical element of an EBF.

A link must be provided for compact flanges and web, adequate shear capacity, adequate flexural and axial load capacity, limited rotation relative to the rest of the beam and limit drift of the EBF. The design of an EBF is usually based on both stress and drift control including rotation angle.

2. "The Seismic Design Handbook, Second Edition", By Farzad Naeim, Chapter 9, Seismic Design Of Steel Structures, By Chia-Ming Uang,Ph.D, Michel Bruneau, Ph.D., P.Eng., Andrew S. Whittaker, Ph.D., S.E., Key-Chyuan Tsai, Ph.D., S.E., Chapter 9, Part 9.4, Pages 436-460. This chapter presents the Eccentrically Braced Frames (EBF) that combines the advantages of both steel moment frames (excellent ductility manner) and braced frames (have a large lateral stiffness).

3. "Finite Element Investigation of Steel Built-up Shear Links Subjected to Inelastic Deformation", By Peter Dusicka, Ahmad M. Itani and Ian G. Buckle, Center for Civil Engineering Earthquake Research (CCEER) Department of Civil and Environmental Engineering, MS 258, University of Nevada, USA. In general the study explains the links were categorized into groups; with and without stiffeners. Stiffeners are necessary to delay the onset of web buckling during inelastic link deformation. However, by utilizing low yield point steels, the web thickness could be increased and stiffeners excluded.

4. "Experimental and Analytical Investigation of Tubular Links for Eccentrically Braced Frames", By Jeffrey W. Bermana, Michel Bruneaub, 30 November 2006.

This paper describes first an experimental program, a proof-of- concept experiment which showed that hybrid tubular links can achieve and exceed the maximum rotation for links specified in the AISC seismic provisions, indicating that they can provide ductility levers.

5. "Testing of a Laterally Stable Eccentrically Braced Frame for Steel Bridge Piers", By Jeffrey W. Berman. This paper describes the design and testing of a proof-of-concept Eccentrically Braced Frames specimen that utilized a hybrid rectangular shear link. The proof-of-concept testing of a single link rotation of 0.151 radians (8.65°). (Almost twice the maximum allowed in building codes for I-shaped links) without strength degration and showed no signs of lateral torsion buckling.

# CHAPTER TWO

# LINK BEHAVIOR FOR ECCENRTICALLY BRACED FRAMES

## 2.1. Link Plastic Rotation Angle

Link plastic rotation angle is defined as the inelastic angle between the link and the portion of the beam outside the link as shown in Figure (2.1d).



a.  K-Braced Type
    Under Lateral Loading

b. Inelastic Deformation

c. Inelastic Deformation Patterns
   Loading in the Reverse Direction

$\gamma_p$ = link plastic rotation angle (rad)

d. Link Plastic Rotation Angle (rad.)
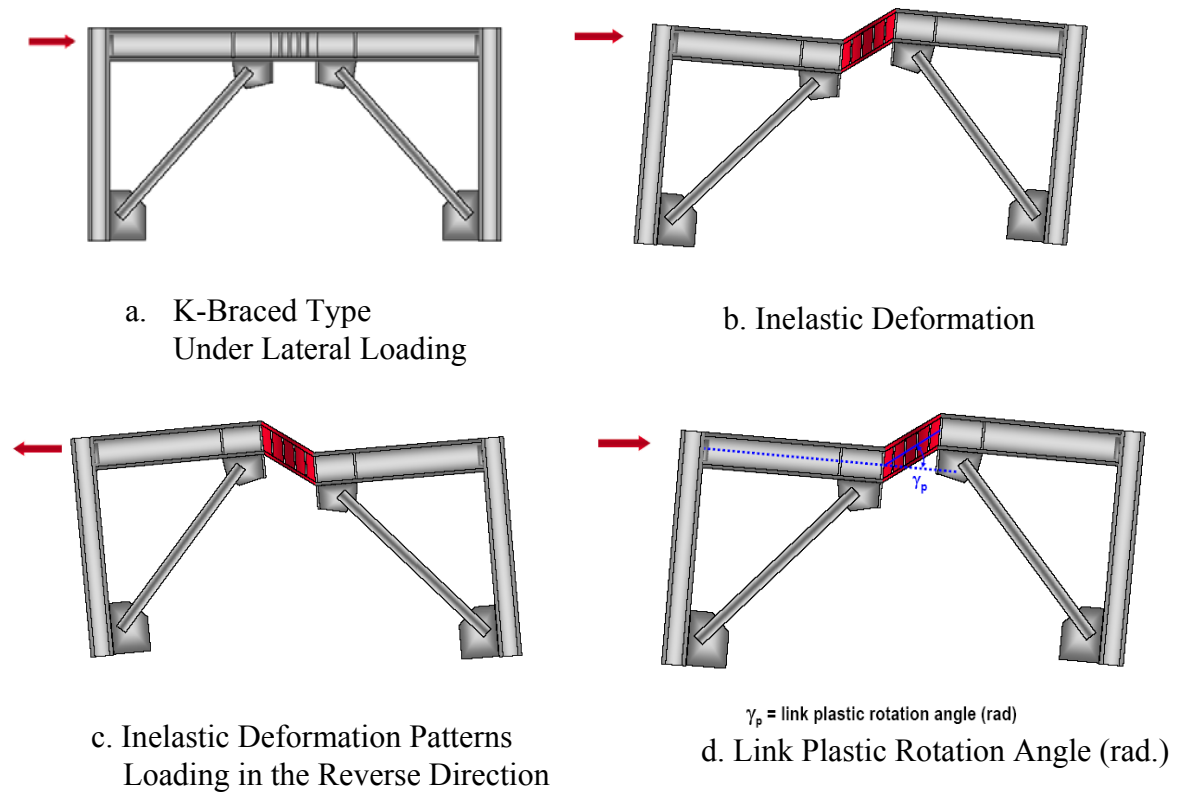
Figure (2.1): K-Braced Type Behavior

Inelastic deformation patterns are shown in Figure (2.1.b) and (2.1.c). The K-braced type shows that the geometry of the two triangular are stiff and stable elements and the link connection between them is considered a weak element, therefore the inelastic deformation will occur in the link.

The plastic rotation angle $\gamma_p$ is primary kinematic variable used to characterize inelastic deformation demands on a link. $\gamma_p$ is defined as the inelastic angle between the link and adjoining beam, in a rigid-plastic EBF mechanism. The link plastic rotation angle is expressed in radians.

The inelastic deformations for D-braced type (single diagonal EBF) with the link attached to the column are shown in Figure (2.2). In this case the yielding will occur in the link.



a. D-Braced Type under Lateral Loading

b. Inelastic Deformation

c. Inelastic Deformation Patterns
   Loading in the Reverse Direction

d. Link Plastic Rotation Angle
   (Single Diagonal EBF)

$\gamma_p$ = link plastic rotation angle (rad)
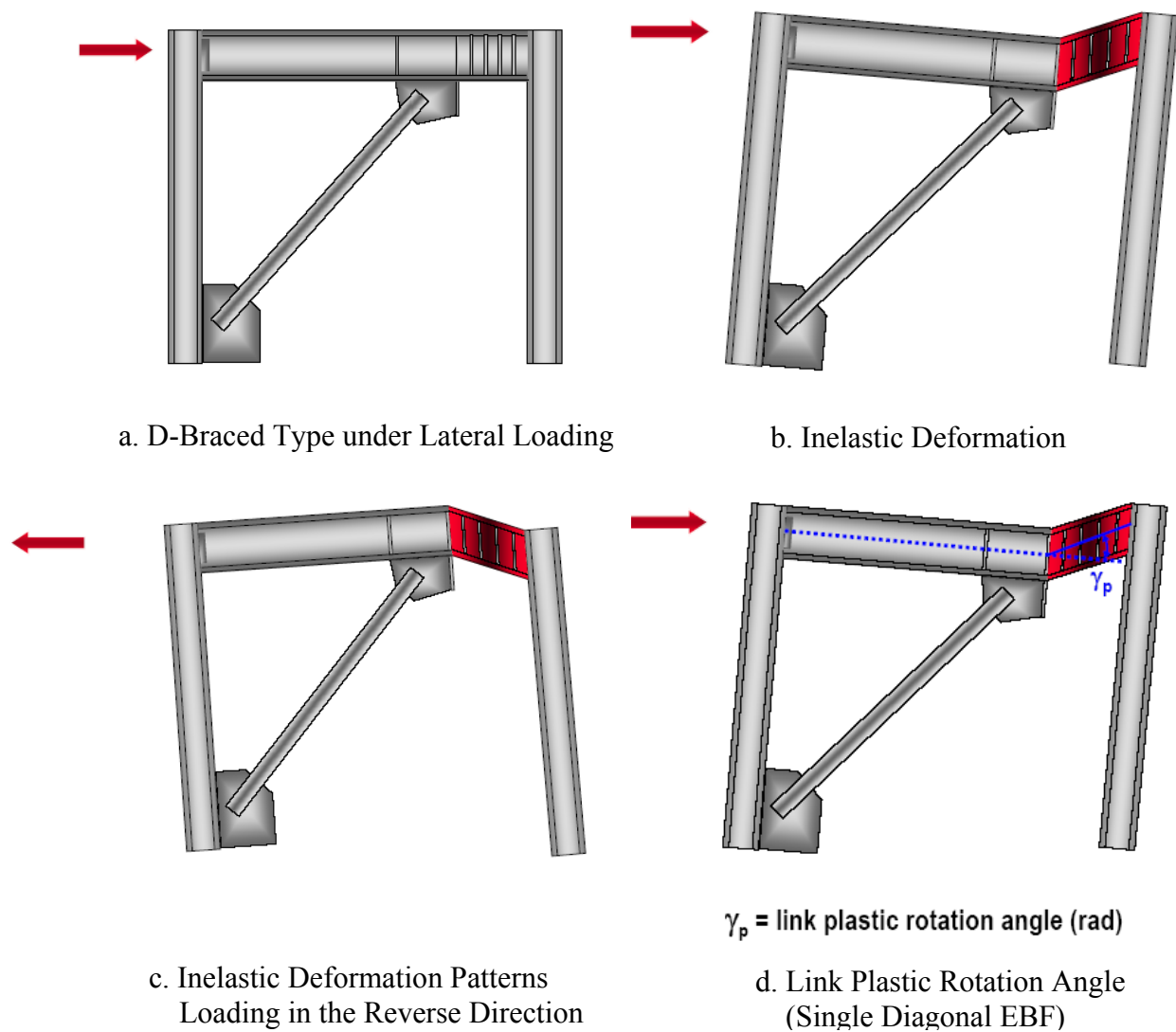
Figure (2.2): D-Braced Type Behavior

The inelastic deformations for V-braced type with two links attached to the column at both ends are shown in Figure (2.3).



a. V- Braced Type under Lateral Loading

b. Link Plastic Rotation Angle (Double Diagonal EBF)
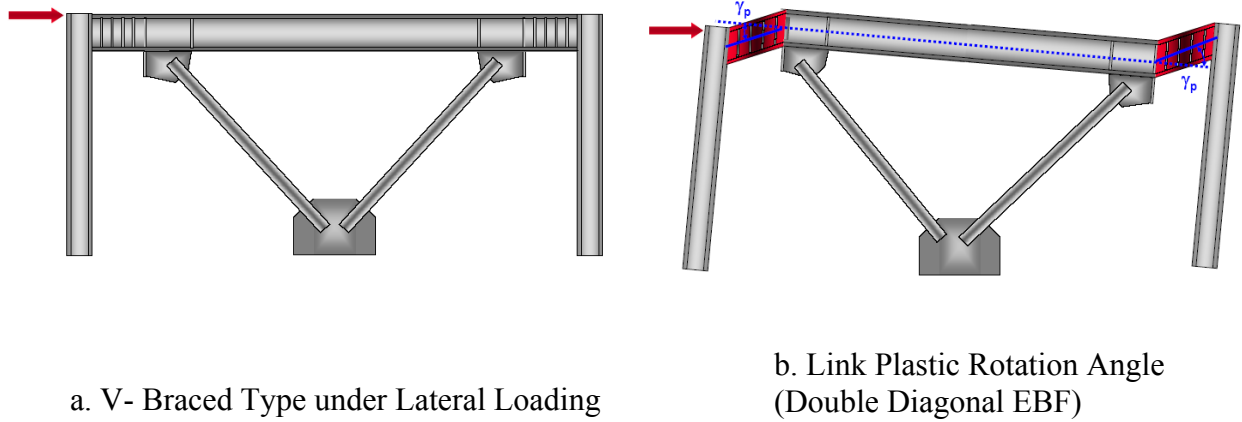
Figure (2.3): V-Braced Type Behavior

It should be noted that for an EBF with links attached to columns, the link-column connection must accommodate very large inelastic deformation demands.

## 2.2. Forces in Links

If a lateral force is applied to the three types of the frames shown in Figure (2.4), internal resultant forces, moment M, shear V, and axial load P are generated in the link. The forces generated in the links are nearly similar in each case. The three cases are illustrated as shown in Figure (2.4): a single diagonal EBF (D- braced type) and an EBF with link at mid-span (K – braced type) and a double diagonal EBF (V-braced type).

Links generally show very high shear, which is constant along the length of the link. Links also show very large bending moments at the end of opposite sign with the reverse curvature bending. The axial forces in the links generally are very small, and in some cases are not developed. The other parts of the beams outside the links show high axial forces, smaller shear and smaller moment.
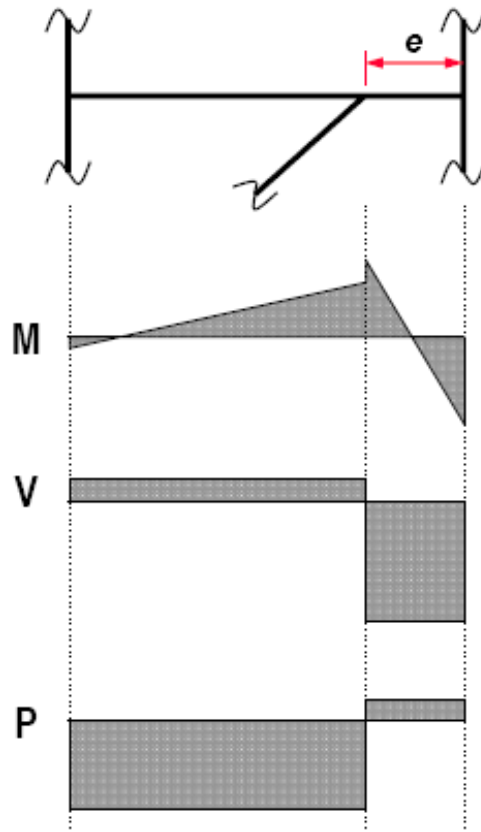
a. D-Braced EBF Internal Force
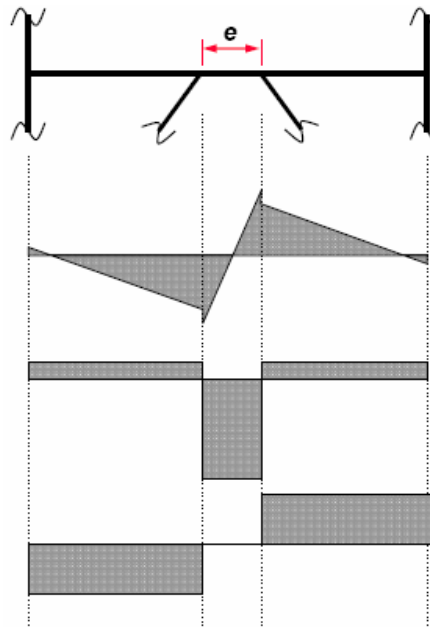


b. K-Braced EBF Internal Force

Figure (2.4): Forces in Links

## 2.3. Shear versus Flexural Yielding Links

Link plastic strength will be controlled by shear or flexure.
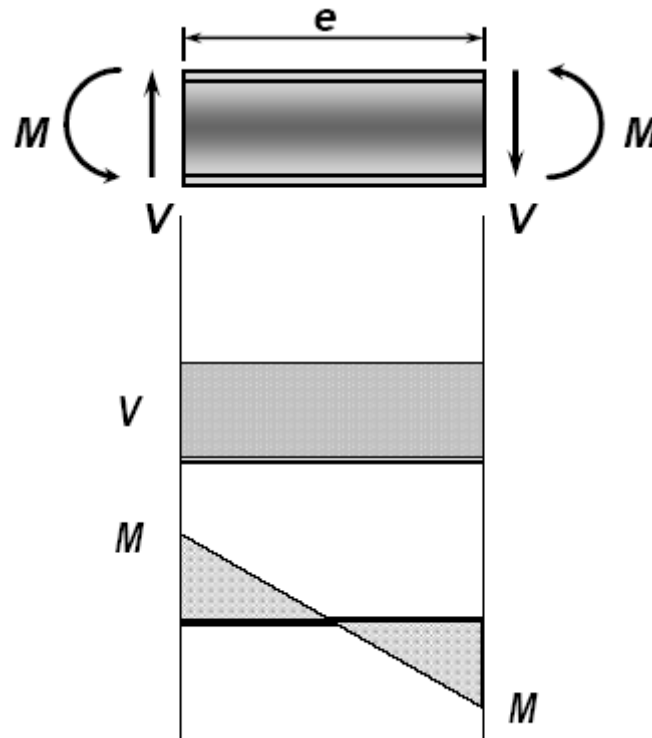


Figure (2.5): Link Shear-Moment Free Body Diagram

The links carry both large shear force and large end moments, consequently, as link is loaded beyond its elastic range; it is possible that either shear yielding or flexural yielding occur.

The behavior of the link can be controlled if it will yield in shear, in flexure, or in combined shear and flexure, the link length, e, is a key parameter that controls inelastic behavior. Inelastic response of short links is dominated by shear, whereas the inelastic response of longer links is dominated by flexure.

Understanding how link length can be used to control inelastic behavior can be approached by examining a free-body diagram of a link, as shown in Figure (2.5). It can be noted that the Shear force, V, is constant along the length of the link, while it is also subjected to equal and opposite end moments M.

A simplistic but reasonable assumption is made that the link end moments are equal in magnitude. It is also assumed that axial force in the link is small, and can be neglected.

The Shear yielding of the link will occur when the shear force reaches fully plastic shear capacity, $V_p$, of the link section. Note that shear yielding in a wide-flange section occurs primarily in the web. $V_p$ can be computed by simply multiplying the web area of the section by the yield stress in shear.

The plastic shear capacity can be expressed in the following equation

$$V_p = 0.6F_y\left(d - 2t_f\right)t_w$$

Where $F_y$ is the specified minimum yielding stress; d is the overall beam depth; $t_f$ is the thickness of the flange; and $t_w$ is the thickness of the web.

Flexural yielding will occur at the link ends when the end moment reaches the fully plastic moment of the link section ($M_p$). The plastic moment capacity is computed as follows:

$$M_p = ZF_y$$

Where Z is the plastic section modulus depending solely on the geometry of the cross section. It can be determined simply by computing the first moment of area of the section about its plastic neutral axis. The values of Z for all hot-rolled sections can be found in the AISC Manual; $F_y$ is the specified minimum yield stress and shall not exceed 350 MPa (50 ksi).

Figure (2.6) shows the free-body diagram of a link, and the interaction between moment and shear in the link, the effects of axial force is small therefore it will be neglected. Flexural hinges form at the ends of the link. Based on the Static Equilibrium equation, the link length is equal to twice the moment divided by the shear (e = 2M/V).
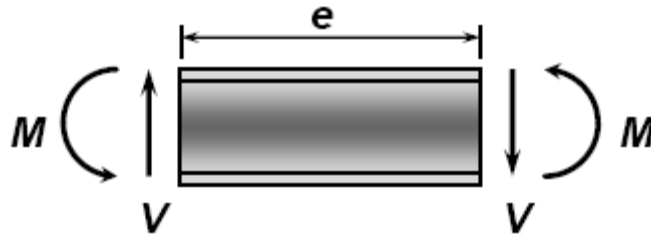
Figure (2.6): Static Equilibrium of Link

There is a relationship between link shear, link end moments, and link length that must be satisfied based on static equilibrium of the link. By summing moments for the free body diagram of the link.

When both end moments reach the plastic moment, $M_p$, a shear hinge is said to be formed when the shear reaches $V_p$. When both flexural and shear hinges form simultaneously, a balanced yielding condition occurs.

To determine the value of link length for which shear and flexural yielding occur simultaneously, Figure (2.7) shows a free body diagram with a link shear equal to $V_p$ and link end moments equal to $M_p$. The static equilibrium of the link, derived by shear and flexural yielding will occur simultaneously at a link length of $e = 2M_p/V_p$.
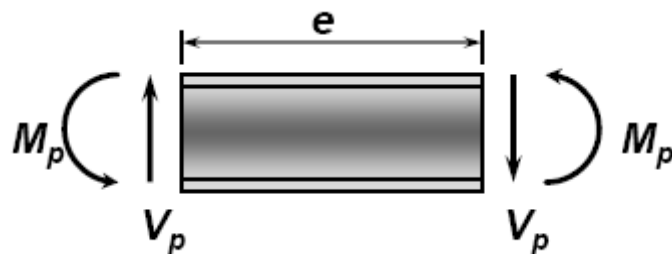


Figure (2.7): Shear and Flexural Yielding Occur Simultaneously

For links with e < $2M_p/V_p$, the link shear will reach $V_p$ before the end moments reach $M_p$, and the link will yield in shear as can be illustrated in Figure (2.8).

In shear yielding links, web yielding takes place along the entire web depth since shear stress is relatively uniform over the web depth in the inelastic range. The yielding also occurs along the entire length of the link, since shear force is constant along the length of the link. It should be noted that tests with short yielding links showed that eccentrically braced frames are very ductile and stable frames for resisting seismic loadings as given by (Farzad Naeim, 2001)



Shear yielding will occur when $V=V_p$ and $M< M_p$

Or, when: $e \leq \dfrac{2M_p}{V_p}$
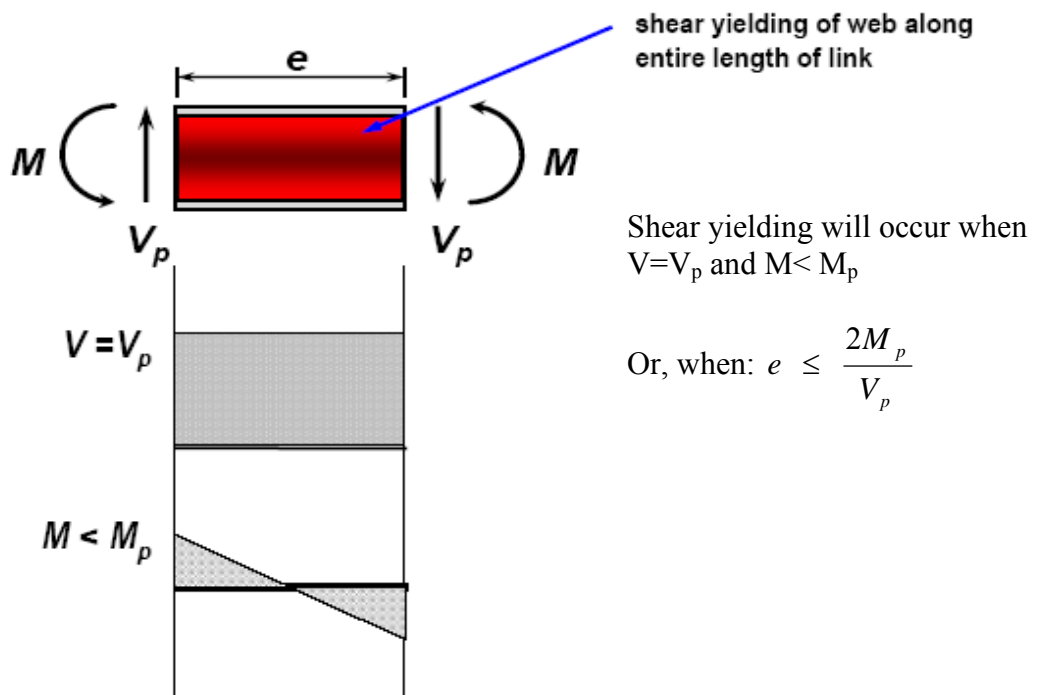
Figure (2.8): Shear Yielding Link

For links with e > $2M_p/V_p$, the link end moments will reach $M_p$ before the link shear reaches $V_p$, and the link will yield in flexure as illustrated in Figure (2.9).
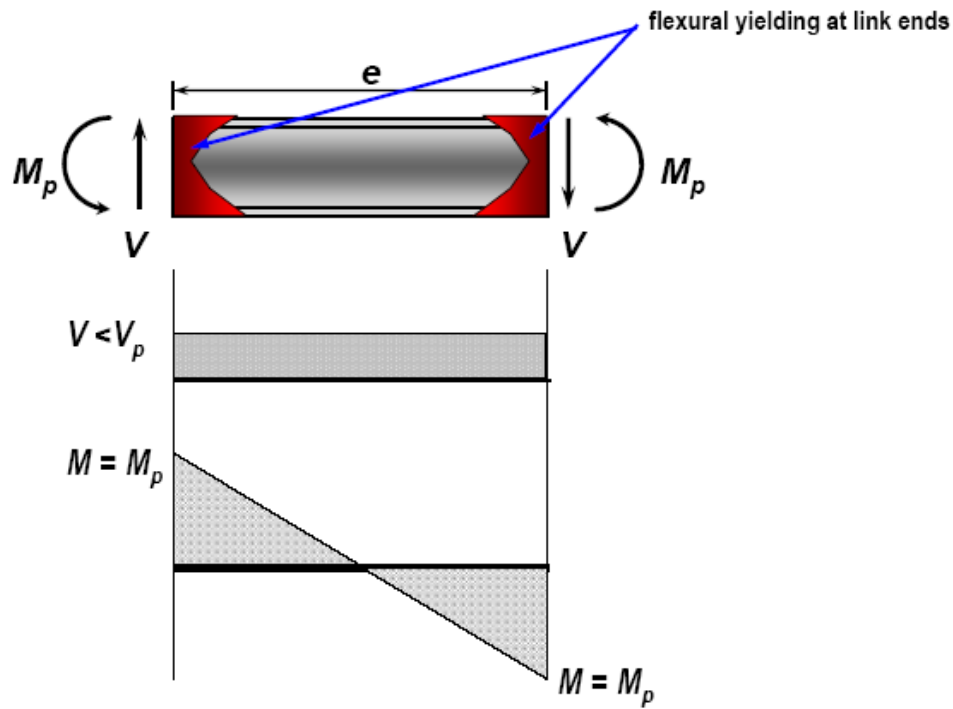
Figure (2.9): Flexural Yielding Link (Engelhardt, 2005)

Note that for a flexural yielding link, flexural yielding occurs only at the link ends. Because of the high moment gradient in a link (high shear = high moment gradient), flexural yielding is normally concentrated within a very short length at the link ends. A key reason why flexural yielding links provide lower levels of ductility is because only a relatively small portion of the link yields. It is worth to note that experimental results have shown that the inelastic deformations capacity of an EBF can be greatly reduced when long links are used.

These simple results are based on simple plastic theory, and assume there is no shear-flexure interaction and no strain hardening in the link.

The assumption of no shear-flexure interaction implies that $V_p$ is not affected by the presence of moment, and that $M_p$ is not affected by the presence of shear. While this is theoretically incorrect, experiments have shown there is, in fact, little shear-flexure interaction at the yield limit state of the link.

Experiments have shown that a link can develop a shear of $V_p$ even in the presence of very high end moments. Similarly, a link can develop a moment of $M_p$, even in the presence of very high shear.

Consequently, from a design perspective, shear flexure interaction when computing the plastic strength of a link is normally ignored.

Experiments have shown that links experience very high degrees of strain hardening. For example, in shear yielding links, ultimate shear forces $V_{ult}$ on the order of 1.25 to 1.5 $\times$ $V_p$ are observed in experiments. Similarly, in flexural yielding links, end moments on the order of 1.25 to 1.5 $\times$ Mp are observed in experiments.

Consequently, the effects of strain hardening must be considered when evaluating inelastic behavior of links.

## 2.4. Link Nominal Shear Strength, $V_n$

The link nominal shear strength $V_n$ is the link shear that will result in first significant yield of the link in shear.

The computation of $V_n$ neglects shear-flexure interaction. Experiments have shown it is reasonable to neglect shear-flexure interaction for the yield limit state of the link, i.e., for defining the plastic strength of the link.

$$V_n = \text{lesser of} \begin{cases} V_p & \text{controls for:} \quad e \leq \dfrac{2M_p}{V_p} \\ \\ 2M_p / e & \text{controls for:} \quad e \geq \dfrac{2M_p}{V_p} \end{cases}$$

For e < $2M_p/V_p$, link nominal shear strength will be controlled by shear yielding, and $V_n = V_p$.

For e > $2M_p/V_p$, link nominal shear strength will be controlled by flexural yielding at the link ends, and $V_n = 2 M_p/e$. In this case, the link nominal shear strength represents the value of link shear when the end moments reach $M_p$.

Note that when sizing a link for strength, all computations are done in terms of shear, regardless of whether link strength is controlled by shear yielding or by flexural yielding. Sizing link shear strength

$V_u \leq \emptyset V_n$  Where $V_u$ factor shear force in link according to ASCE, $\emptyset V_n$ link design shear strength. The required shear strength of the link $V_u$ based on the LRFD load combination with code specified earthquake and gravity load.

Case study:  W16x36  A572-Grade 50

A simple example of computing link nominal shear strength, for a W16x36 link of A572-Grade 50 ($F_y$ minimum yield stress 350 MPa, $F_u$ tensile stress 450 MPa) steel section is shown in Figure (2.10).
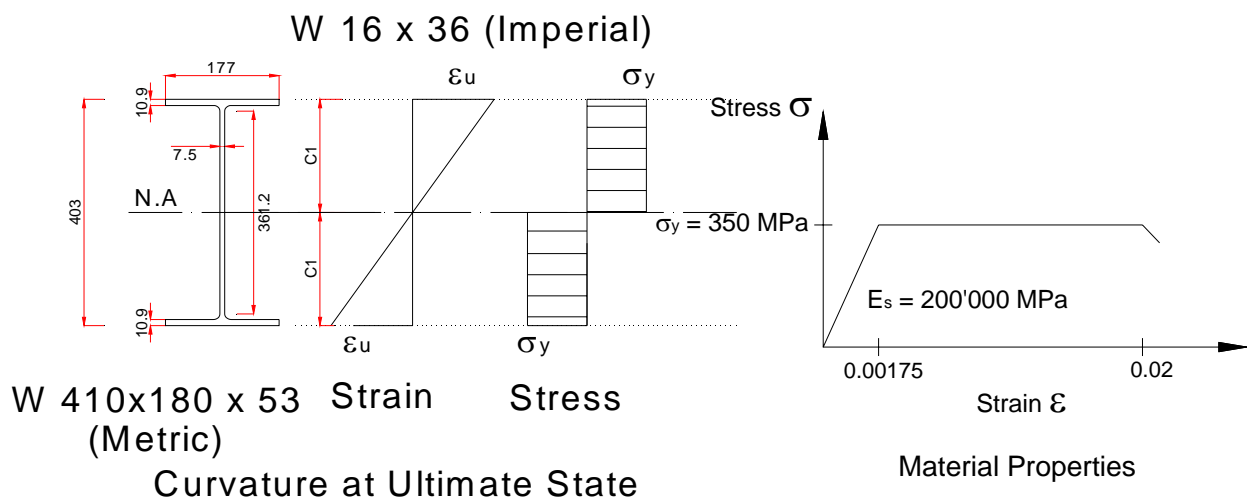


Figure (2.10): Cross Section and Material Properties

The calculation of $M_p$, $V_p$, $M_p/V_p$, and $2\,M_p/V_p$. are as follows:

$$\frac{M_p}{V_p} = \frac{376 \text{ kN.m}}{600 \text{ kN}} \times 1000 = 612 \text{ mm} \qquad \frac{2M_p}{V_p} = 2 \times 612 = 1224 \text{ mm}$$

$V_n = \textbf{lesser of}$
$$\begin{cases} \mathbf{V_p} & \mathbf{= 600 \text{ kN}} \\ \\ \mathbf{2M_p / e} & \mathbf{= 734 / e} \end{cases}$$

Figure (2.11) shows the value of link nominal shear strength for an A572-Grade 50 W16x36 link.

$V_n = V_p = 600$ kN will control when $e \leq 1224$ mm ($2\,M_p/V_p$).

$V_n = 2\,M_p/e = 734/e$, will control when $e \geq 1224$ mm ($2\,M_p/V_p$).

Figure (2.11) shows that the link nominal shear strength is constant and it is equal to $V_p$ when shear yielding link control, the link ultimate shear strength varies when flexural yielding link occur. The maximum strength of a link is achieved when shear yielding controls. That is, shear yielding links provide greater link strength (and therefore greater lateral frame strength for an EBF) than flexural yielding links.
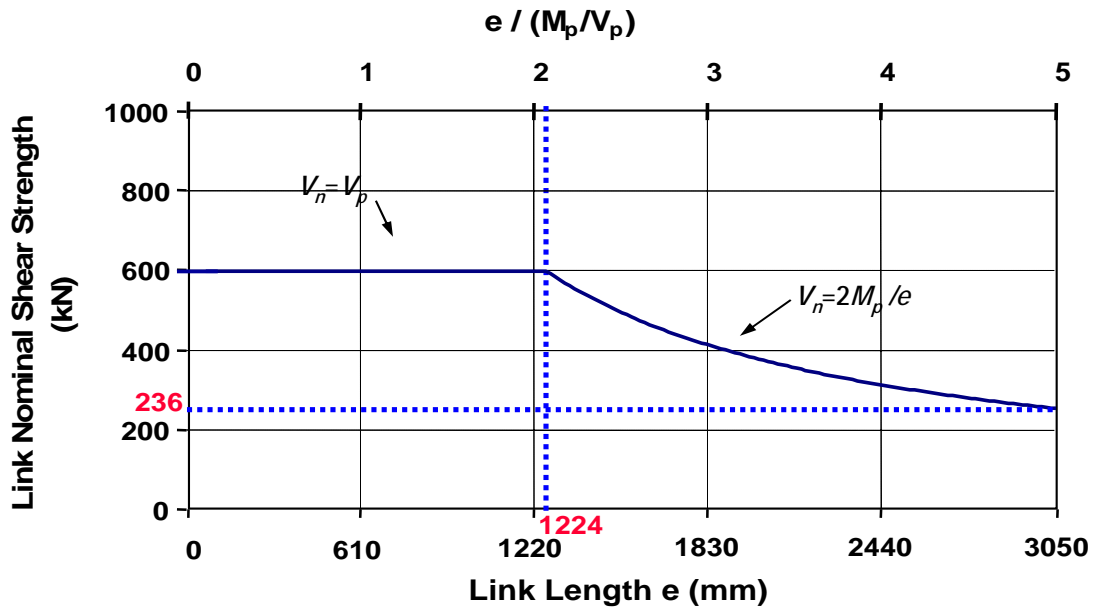
Figure (2.11): Relationship between Link Nominal Shear Strength (kN) and Link Length
e (mm)

## 2.5.    Post-Yield Behavior of Links:   Strain Hardening

The value of $V_n$ (link nominal shear strength at idealized case), shown in the
Figure (2.12) represents the shear at first significant yield of the link $V_y$. Note that after
first significant yield $V_y$, the link shear strength continued to increase due to strain
hardening. The ultimate link shear at strain harden $V_{ult}$ is substantially greater than $V_y$.
Experiments have shown that $V_{ult} \approx 1.25$ to $1.5\ V_y$ for both shear and flexural yielding
link.
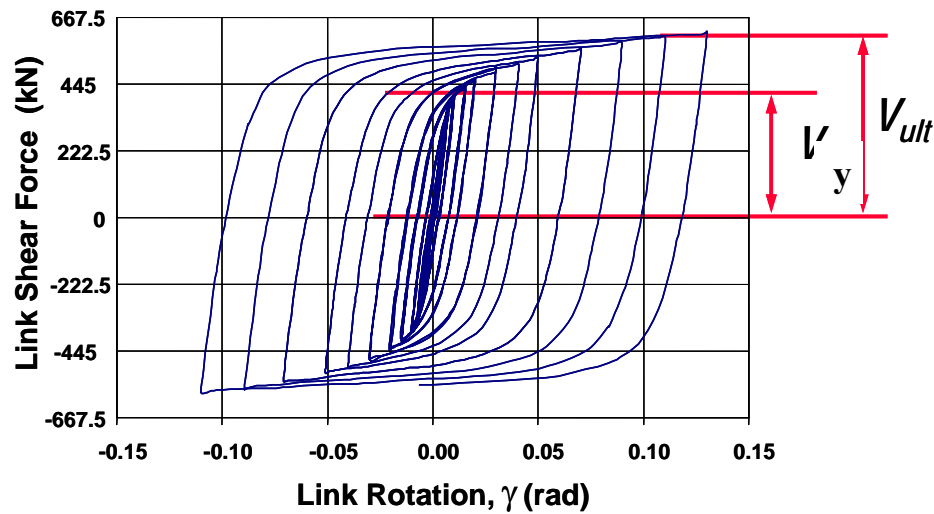
Figure (2.12):Post-Yield Behavior of Link

An important effect of strain hardening is that both shear and flexural yielding will occur over a range of link lengths. A link length of $e = 2\,M_p / V_p$ represents theoretical the dividing line between shear yielding and flexural yielding links, and it is used as a basis for computing link nominal shear strength (i.e. link shear at first significant yield). However, once the link has achieved its nominal strength, the link shear will continue to increase due to strain hardening. As a result, a link that initially yielded in shear may still experience flexural yielding, as the link shear continues to increase. Similarly, a link that initially yielded in flexure may still experience shear yielding, as the link end moments continue to increase due to strain hardening.

As an example, consider a link with $e = 1.8\,M_p/V_p$. This link will initially yield in shear, at this point, the link shear will equal $V_p$ and link end moments will be less than $M_p$.

Due to strain hardening, say that the link ultimately achieves a shear strength of $V_{ult} = 1.5\ V_p$. At this point, the link end moments must equal (by static equilibrium of the link): $M_{ult} = (e \times V_{ult})/2 = [(1.8 M_p/V_p) \times (1.5\ V_p)]/2 = 1.35\ M_p$. Thus, even though this link initially yielded in shear, it is also experiences flexural yielding.

As another example, consider a link with $e = 2.3 M_p/V_p$. This link will initially yield in flexure, and $V_n = 2\ M_p/e = 2\ M_p / (2.3 M_p/V_p) = 0.87\ V_p$. At this point, the link end moments will be equal to $M_p$, and the link shear will be less than $V_p$. Due to strain hardening, say that the link end moments ultimately achieve $M_{ult} = 1.5\ M_p$. At this point, the link shear must equal (by static equilibrium of the link):

$$V_{ult} = (2\ M_{ult})/e = (2 \times 1.5\ M_p) / (2.3 M_p/V_p) = 1.3\ V_p.$$

Thus, even though this link initially yielded in flexure, it ultimately also experienced shear yielding.

Thus, whereas $e = 2\ M_p / V_p$ represents the dividing line between shear and flexural yielding links from the point of view of first significant yield, after first yield a combination of shear and flexural yielding will occur over a rather wide range of link lengths.

Experiments have shown that to obtain a link that yields predominantly in shear (with little flexural yielding even after strain hardening), the link length should be kept below about $1.6\ M_p/V_p$. To obtain a link whose inelastic behavior is dominated by flexural yielding (with little shear yielding even after strain hardening), the link length should be greater than about $2.6\ M_p/V_p$.

For link lengths between 1.6 and $2.6\ M_p/V_p$, the link will experience significant degrees of both shear and flexural yielding as it strain hardens under inelastic cyclic loading.

The choice of link lengths of 1.6 $M_p/V_p$ and 2.6 $M_p/V_p$ for demarcating zones of inelastic link behavior is somewhat arbitrary, as there are no sharply defined boundaries between shear and flexural yielding as link length is varied. Nonetheless, these value appears reasonable based on experimental observations of link behavior.

The links lengths of 1.6 $M_p/V_p$. and (e ≤ 1.6 $M_p/V_p$.), are also used by the AISC Seismic Provisions to divide links into three ranges of inelastic behavior: predominantly shear yielding (e ≤ 1.6 $M_p/V_p$.), predominantly flexural yielding (e ≥ 2.6 $M_p/V_p$.), and combined shear and flexural yielding (1.6 $M_p/V_p$. < e < 2.6 $M_p/V_p$.).

Designers can use these length limits to control the inelastic behavior of links.


### 2.5.1 Shear Yielding Links

Critical length for strain hardener short link: Based on plastic theory test result (Engelhardt,2005), shows that stiffened short link at large inelastic deformation can strain harden and develop shear strength equal to 1.5 $V_p$. The end moment of a link will continuous to increase due to strain hardening and therefore flexure hinges can develop. Due to high strains these end moments are limited to 1.2Mp, and then the shear link will be modified as follows

e = 2(1.2 $M_p$)/1.5$V_p$=1.6 $M_p/V_p$

Provide best overall structural performance for strength, stiffness, and ductility

The previous clarify described how link length can be used to control whether a link will yield primarily in shear, primarily in flexure, or in combined shear and flexure.

The next question is which mode of yielding is preferred. The answer to this question is clear from both experimental and analytical evidence: shear yielding links provide for the best overall strength, stiffness and ductility of an EBF. So, in general,

for good seismic performance, EBFs with shear yielding links ($e \leq 1.6\ M_p/V_p$) are preferred.

In a schematic fashion, links are typically tested in the laboratory by restraint of link ends against rotation (either complete rotational restraint, or a restraint that provides limited rotational flexibility that simulates rotational restraint provided by an adjoining beam or column). Link deformation shown in Figure (2.13) is normally characterized by the link rotation angle ($\gamma$). The value of $\gamma$ is normally computed simply by taking the relative end deflection of the link, and dividing by the link length.



$$\gamma = \frac{\Delta}{e}$$
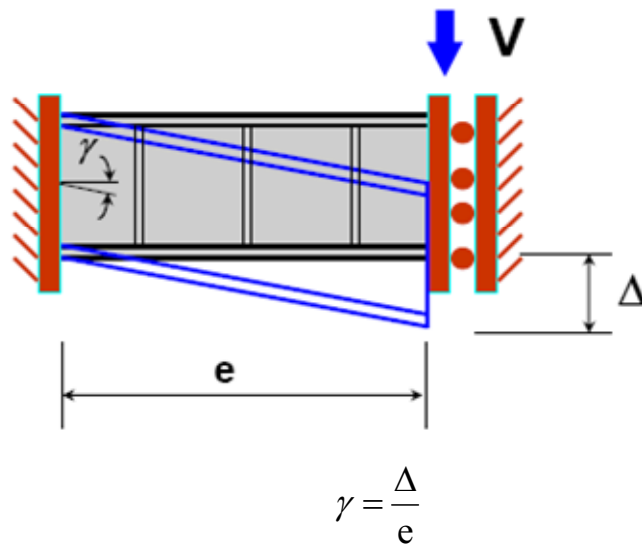
Link Deformation :(radian)

Figure (2.13): Link Deformation

The link rotation angle $\gamma$ includes both elastic and inelastic contributions. The elastic portion of the link rotation (resulting from elastic link deformations or elastic rotations of the link ends) can be subtracted from the total rotation $\gamma$ to obtain the link plastic rotation angle $\gamma_p$.

### 2.5.2 Long Yielding Links

Critical length for strain harden long link: For long links "e" more than $(2M_p/V_p)$ the inelastic deformation capacity of an EBF can be greatly reduced, in this case the flexural hinge dominate the link response and e will be larger than $2.6M_p/V_p$.

Links with a length beyond $1.6$ $M_p/V_p$ are no longer predominantly shear yielding links, and generally result in EBFs with less strength, stiffness and ductility, as compared to EBFs with shear links.

Consequently, these longer links should be avoided in EBFs. Nonetheless, longer links are sometimes needed in EBFs to satisfy architectural constraints that call for large frame openings (to accommodate a door, window, etc), or other non-structural constraints.

The AISC seismic provisions permit EBFs to be designed with any length of link, and appropriate detailing provisions and rotation limits are provided for each length range (shear yielding, flexural yielding, combined shear and flexural yielding). Nonetheless, it should be kept in mind that shear yielding links are preferred for best structural performance of an EBF.

## 2.6. EBF Rigid-Plastic Kinematics

Applying simple plastic theory, the kinematics of the plastic mechanisms for the K-Type bracing, D- Type Bracing, and V- Type bracing are as follow.

### 2.6.1 Kinematic Mechanism for K-Type Bracing

Figure (2.14) represents the geometry of rigid-plastic mechanisms of EBFs that can be used to relate link plastic rotation angle $\gamma_p$ to the frame plastic inter-story drift angle $\theta_p$. This relationship is used to estimate link plastic rotation demands in the AISC Seismic Provisions.

For the case of link at mid span of the beam (K-braced EBF type) $\gamma_p$ is obtained by multiplying $\theta_p$ by L/e as in the following $\gamma_p = \dfrac{L}{e}\theta_p$
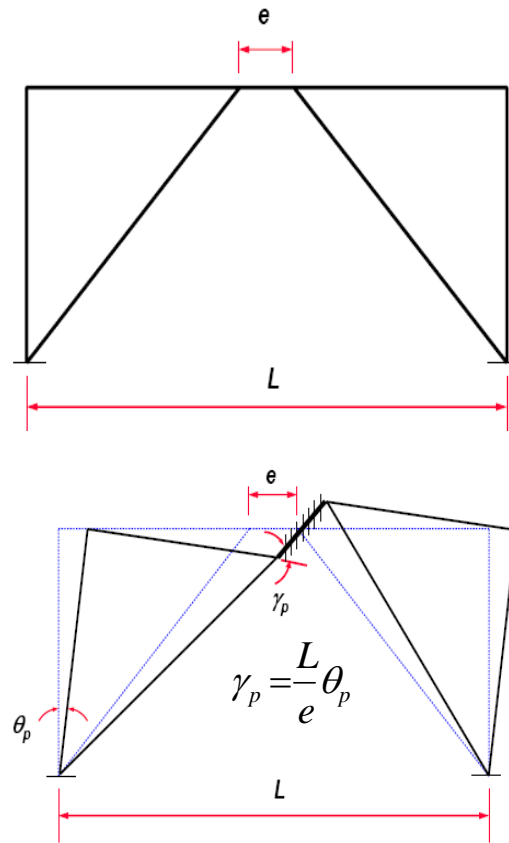


Figure (2.14): Kinematic Mechanism for K-Type Bracing

### 2.6.2 Kinematic Mechanism for D-Type Bracing

For D- Braced Type (the single diagonal EBF), shown in the Figure (2.15) represents the relationship between link plastic rotation angle $\gamma_p$ and frame plastic inter-story drift angle $\theta_p$ is the same as for the EBF with a link at mid-span (K-braced type).

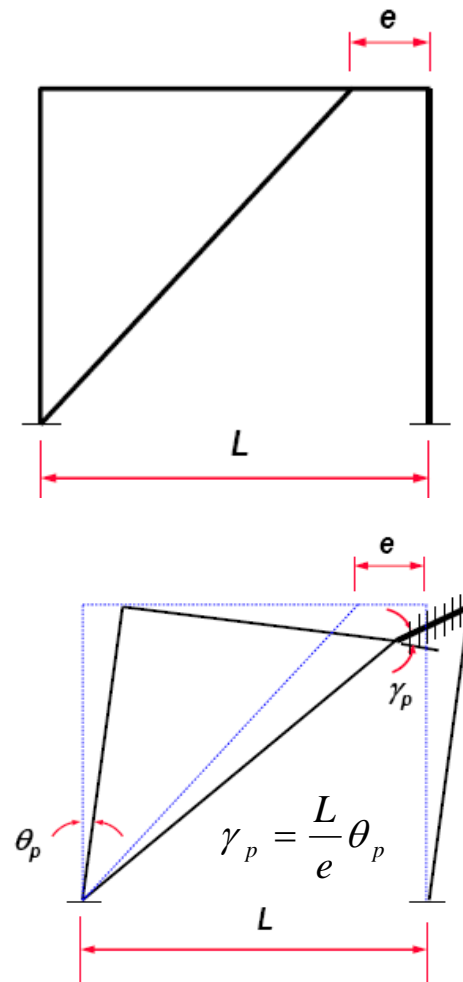$$\gamma_p = \frac{L}{e}\theta_p$$

Figure (2.15): Kinematic Mechanism for D- Type Bracing

### 2.6.3 Kinematic Mechanism for V-Type Bracing

The geometry of rigid-plastic mechanisms of V-braced EBF in Figure (2.16), shows that the link rotation angle demand is one-half the previous two types of EBF as shown in the following equation $\gamma_p = \dfrac{L}{2e}\theta_p$
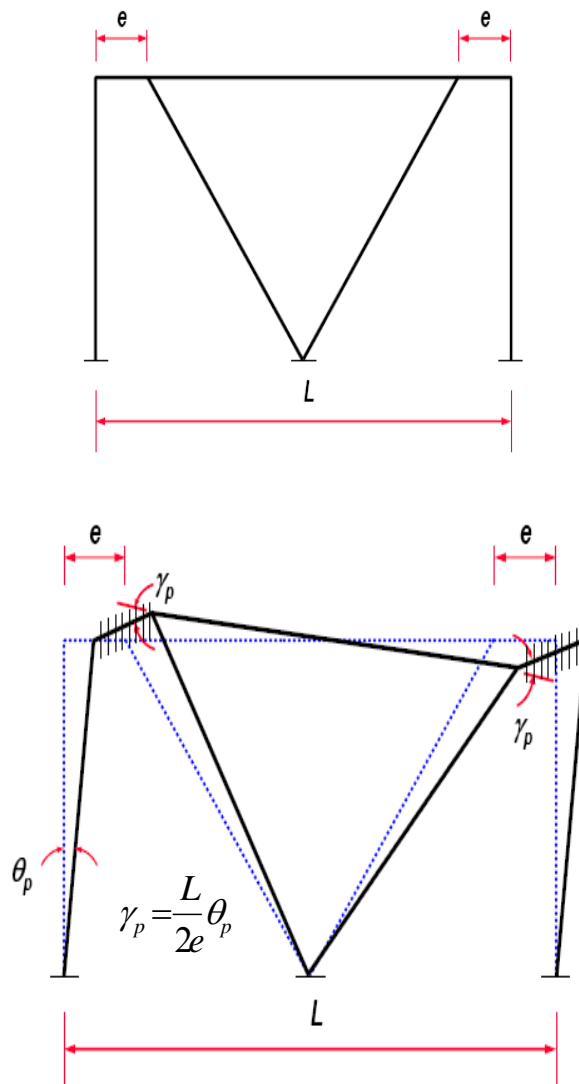


Figure (2.16): Kinematic Mechanism for V-Type Bracing

# CHAPTER THREE
# MODELS ANALYSIS AND PROCEDURES

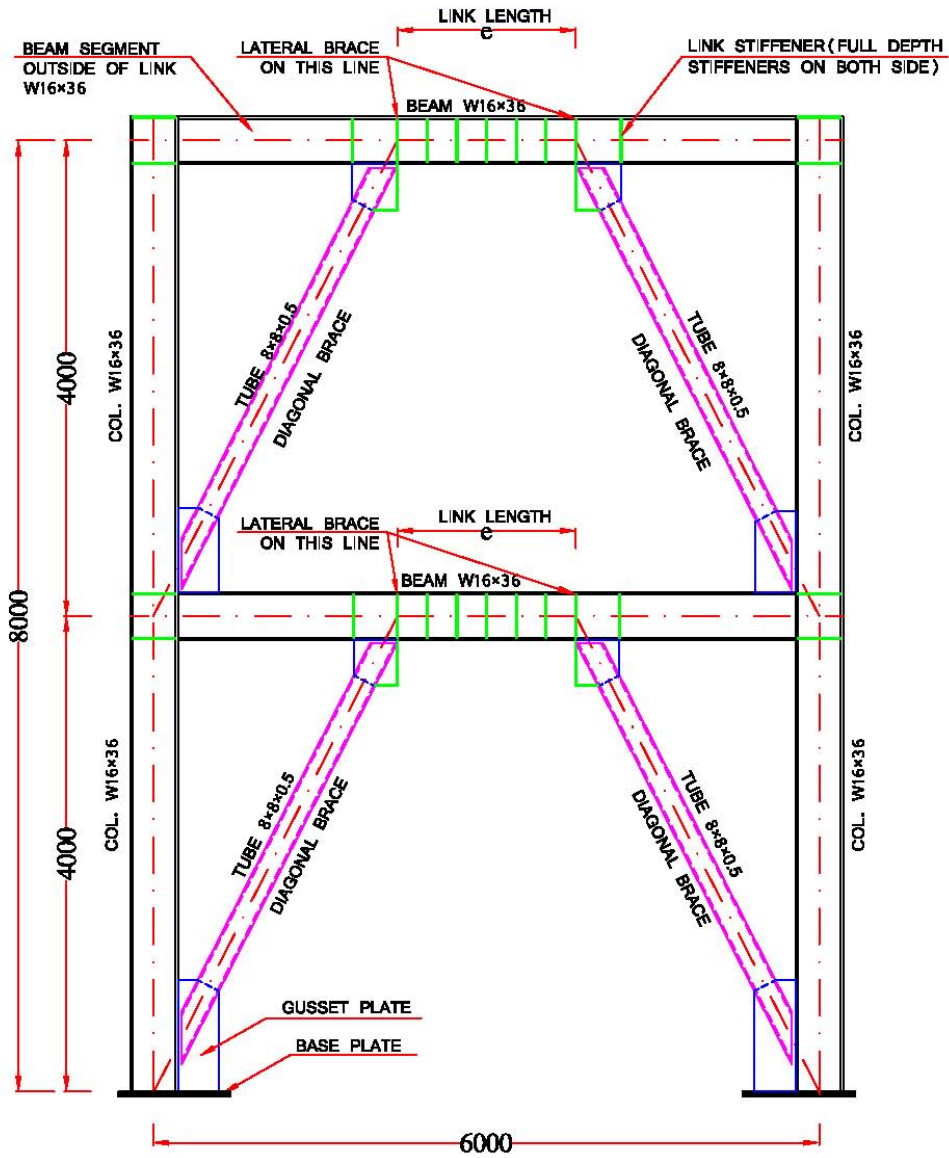## 3.1. Geometric and Material Assumptions for all Models

The generated 2D model frames will be those of Eccentrically Braced Frames with a total height 8 meters, all the models are having the following characteristic and governing parameters:

(1) The number of stories taken are two, with a typical story height of 4 meters.

(2) All models have a bay width (span) equal 6 meters.

(3) Material: the yielding stress of the steel $F_y$ equal 350 MPa (50 ksi).

(4) Types of the frame elements are as listed in Table (3.1) and Figure (3.1), (3.2), (3.3).
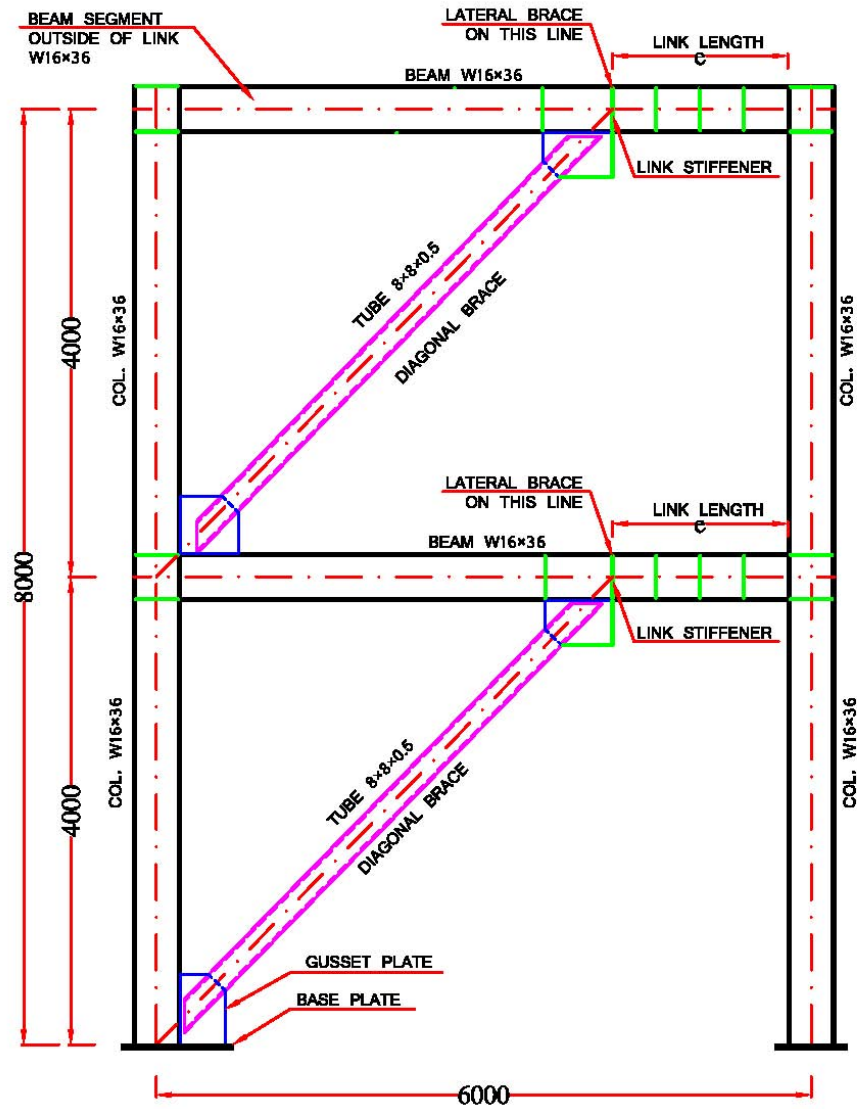
Table (3.1): Dimension of Columns, Beams, and Bracings

| Section Element | Description |
|-----------------|-------------|
| Columns | W16x36 |
| Beams | W16x36 |
| Bracing | Tube 8x8x0.5 |

The link cross section segment is the same as the cross section of the beam, and the web of the link shall be single thickness without doubler-plate reinforcement and with out web penetrations (AISC Seismic Provisions, 2005).
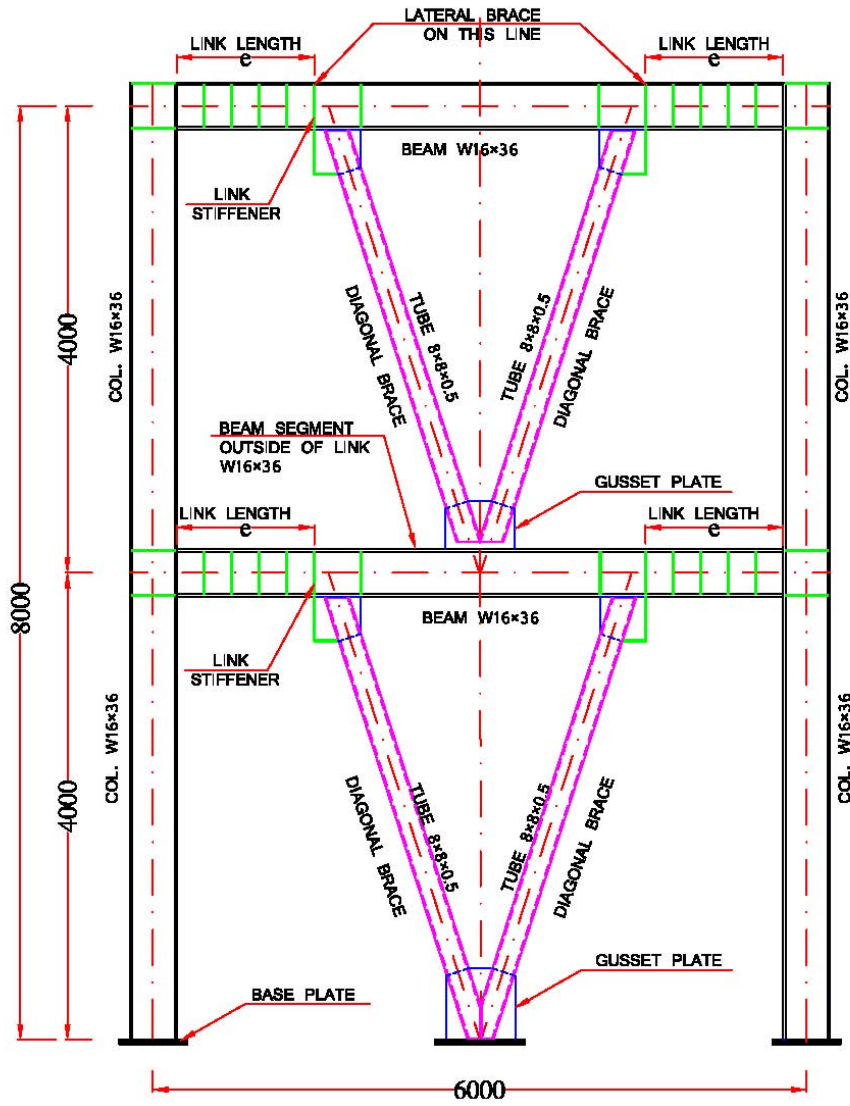
Figure (3.1): Model Frame Elements Profile for K-Braced Type

Figure (3.2): Model Frame Elements Profile for D-Braced Type

Figure (3.3): Model Frame Elements Profile for V-Braced Type

## 3.2. Elastic Stiffness

The stiffness, k, of a structure is a measure of the resistance offered by an elastic structure to deformation.

Three types of EBF are considered in the modeling taking in consideration different lengths and locations of links.

The first parameter studied is stiffness. The Steel Moment Resisting Frame (MRF) can behave in very ductile manner and very flexible, this case means that the link length is the same as the beam (e=L).

Concentrically Braced Frame (CBF) shows a large stiffness, but their energy dissipation capacity is affected by brace buckling and e=0.

The system of the Eccentrically Braced Frame (EBF) combines the advantage of both the Steel Moment Frame and Concentrically Braced Frame, EBF dissipates energy by controlled yielding of shear or moment links.

Seismic resisting structures are expected to maintain adequate stiffness during earthquake duration. The EBF must resist the lateral forces without damaging drift level and it must have a proper stiffness for occupant comfort.

The variation of the lateral stiffness of three types of EBF (D-braced, K-braced, and V-braced) with respect to different link length are studied and modeled in SAP 2000 as shown in Figure (3.4), (3.6), (3.8).

The mathematical models evaluate lateral stiffness of braced frames, and the use of shorter links (shear yielding link) leads to more stiffness than the long links. The variations of the lateral stiffness of EBF with respect to the link length for different types of bracing are shown in Figure (3.8). The Figure clearly shows the advantage of using a short link for drift control.

### 3.2.1. Elastic Stiffness for K-Braced EBF

Figure (3.4) shows the story drift shape of K-braced EBF. Note that the deformation shape increases with the increase of link length. The deformation rate is 2.9 times higher in long link than it is in short link. Consequently, the relative lateral stiffness for the short link was 2.9 times as high as that for the long link.

(a) Short Link e=600mm Lateral
Displacement Δ=0.0201 mm

(b) Intermediate Link e=1200mm Lateral
Displacement Δ=0.0346 mm

(c) Long Link e=1800mm Lateral
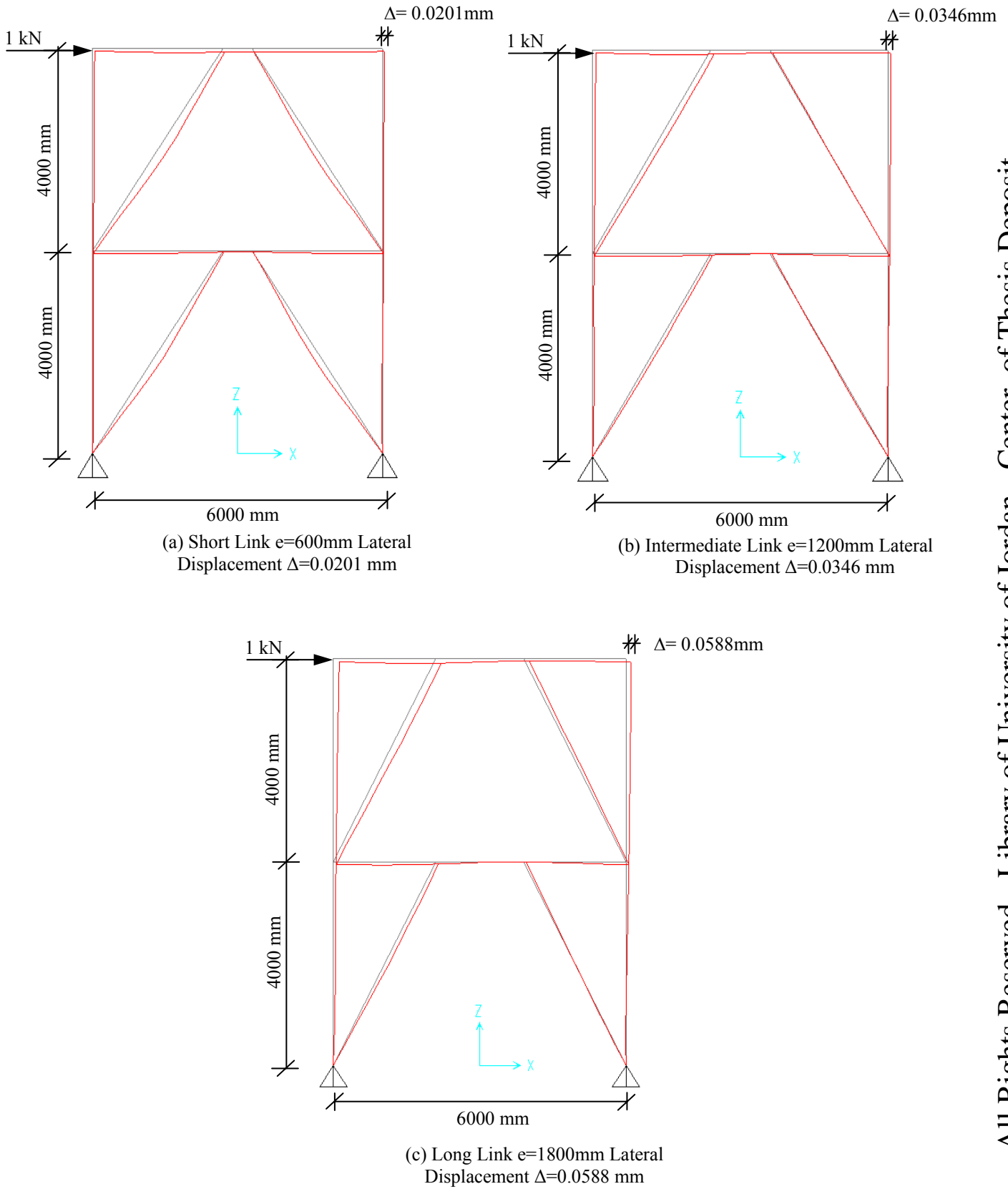Displacement Δ=0.0588 mm

Figure (3.4 a, b, c): Lateral Drift for K-Braced EBF Vary with Link Length

Table (3.2): Relative Stiffness Associated to Link Length for K-Braced EBF

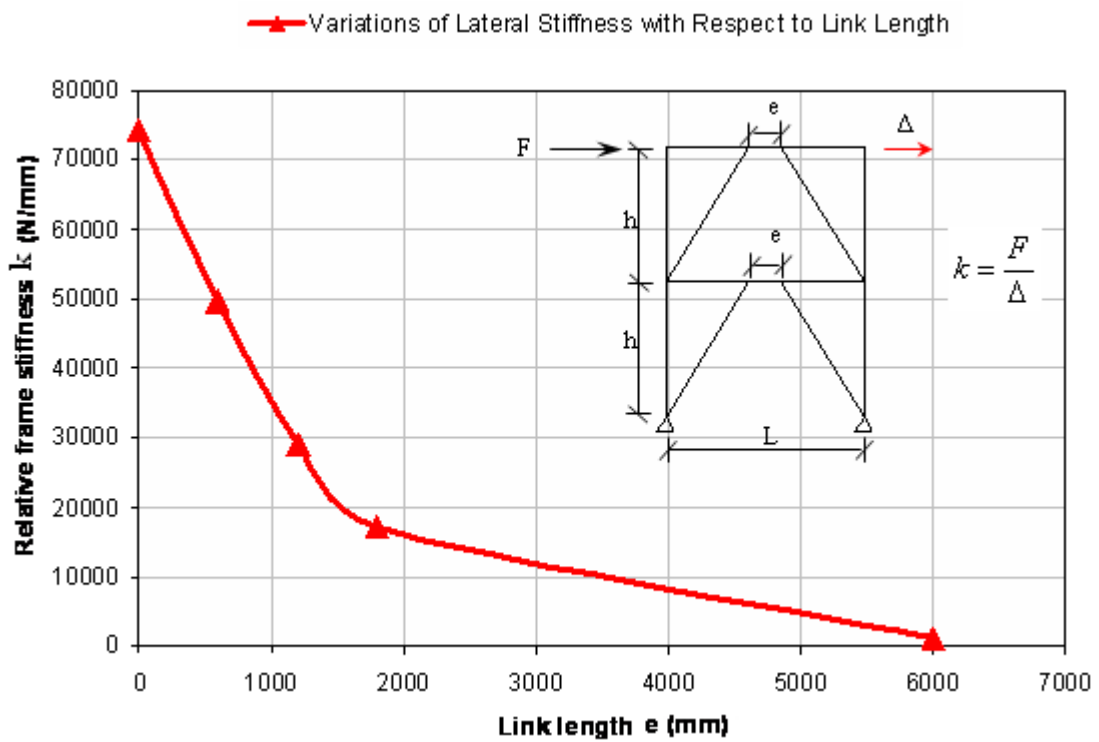| e<br>(mm) | k<br>(N/mm) |
|-----------|-------------|
| 0 | 74074 |
| 600 | 49751 |
| 1200 | 28901 |
| 1800 | 17006 |
| 6000 | 1093 |



Figure (3.5): Variation of Lateral Stiffness with Respect to Link Length for K-Braced

### 3.2.2. Elastic Stiffness for D-Braced EBF

Take stiffness for D-braced EBF, Figure (3.6), shows several link length of EBF (e=600mm, e=1200mm, and e=1800mm), an important parameter of an EBF is the brace offset (e). Figure (3.7) show a plot of link length versus relative frame stiffness for various aspect of link length.

Table (3.6) shows that short link (shear link, e=600 mm) has a relative lateral stiffness 2.6 times that of the long link (flexural link, e=1800 mm). This proves that short link outperforms long link when comparing each type's relative stiffness.

Figure (3.7) demonstrates that the link length is inversely proportional to the stiffness. CBF system has no link, therefore, the stiffness value is the largest since (e=0). On the other hand, when the link length is largest (e=L), the stiffness will be at its minimum.

(a) Short Link e=600mm Lateral Displacement Δ=0.1372 mm

(b) Intermediate Link e=1200 mm Lateral Displacement Δ=0.2378 mm

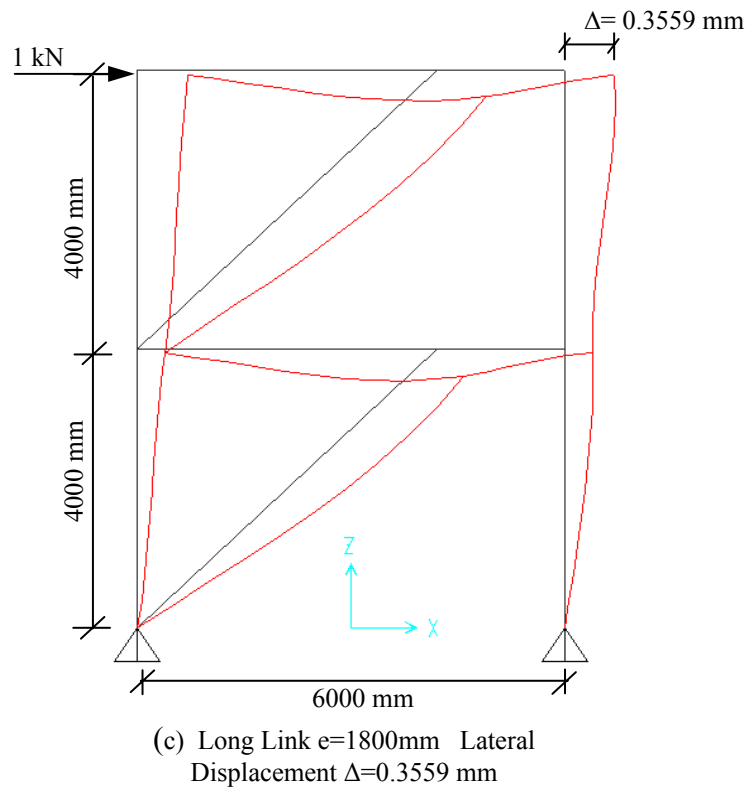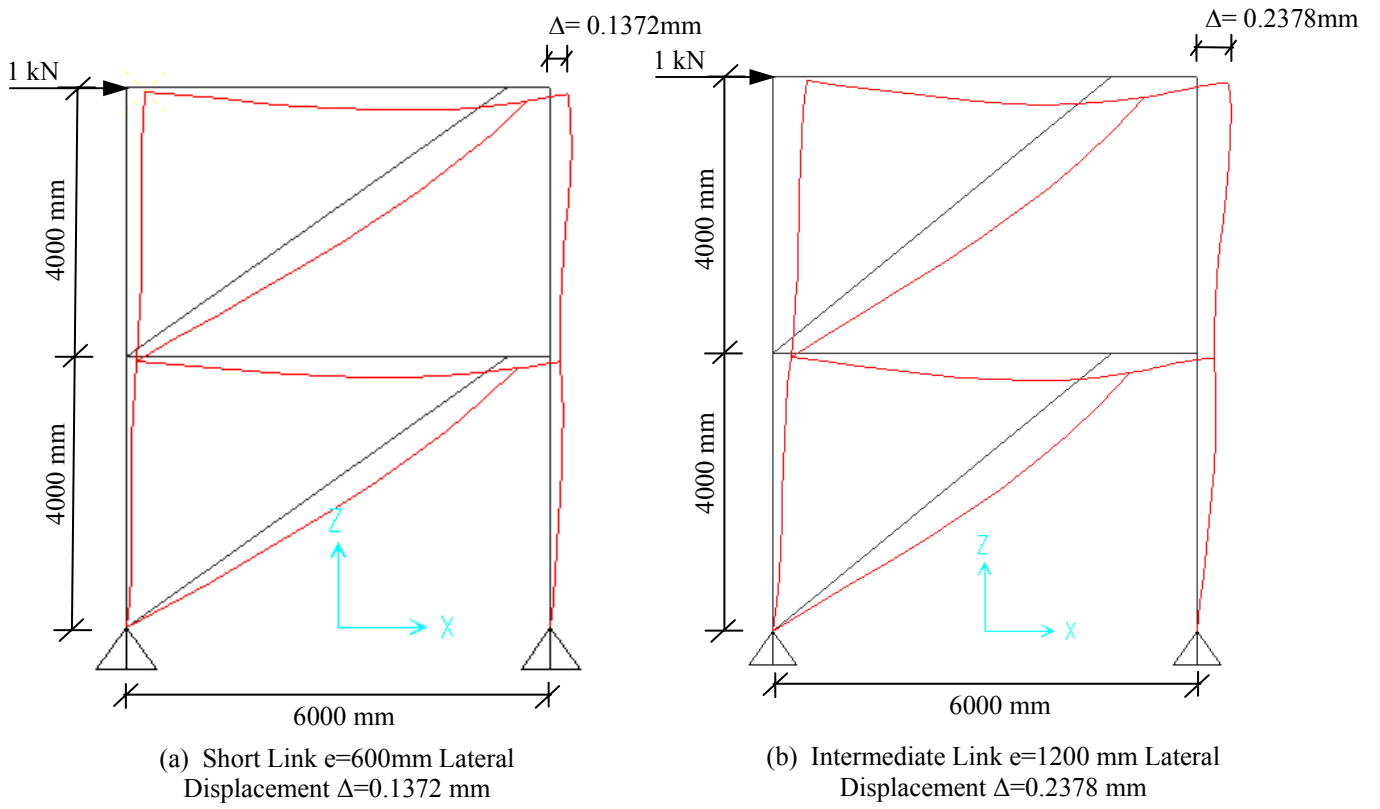(c) Long Link e=1800mm Lateral Displacement Δ=0.3559 mm

Figure (3.6 a, b, c): Lateral Drift for D-braced EBF Vary with Link Length

The red lines in Figure (3.6) are used to show the deformation shape of the frame. Grey lines are used to show frame prior to deformation.

Table (3.3): Relative Stiffness Associated to Link Length for D-braced EBF

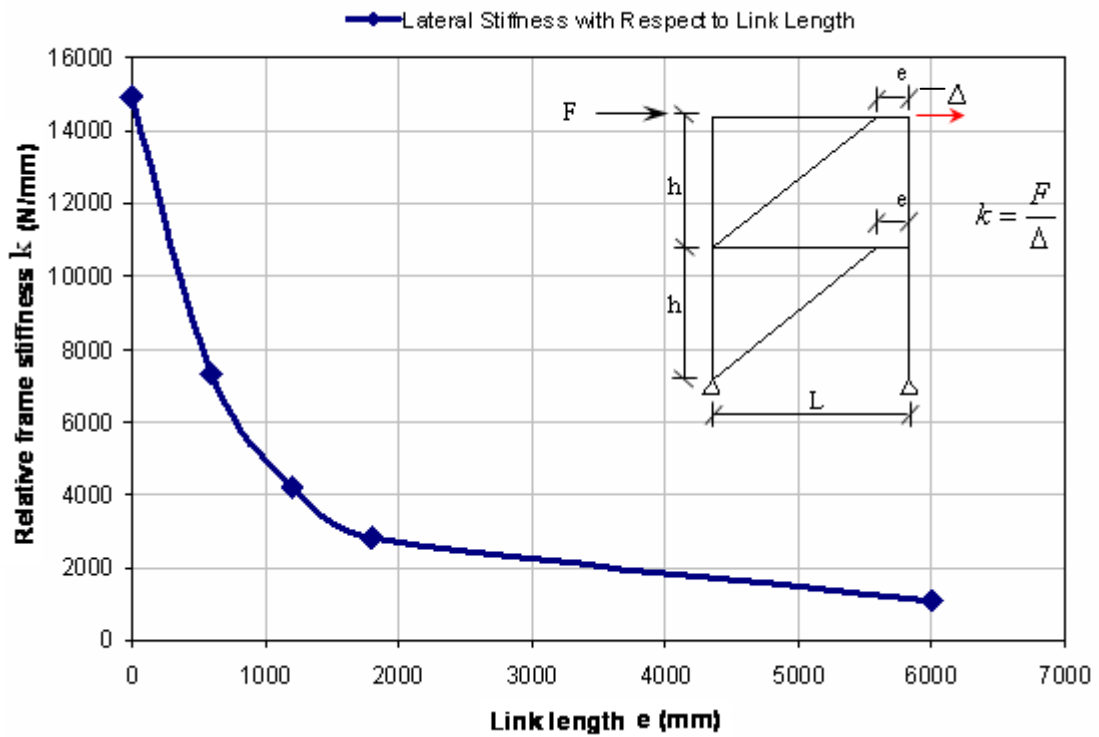| e (mm) | k (N/mm) |
|--------|----------|
| 0      | 14925    |
| 600    | 7288     |
| 1200   | 4205     |
| 1800   | 2809     |
| 6000   | 1093     |



Figure (3.7): Variation of Lateral Stiffness with Respect to Link Length for D-Braced

### 3.2.3. Elastic stiffness for V-Braced EBF

Figure (3.8) illustrates the deformation shape for a V-braced EBF. Note that long link has a maximum deformation reaching a rate 2.95 that of the short length.



(a) Short Link e=600mm Lateral Displacement Δ=0.0362 mm

(b) Intermediate Link e=1200 mm Lateral Displacement Δ=0.0606 mm

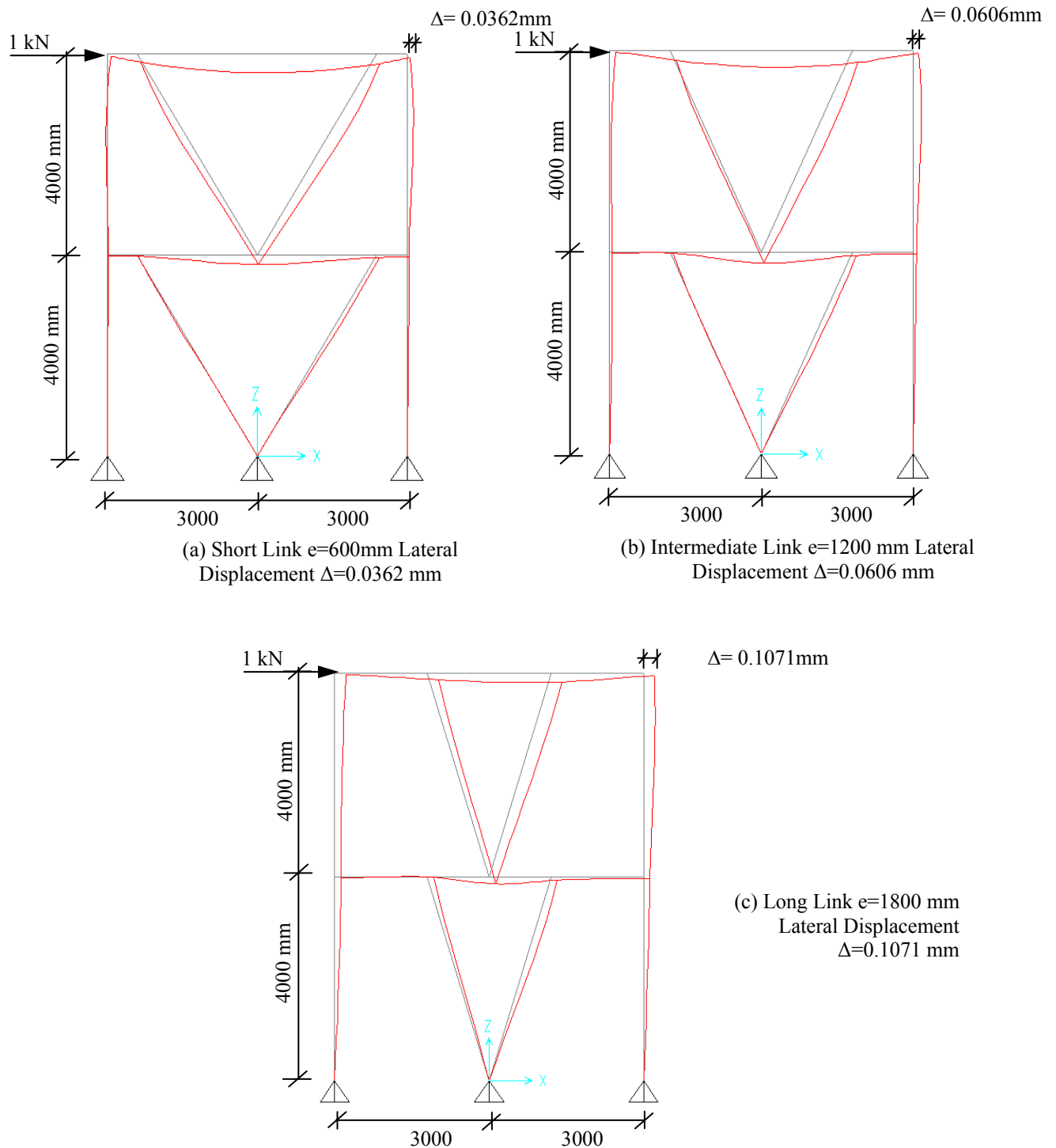(c) Long Link e=1800 mm Lateral Displacement Δ=0.1071 mm

Figure (3.8 a, b, c): Lateral Drift for V-braced EBF Varies with Link Length

Table (3.4): Relative Stiffness Associated to Link Length for V-Braced EBF

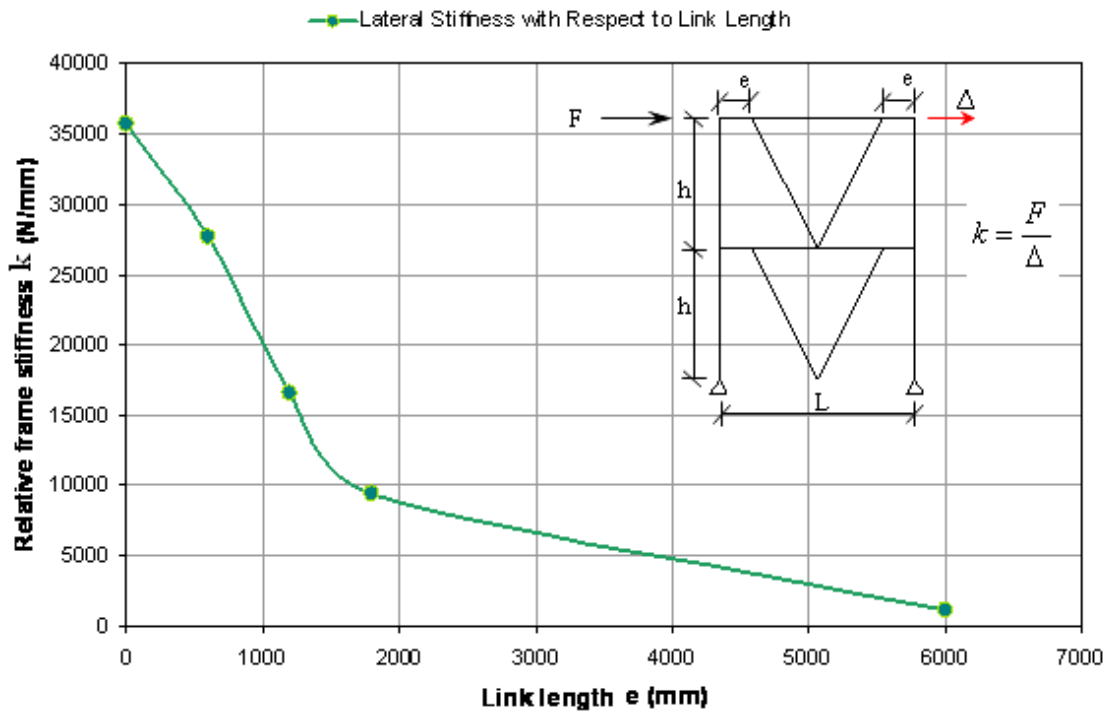| e (mm) | k (N/mm) |
|--------|----------|
| 0 | 35714 |
| 600 | 27624 |
| 1200 | 16501 |
| 1800 | 9337 |
| 6000 | 1093 |



Figure (3.9): Variation of Lateral Stiffness with Respect to Link Length for V-Braced

### 3.2.4. Comparison of Elastic Stiffness between the Three Braced Types of EBF

As can be seen in Table (3.5) and Figure (3.10), K-braced EBF is the best system when comparing relative frame stiffness and short link is the best of the three link length categories.

When studying the relative frame stiffness of the three types of EBF, it is found that K-braced EBF is 6.8 times stiffer than D-braced EBF and 1.8 times stiffer the V-braced EBF. Figure (3.10) clearly illustrates that it is advantages to used K-braced EBF with a short link due to its limitation on drift control under earthquake (lateral force).

Table (3.5): Relative Stiffness Associated to Link Length for Different Types of EBF

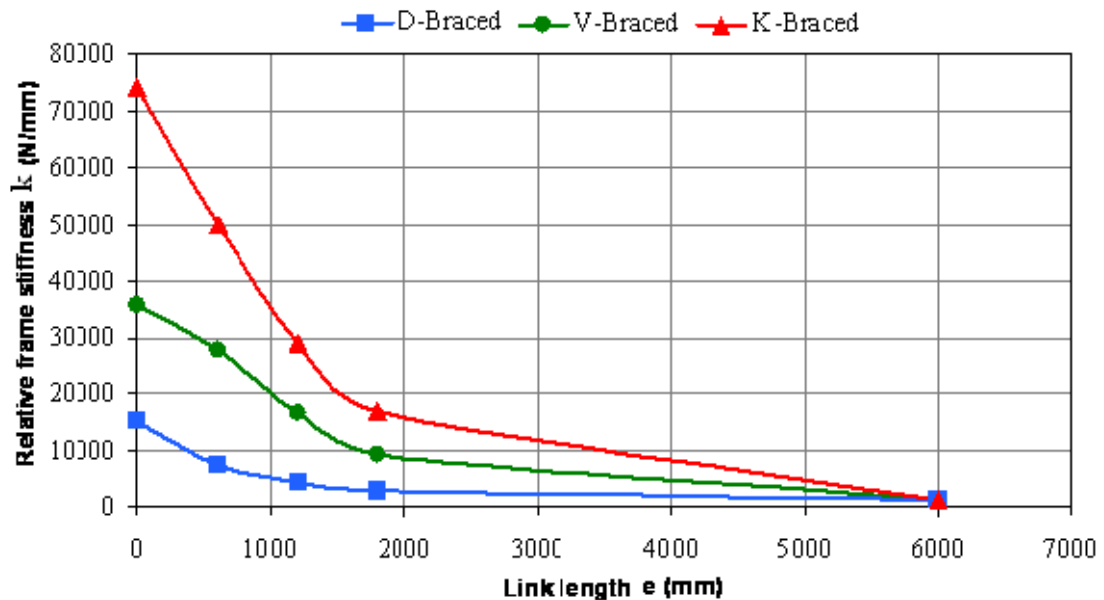| Link Length | V-braced EBF | D-braced EBF | K-braced EBF |
|---|---|---|---|
| e (mm) | k (N/mm) | k (N/mm) | k (N/mm) |
| 0 | 35714 | 14925 | 74074 |
| 600 | 27624 | 7288 | 49751 |
| 1200 | 16501 | 4205 | 28901 |
| 1800 | 9337 | 2809 | 17006 |
| 6000 | 1093 | 1093 | 1093 |



Figure (3.10): Variation of Lateral Stiffness with Respect to Link Length for Different Types of EBF

## 3.3. Nonlinear Static Procedure Analysis (NSPA)

In performance-based earthquake engineering it is necessary to obtain realistic estimates of inelastic deformations in structures, so that these deformations may be checked against deformation limits as specified in the performance criteria. The available methods for determining the inelastic deformations are as follows:

- Nonlinear static procedure analysis.

- Nonlinear dynamic response history analysis.

In this study nonlinear static procedure analysis (NSPA) is used. The NSPA is a simple method for determining the inelastic deformation and provide estimate reasonable for the location of inelastic behavior, also it is less time consuming than the nonlinear dynamic history analysis.

Static nonlinear analysis is a procedure, in which the magnitude of the structural loading or displacement is incrementally increased in accordance with a certain predefined pattern. With the increase in the magnitude of loading or displacement, weak links and failure mechanism of the structure are found. The NSPA is an attempt by the structural engineering profession to evaluate the real strength of the structure and it promises to be a useful and effective tool for performance based design.

Nonlinear static analysis, commonly referred to as pushover analysis, is a method for determining the ultimate load and deflection capacity of a structure.

The Federal Emergency Management Agency FEMA-273 documents have developed modeling parameters, acceptance criteria (Immediate Occupancy (IO), Live Safety (LS), and Collapse Prevention (CP)) and analysis procedures for NSPA.

These documents define force-deformation criteria for hinges used in NSPA. As shown in Figure (3.11), points labeled A, B, C, D and E are used to define the force-deflection behavior of the hinge and three points labeled IO, LS, and CP are used to define the acceptance criteria for the hinge. (IO, LS and CP stand for Immediate Occupancy, Live Safety and Collapse Prevention respectively.) The values assigned to each of these points vary depending on the type of member as well as many other parameters defined in the FEMA-273 documents as shown in Table (3.6) and Table (3.7), where $M_{ce}$ is the expected moment strength, and $V_{ce}$ is the expected shear strength.

The rules for determining building performance are given below for each performance level, acceptance criteria state IO in any story, in the direction of the applied earthquake loads, not more than 10% of beams are in the significant damage state whereas all other structural members are in the minimum damage state, retrofitting is not required.

Acceptance criteria state LS in any story, the damage is not more than 20% of beams and some columns are in the extreme damage state. Retrofitting of the building may be required depending on the number and distribution of members in the extreme damage state.
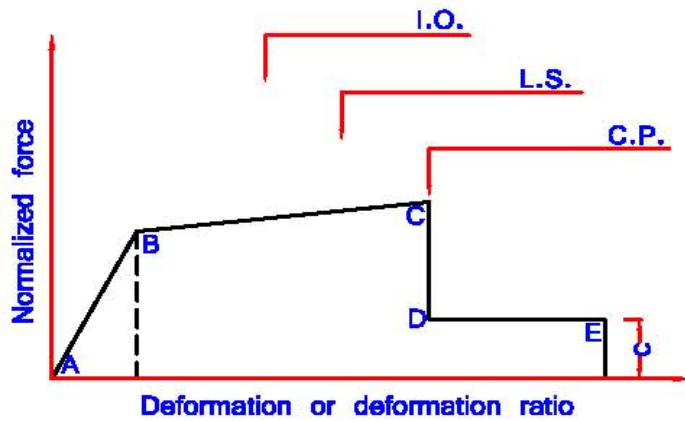
Acceptance criteria state CP in any story, Occupancy of the building should not be permitted. Decision on retrofitting or demolishing of the building depends on the feasibility of retrofitting. If the building fails to satisfy any of the above performance levels, it is accepted as in the collapse state.
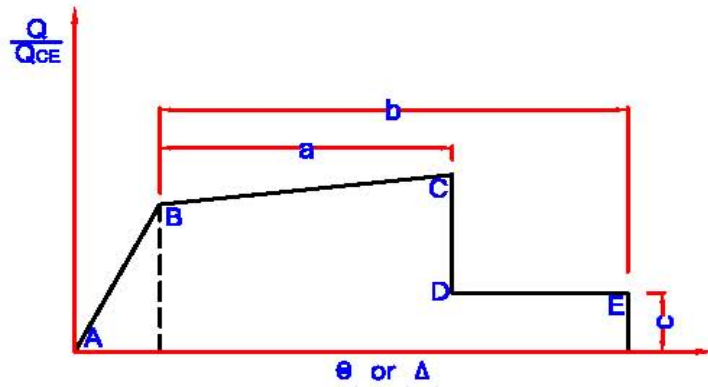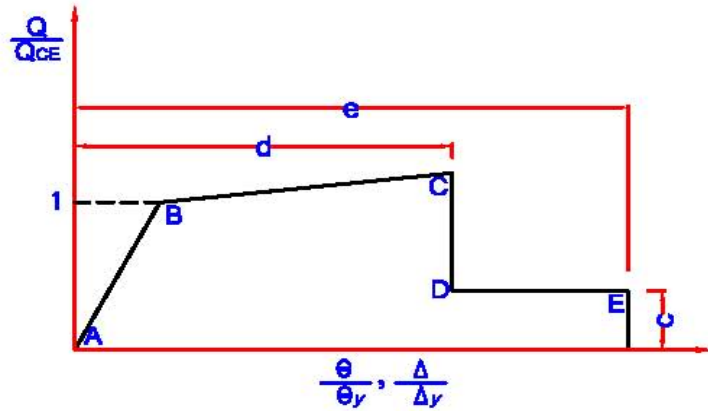
Figure (3.11): Definition of the ( a,b,c,d,e ) Parameters, and the Generalized Load-Deformation Behavior

Table (3.6): Modeling Parameters and acceptance Criteria for Nonlinear Procedure- Braced Frames (FEMA-273 from Table 5-8)

| Component/Action | $\frac{\Delta}{\Delta_y}$ | | Residual Strength Ratioo | Plastic Rotation, Deformation Limits Primary | | |
|---|---|---|---|---|---|---|
| | $d$ | $e$ | $c$ | IO | LS | CP |
| beams[1]: | | | | | | |
| a. $\frac{b}{2tf} < \frac{52}{\sqrt{F_{ye}}} = 7.354$ | 10 | 12 | 0.6 | 2 | 7 | 9 |
| b. $\frac{b}{2tf} > \frac{95}{\sqrt{F_{ye}}} = 13.435$ | 5 | 7 | 0.2 | 1 | 3 | 4 |
| c. For $\frac{52}{\sqrt{F_{ye}}} \leq \frac{b}{2tf} \leq \frac{95}{\sqrt{F_{ye}}}$ use linear interpolation | 9.387 | 11.387 | 0.551 | 1.877 | 6.51 | 8.387 |

Table (3.7): Modeling Parameters and acceptance Criteria for Nonlinear Procedures- Fully Restrained (FR) Moment Frames (FEMA-273 from Table 5-8)

| Component/Action | $\frac{\Delta}{\Delta_y}$ | | Residual Strength Ratioo | Plastic Rotation, Deformation Limits Primary | | |
|---|---|---|---|---|---|---|
| | $d$ | $e$ | $c$ | IO | LS | CP |
| a. $\frac{2M_{CE}}{eV_{CE}} \leq 1.6$ | 16 | 18 | 0.80 | 1.5 | 12 | 15 |
| b. $\frac{2M_{CE}}{eV_{CE}} \geq 2.6$ | Same as for beam in FR moment frame (see table 5-4) | | | | | |
| c. $1.6 \leq \frac{2M_{CE}}{eV_{CE}} \leq 2.6$ | Use linear interpolation | | | | | |

## 3.4. Nonlinear Static Procedure Analysis Using SAP2000

Nonlinear static procedure analysis (NSPA), known as pushover analysis is a method used to locate plastic hinge due to lateral force (seismic load). There are number of software packages used to determine inelastic behavior in structures. Such as SAP2000, wFRAME, DRAIN-2DX, ADNINA, and SC-push 3D. SAP2000 was used in this study. Moreover, it has built in default plastic hinge property for building structure based on FEMA 273 recommendations; also the load patterns are easy to create.

## 3.4.1. Overview of SAP2000 Model

The NSPA procedure defined earlier in this section can be broken down into the following steps:

(1) Creating the basic computer model.

(2) Defining section properties, W16x36 is chosen for both beams and columns, while Tube 8x8x0.5 is used for braced elements.

(3) Define properties and acceptance criteria for the pushover hinges, the following modeling parameters and acceptance criteria (d, e, c) and (IO, LS, CP) for NSPA is used to define shear plastic hinge or moment plastic hinge depending on link length.

It might be worth mentioning at this junction that if the short link in EBF is used, then the hinge in use is shear plastic hinge (shear force is the dominant in the link). On the other hand, if a long link in EBF is used, the hinge is considered moment plastic hinge. It is important to note that any effect of axial force is small and it will be neglected.

(4) Define the pushover cases. The first case is the gravity static nonlinear load in this study; the gravity load was started from zero as initial condition. Note that load application control for NSPA gravity load was chosen to be full load, and the results saved took into account the final state only.

The second case is lateral load. It was continued from the end of nonlinear case gravity load. Note that the load application control for lateral load is displacement control. Displacement control was used in order to find the formation of plastic hinges. Moreover, since the magnitude of the applied lateral load is not known in advance, displacement control was chosen in this study, the pushover load was defined as displacement control. The structure was pushed to a pre-specified displacement. Since the displacement component is monotonically increasing during loading, conjugate displacement was used.

### 3.4.2. Formation of Plastic Hinges and Mechanisms

When bending moment is applied to any structural element, it will gradually increase until the element reaches plastic limit. The moment in this case is called plastic moment ($M_p$). Plastic moment will result in plastic behavior. A plastic hinge is a type of energy damping device allowing rotation (deformation). Plastic hinge formation occurs due to plastic moments, hinges are usually situated:

(1) Under concentrated load.

(2) At location of no shear force under distributed load.

(3) At joints connecting different elements together.

(4) At fixed support.

Formation of plastic hinges redistributes the moments in a sequential manner until moments at critical sections reach plastic moment value.

There are number of mechanisms dealing with plastic hinge formation:

(1) Independent Mechanism

The independent mechanism is denoted as a structure failure technique through which numbers of plastic hinges are formed under a limited or a combination load applied in the same direction.

(a) Beam mechanism

This mechanism is generated in frame element whether they are vertical, horizontal or inclined under concentrated or uniform loads.

(b) Sway mechanism

This mechanism is generated in frame elements. The motion in this mechanism is due to side sway.

(c) Joint mechanism

This mechanism is generated at the junction of three or more elements. The joint rotates because lateral displacement generate by external loads.

(2) Combined Mechanism

This is a combination of two or more of the variants of the independent mechanism. Figure (3.12) is shown below displays the different types of mechanism.

**(a) BEAM MECHANISMS**

**(b) PANAL MECHANISMS**

**(C) JOINT MECHANISM**

**INDEPENDENT MECHANISMS**

**PARTIAL MECHANISM**

**(d) COMPLETE MECHANISM**

**COMBINED MECHANISMS**
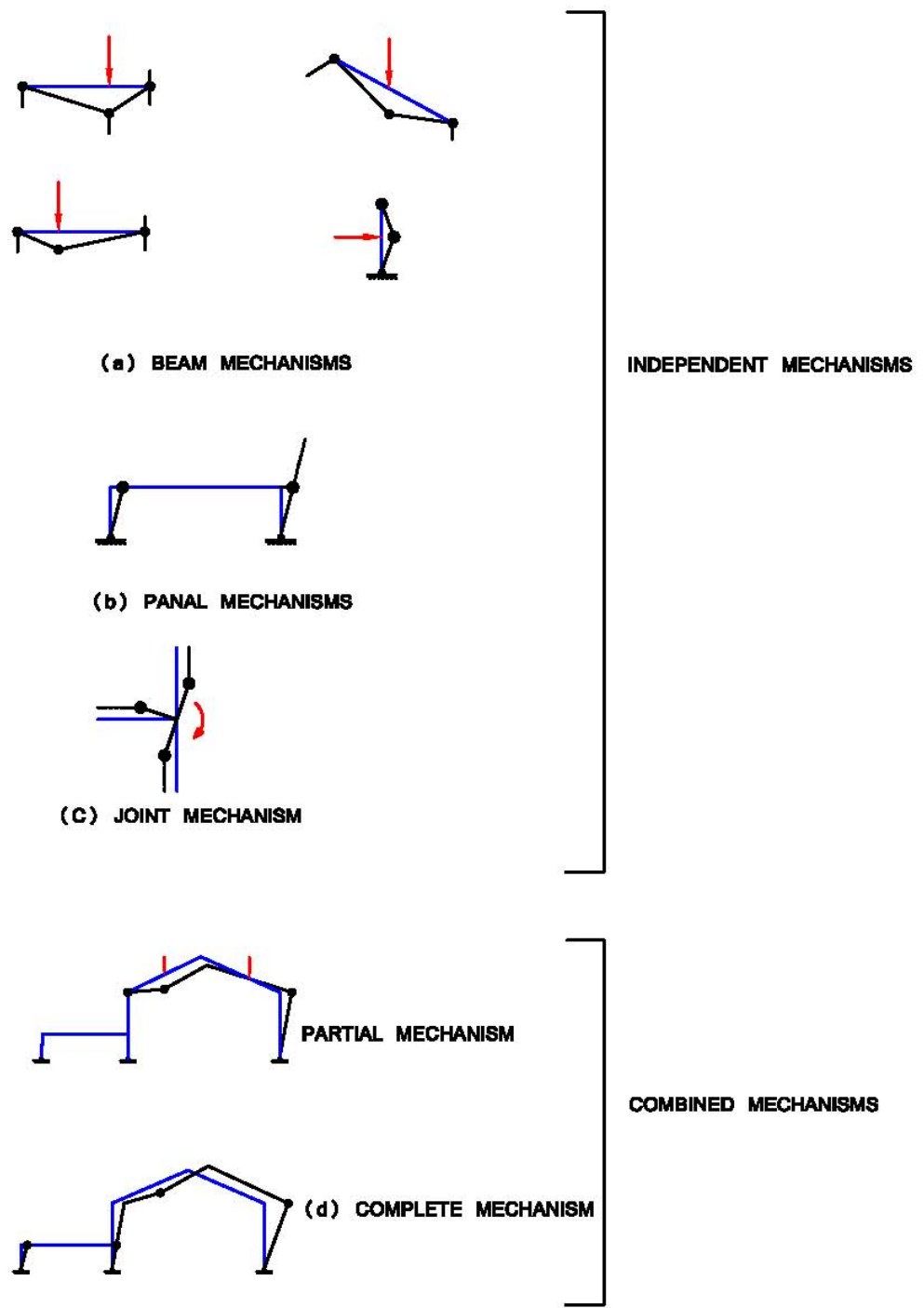
Figure (3.12): Types of Mechanisms

## 3.5. Shear Hinge of Short Link

## 3.5.1. Plastic Hinge Formation for K-Braced Type

The nonlinear pushover analysis of two story eccentrically braced planar frame K type is shown in Figure (3.13). Note that the plastic hinges have only formed in the link. In step 1, yield occurred in the first floor link element no. 12 only. Step 2, yield occurred in the second floor with IO in the first floor link. In step 3 no changes occur. Step 4 shows that the link element 12 in the first floor reach the ultimate capacity state while the second floor link has remained IO. Total failure in the first floor link occurred in step 5. However, the second floor link is still in the IO state. The steps will continue until the total failure in both links occurs as shown in step 10.

The forming of a plastic hinge, in the first floor link preceding the formation of such a hinge in the second floor link is due to shear and moment being applied to the first floor link being higher than those applied to the second floor link. It is clear that the plastic hinge only formed in the link itself rather than in the beams, bracing and columns outside the link. It should be taken into consideration that all joints used in this model were defined as shear hinge joints.
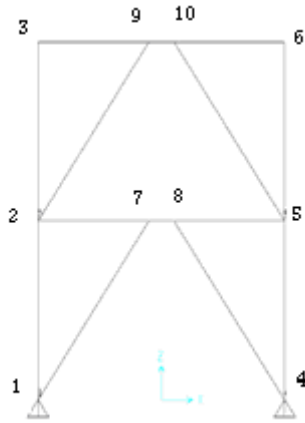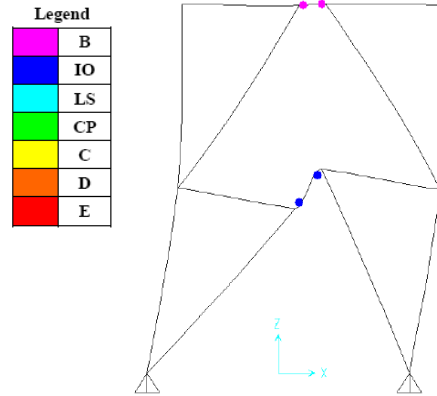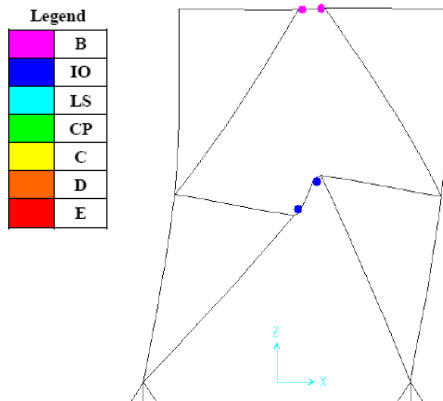
(Figure 3.13a): Joints Labels
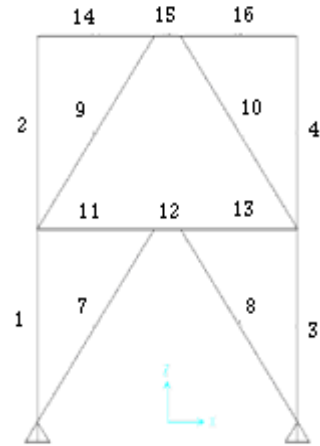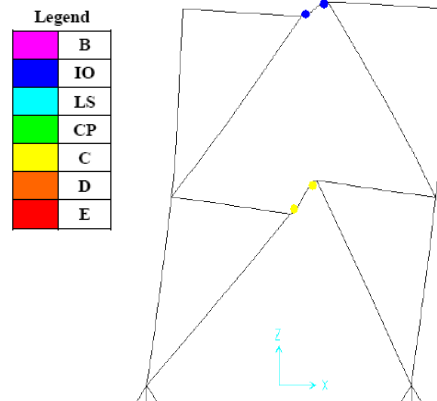


(Figure 3.13b): Elements Labels
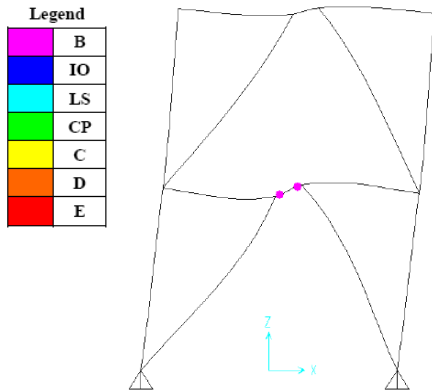


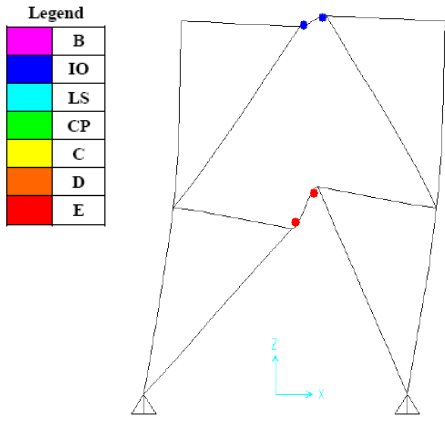(Figure 3.13c): Step(1)Yield (B)
at Joints (7,8)



(Figure 3.13d): Step(2) Acceptance
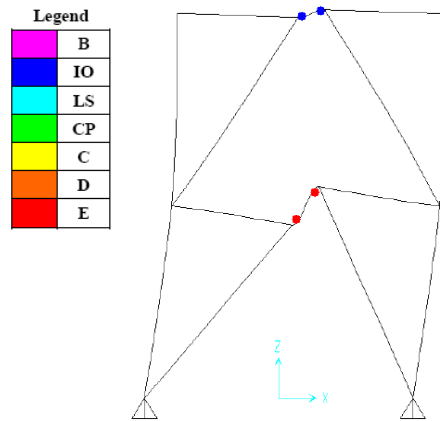Criteria (IO) at Joints (7,8) and Yield
at Joints (9,10)



(Figure 3.13e): Step(3) Acceptance
Criteria (LS) at Joints (7,8) and
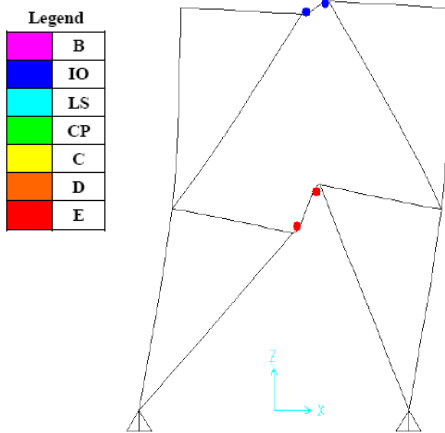Acceptance Criteria (IO) at Joints (9,10)



(Figure 3.13f): Step(4) Ultimate
Capacity (C) at Joints (7,8) and
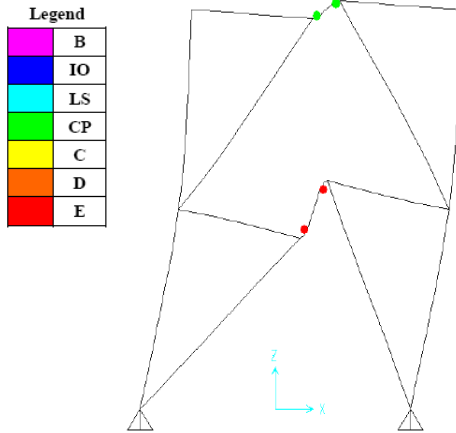Acceptance Criteria (IO) at Joints (9,10)

(Figure 3.13g): Step(5) Total
Failure (E) at Joints (7,8) and
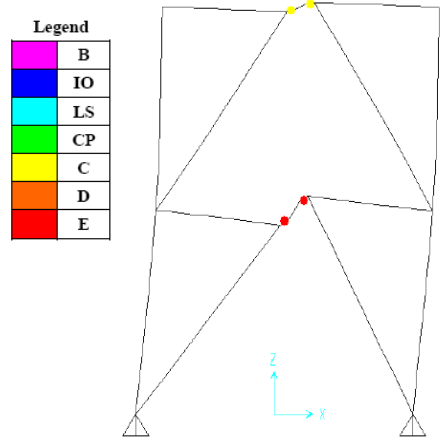Acceptance Criteria (IO)
at Joints (9,10)



(Figure 3.13h): Step(6) Total
Failure (E) at Joints (7,8) and
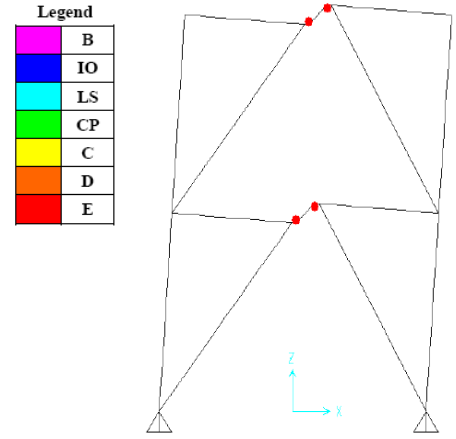Acceptance Criteria (IO)
at Joints (9,10)



(Figure 3.13i): Step(7) Total
Failure (E) at Joints (7,8) and
Acceptance Criteria (IO)
at Joints (9,10)



(Figure 3.13j): Step(8) Total
Failure (E) at Joints (7,8) and
Acceptance Criteria (CP)
at Joints (9,10)



(Figure 3.13k): Step(9) Total
Failure (E) at Joints (7,8)
and Ultimate Capacity (C)
at Joints (9,10)



(Figure 3.13l): Step(10) Total
Failure (E) at Joints (7,8)
and Joints (9,10)

Figure (3.13): Plastic Hinge Formation for K-braced Type Short Link

The SAP 2000 result gives the plastic deformation and the shear force for different stages and for various bracing types; they are shown in Table (3.8), (3.9), and (3.10). Table (3.8) Shows Plastic Deformation and the Shear Force $V_2$ in K-Braced type.

Table (3.8): Short Link 12H1 (FH1) in K-Braced

| Case | Deformation (mm) | Shear Force V2 (kN) |
|---|---|---|
| Yield | 6.6 | 630 |
| Ultimate | 138 | 944 |
| Failure | 223 | 0 |

### 3.5.2. Plastic Hinge Formation for D-Braced Type

The sequence which took place in this process is quite close to that which occurs when using K-braced type short link. It should be mentioned that the same modeling parameters and acceptance criteria are used for different bracing configurations for a specified type of hinge (shear hinge). Figure (3.14) refers to steps of (NLPA) which show the formation of plastic hinge for D-braced short link. Table (3.9) Shows Plastic Deformation and the Shear Force $V_2$ in D-Braced Type.
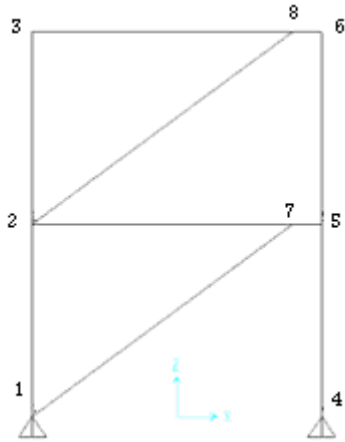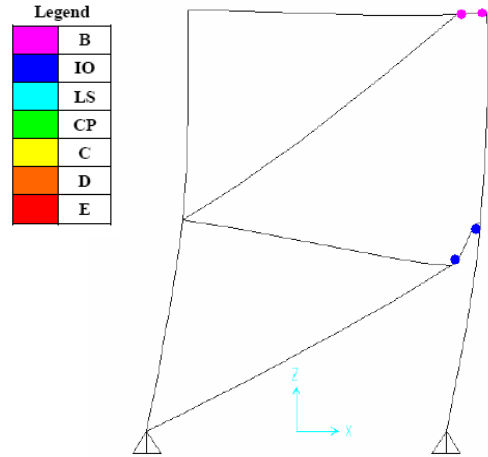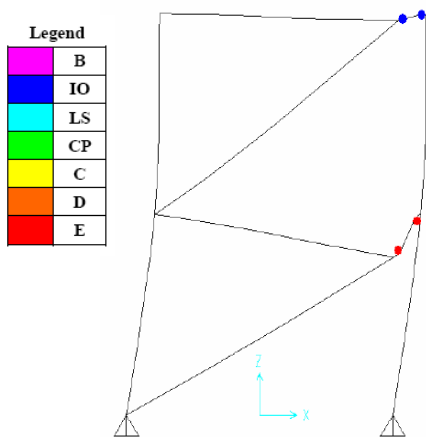
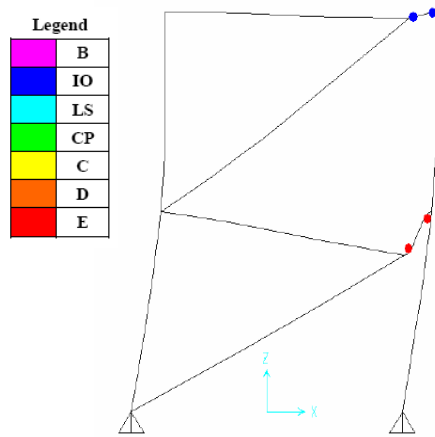(Figure 3.14a): Joints Labels
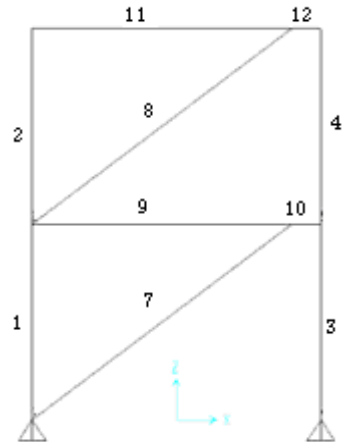


(Figure 3.14b): Elements Labels
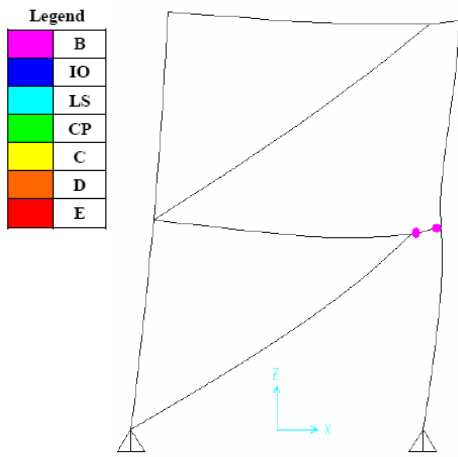


(Figure 3.14c): Step(1)Yield (B)
at Joints (5,7)



(Figure 3.14d): Step(2) Acceptance
Criteria (IO) at Joints (5,7)
and Yield at Joints (6,8)



(Figure 3.14g): Step(5) Total
Failure (E) at Joints (5,7)
and Acceptance Criteria (IO)



(Figure 3.14h): Step(6) Total
Failure (E) at Joints (5,7)
and Acceptance Criteria (IO)

at Joints (6,8)



(Figure 3.14i): Step(7) Total
Failure (E) at Joints (5,7)
and Acceptance Criteria (IO)
at Joints (6,8)

at Joints (6,8)



(Figure 3.14j): Step(8) Total
Failure (E) at Joints (5,7)
and Acceptance Criteria (LS)
at Joints (6,8)



(Figure 3.14k): Step(9) Total
Failure (E) at Joints (5,7)
and Ultimate Capacity (C) at Joints (6,8)



(Figure 3.14l): Step(10) Total
Failure (E) at Joints (5,7)
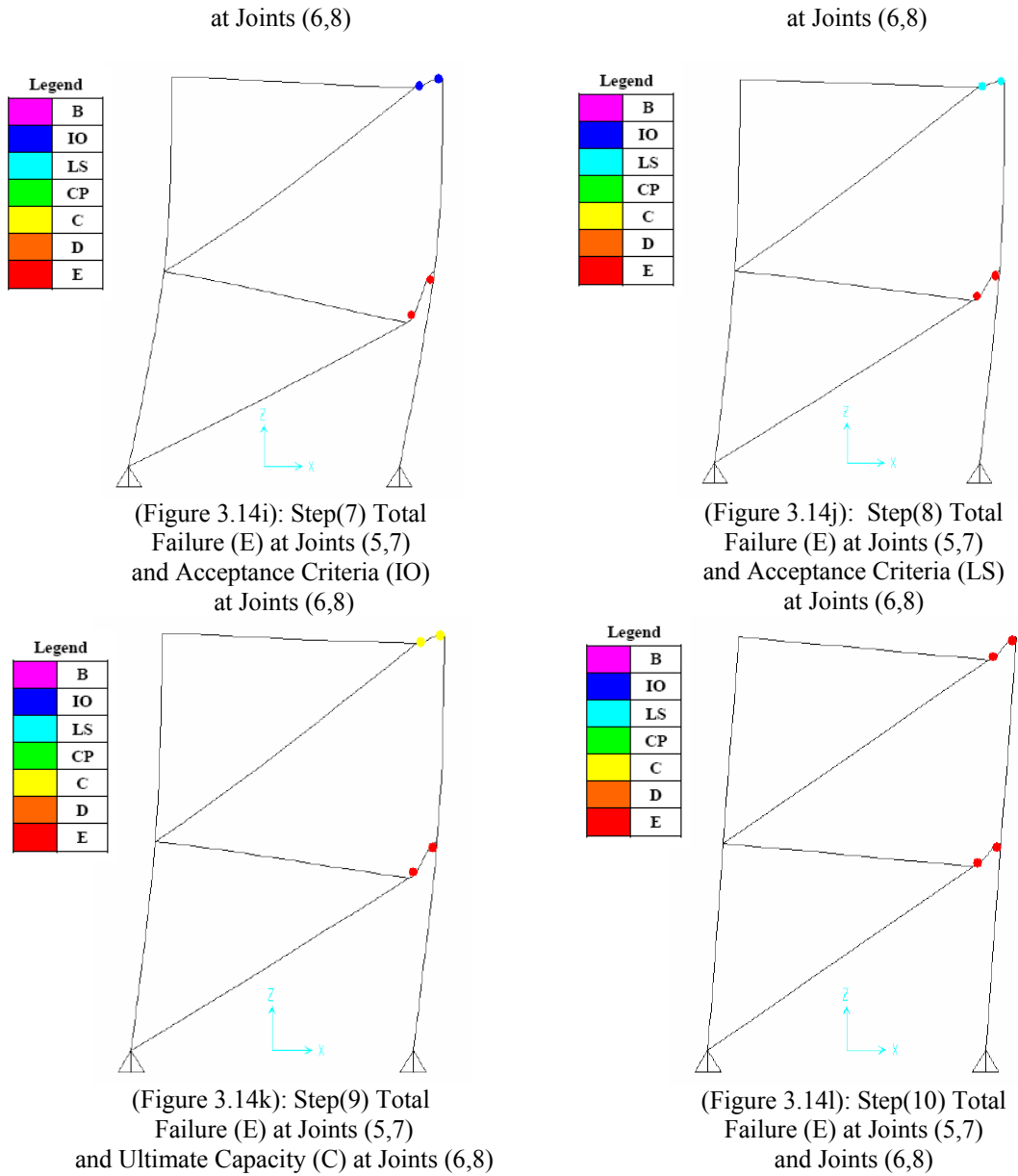and Joints (6,8)

Figure (3.14): Plastic Hinge Formation for D-braced Type Short Link

Table (3.9) :Short Link 10H1 (FH1) in D-Braced

| Case | Deformation (mm) | Shear Force V2 (kN) |
|---|---|---|
| Yield | 9.3 | 630 |
| Ultimate | 145 | 944 |
| Failure | 223 | 0 |

### 3.5.3. Plastic Hinge Formation for V-Braced Type

The sequence which took place in this case is quite close to that which occurs when using previous types of short link. Figure (3.15) refers to steps of (NLPA) of V-braced short link. Table (3.10) Shows Plastic Deformation and the Shear Force $V_2$ in V-Braced Type.
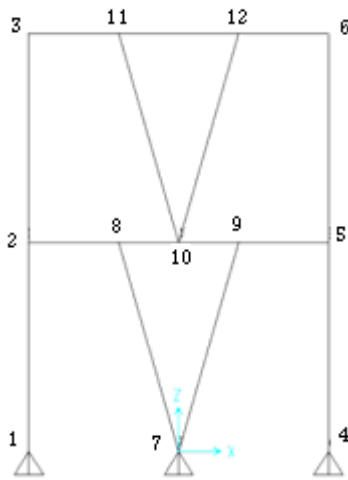


(Figure 3.15a): Joints Labels
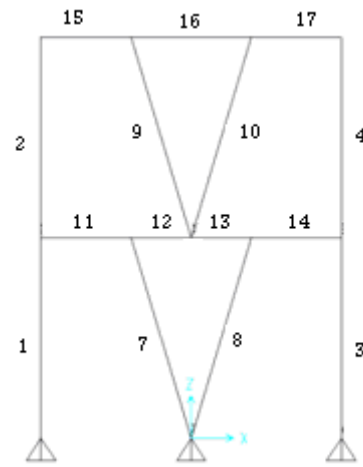


(Figure 3.15b): Elements Labels
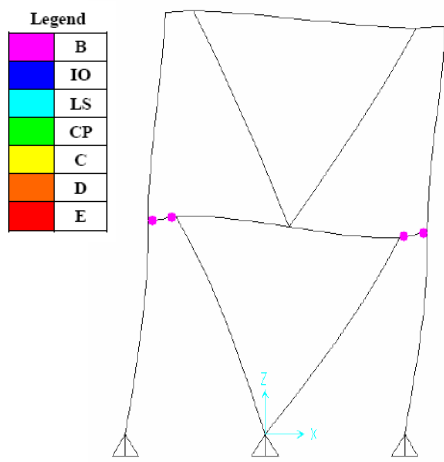


(Figure 3.15c): Step(1)Yield (B) at Joints (2,8) and (5,9)



(Figure 3.15d): Step(2) Acceptance Criteria (IO) at Joints (2,8) and (5,9)
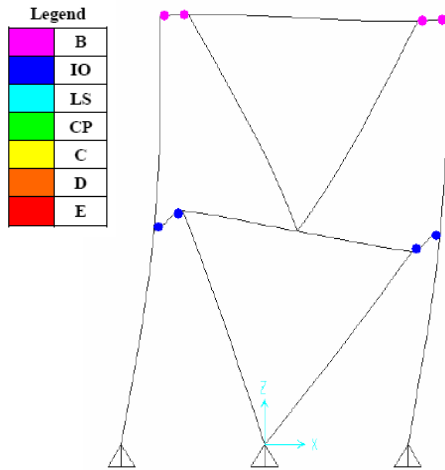
(Figure 3.15e): Step(3) Acceptance Criteria (IO) at Joints (2,8) and (5,9), Yield (B) at Joints (3,11) and (6,12)
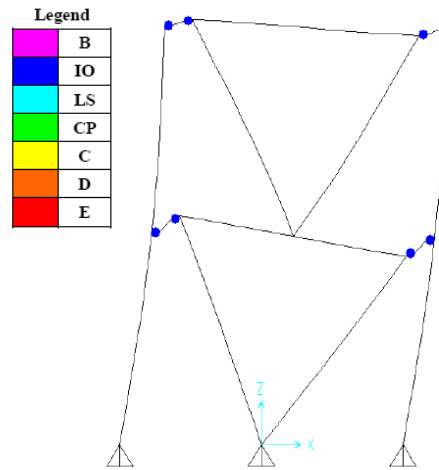


(Figure 3.15f): Step(4) Acceptance Criteria (IO) at Joints (2,8), (5,9), (3,11) and (6,12)



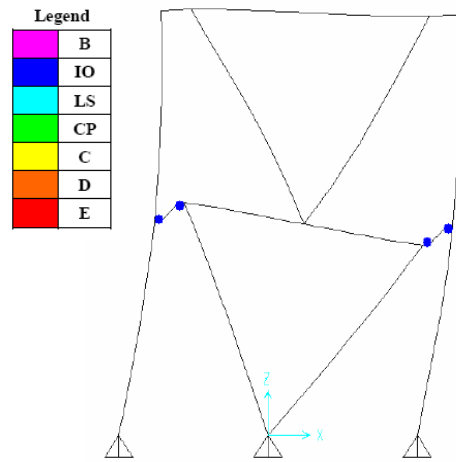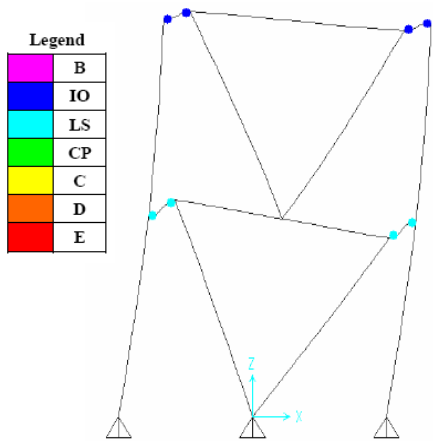(Figure 3.15g): Step(5) Acceptance Criteria (LS) at Joints (2,8) and (5,9), Acceptance Criteria (IO) at Joints (3,11) and (6,12)
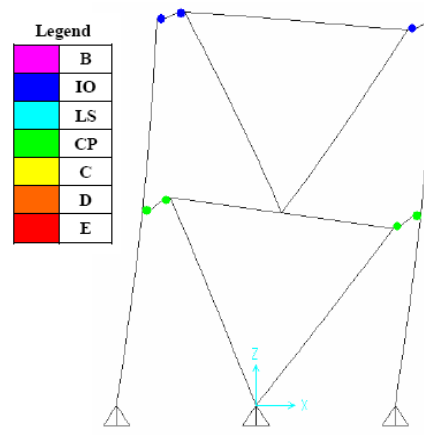


(Figure 3.15h): Step(6) Acceptance Criteria (CP) at Joints (2,8) and (5,9), Acceptance Criteria (IO) at Joints (3,11) and (6,12)
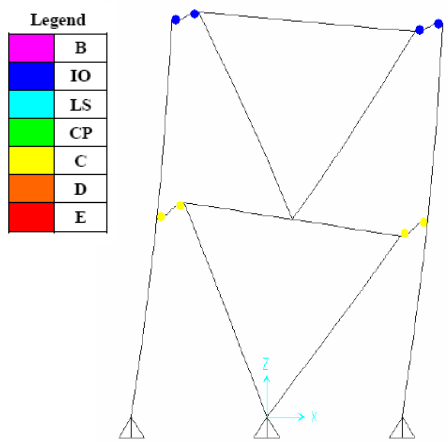


(Figure 3.15i): Step(7) Ultimate Capacity (C) at Joints (2,8) and (5,9), Acceptance Criteria (IO) at Joints (3,11) and (6,12)
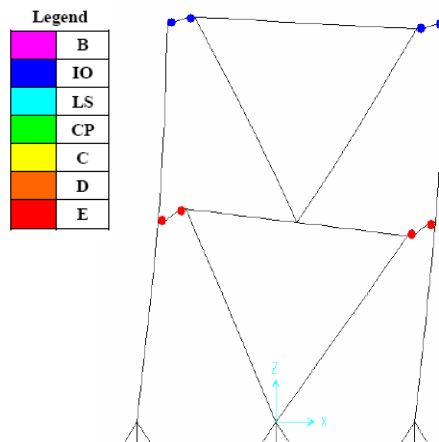


(Figure 3.15j): Step(8) Total Failure (E) at Joints (2,8) and (5,9), Acceptance Criteria (IO) at Joints (3,11) and (6,12)
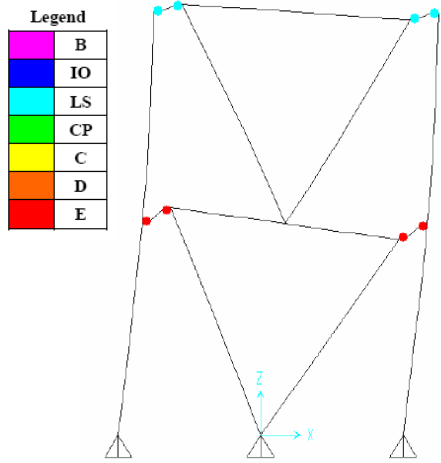
(Figure 3.15k): Step(9) Total Failure (E) at Joints (2,8) and (5,9), Acceptance Criteria (LS) at Joints (3,11) and (6,12)
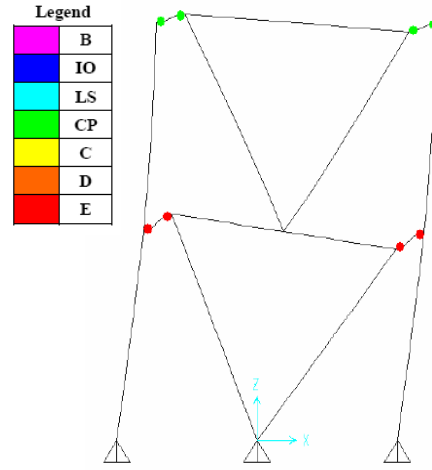


(Figure 3.15l): Step(10) Total Failure (E) at Joints (2,8) and (5,9), Acceptance Criteria (CP) at Joints (3,11) and (6,12)
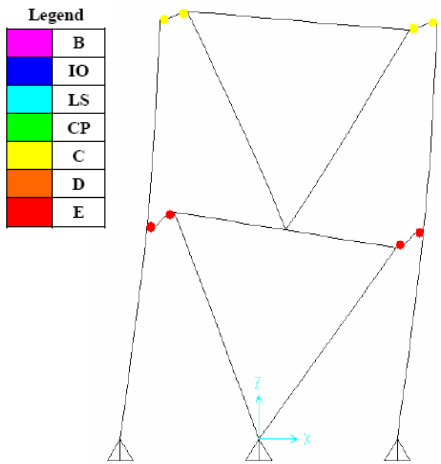


(Figure 3.15m): Step(11) Total Failure (E) at Joints (2,8) and (5,9), Ultimate Capacity (C) at Joints (3,11) and (6,12)
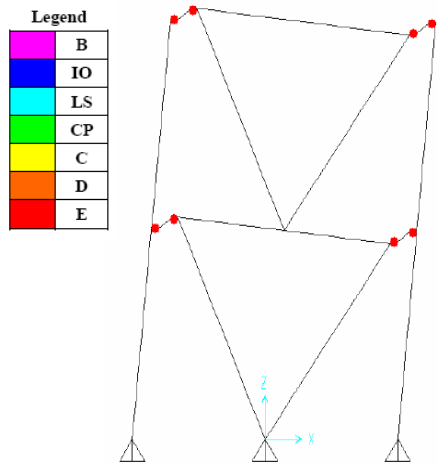


(Figure 3.15n): Step(12) Total Failure (E) at Joints (2,8), (5,9), (3,11) and (6,12)

Figure (3.15): Plastic Hinge Formation for V-braced Type Short link

Table (3.10) :Short Link 11H1 (FH1) in V-Braced

| Case | Deformation (mm) | Shear Force V2 (kN) |
|---|---|---|
| Yield | 12.34 | 630 |
| Ultimate | 282 | 944 |
| Failure | 451 | 0 |
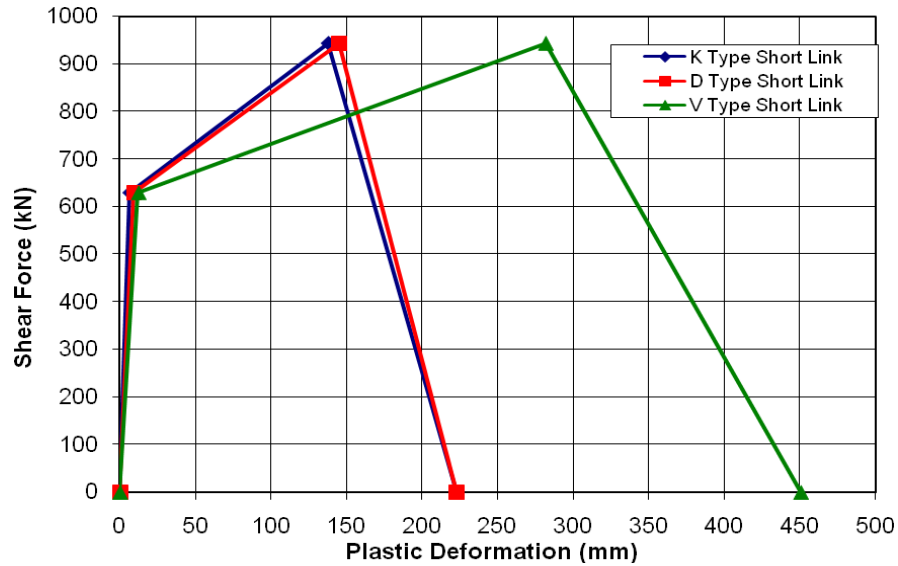
Figure (3.16): Relationship between Plastic Deformation (mm) with Shear Force V2 (kN) for Three Type EBF Short Link

## 3.6. Moment Hinge of Long Link

The type of hinge induced in long link is flexural hinge, because the moment will control, and the long link beam behaves just like a beam in a fully restrained (FR) moment frame. For the purposes of this study the length of link is equal to 1800 mm ($3M_p/V_p$), in order to be assured that flexural yielding dominates the link behavior.

The total failure (point E from the plastic deformation curve) will be at the first floor only when long link is used, also the plastic deformation is formed not only in the link, but also in the joint connecting bracing and column. On the other hand, when short link is used the total failure will be at the two floors, and the plastic deformation happens in the link only, the Figures (3.17), (3.18), and (3.19) illustrate the plastic hinge formation.

Before reaching point B, the deformation, which is linear, will be at the frame element, beyond the point B, the plastic deformation will be in the hinge, in addition to the elastic deformation.

It is worthwhile to mention, that at total failure deformation in the long link case, the story drifts in the first, and the second floors are almost the same, thus the second story is approximately rigid, and the first story behaves nearly as soft story, the essential problem in soft story that total lateral deformation is concentrated at this story, instead of distribution it uniformly on all stories.

### 3.6.1. Moment Hinge for K-Braced Long Link

As shown in the Figure (7.17), it is noted that total failure deformation occurs at the long link end joints (7, 8) within the first floor, also the total failure deformation occurs at the joints connecting bracing and column joints (2, 5) . Moreover, the joint mechanism is not completed at joints 2, and 5 since the beam outside the link, and the lower column does not experience total failure deformation. Step 3 in Figure (3.17) shows the locations where the total failure mechanism occurs.

Table (3.11) shows moment-rotation relationship for K-braced long link, it is noted that yield rotation $\theta_y$ equals to 0.00293 rad.
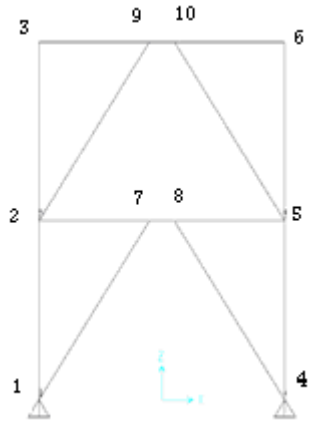
(Figure 3.17a): Joints Labels
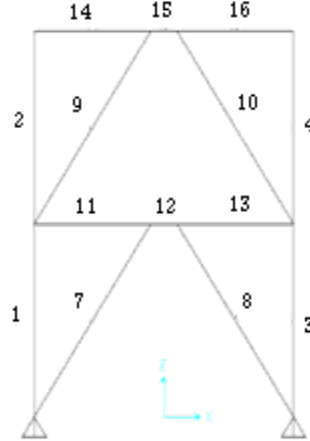


(Figure 3.17b): Elements Labels
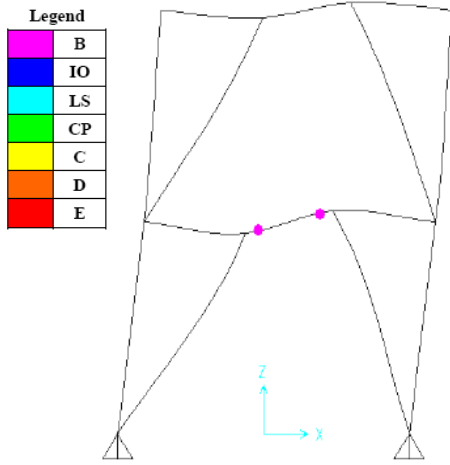


(Figure 3.17c): Step(1)Yield (B)
at Joints (7,8)
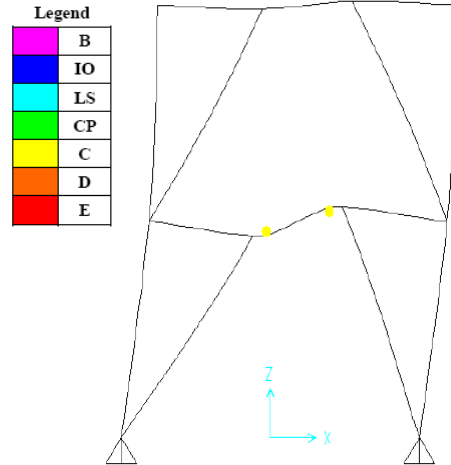


(Figure 3.17d): Step(2) Ultimate Capacity (C)
at Joints (7,8)
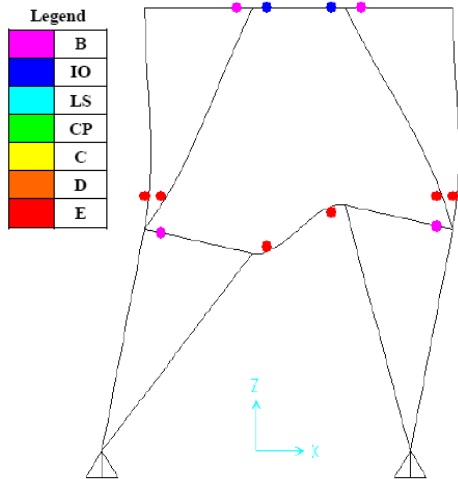


(Figure 3.17e): Step(3) Total Failure
at Joints (2,5,7,8)

Figure (3.17): Plastic Hinge Formation for K-braced Type Long Link

Table (3.11 ) :Moment-Rotation Relationship for K-Braced Long Link 12H1

| Step | State | Rotation $R_2,\theta\%$ (rad.) | Moment Link ,M (kN-m) |
|------|-------|-------------------------------|------------------------|
| 0 | Initial | 0 | 0 |
| 1 | Yield | 0.293 | 396.5 |
| 2 | Ultimate | 0.624 | 449 |
| 3 | Total Failure | 258.68 | 0 |

## 3.6.2. Moment Hinge for D-Braced Long Link

D-braced long link analysis shows that yield deformation is formed firstly at joint 5 which is the end of link attached to column, then yield deformation is formed at the other end of the link, at joint 7, next ultimate deformation is at both ends of the link simultaneously as shown in Figure (3.18). Finally, total failure deformation (joint mechanism) occurs at the link attached to column. It is worthwhile to mention that the rotation is inelastic, and the failure is complete, and sudden in this system, so this system is not adequate in severe seismic environment. Table (3.12) clears the formation steps of plastic hinge, and moment-rotation in each step.

It should be noted that plastic hinge is not formed in the second floor; the second floor story motion behaves approximately like rigid body.



(Figure 3.18a): Joints Labels          (Figure 3.18b): Elements Labels
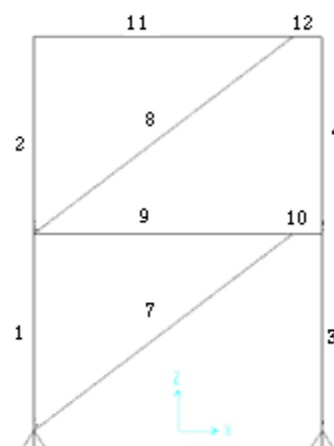
(Figure 3.18c): Step(1)Yield (B) at Joint (5)



(Figure 3.18d): Step(2) Yield (B) at Joint (5,7)



(Figure 3.18e): Step(3) Acceptance Criteria (CP) at Joint (7), Ultimate Capacity (C) at Joint (5)



(Figure 3.18f): Step(4) Ultimate Capacity (C) at Joints (5,7),



(Figure 3.18g): Step(5) Total Failure (E) at Joints (2,5,7)
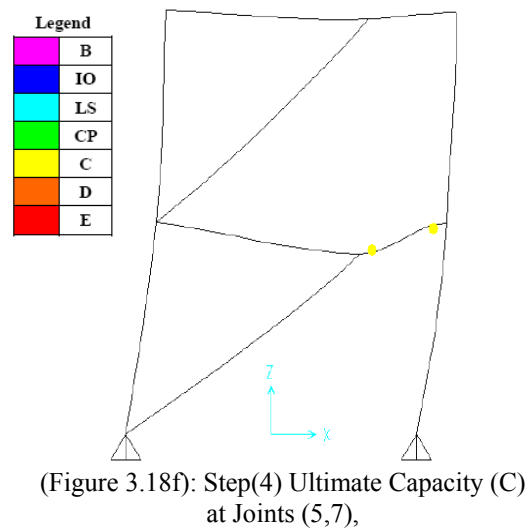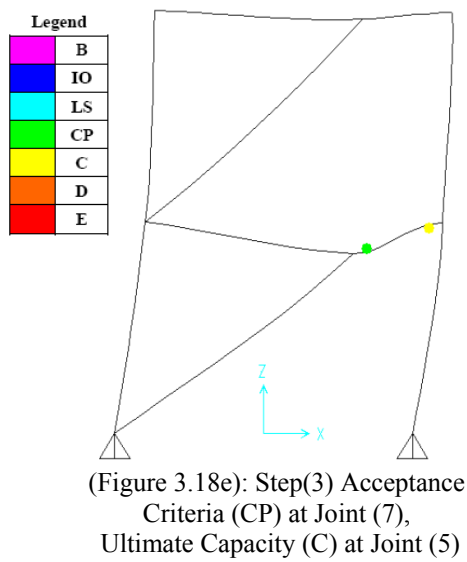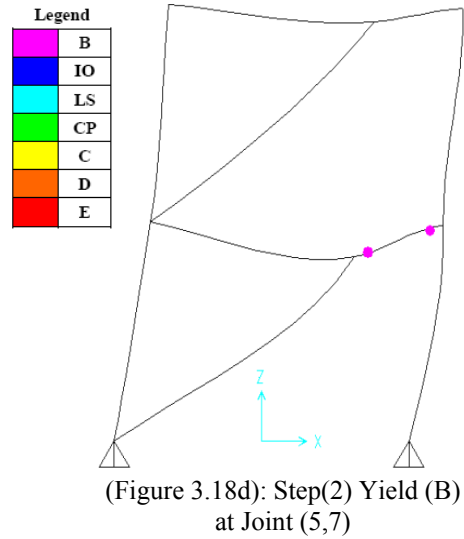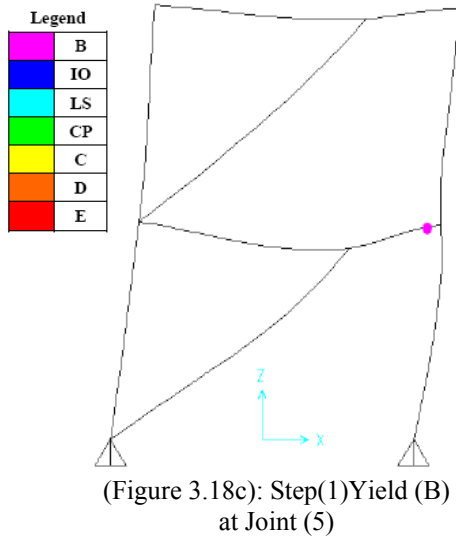
Figure (3.18): Plastic Hinge Formation for D-braced Type Long Link

Table (3.12 ) :Moment-Rotation Relationship for D-Braced Long Link 10H1

| Step | State | Rotation $R_2, \theta$% (rad.) | Moment Link ,M (kN-m) |
|------|-------|-------|-------|
| 0 | Initial | 0 | 0 |
| 1 | One End Yield | 0.214 | 307 |
| 2 | Both End Yield | 0.101 | 398 |
| 3 | One End Ultimate | 0.424 | 449 |
| 4 | Both End Ultimate | 0.441 | 450 |
| 5 | Failure | 168.154 | 0 |

### 3.6.3. Moment Hinge for V-Braced Long Link

Yield deformation is formed firstly at the link end joints (8, 9) in first floor, the yield deformation $\theta_y$ at this step is 0.182% rad. next it is formed at the other end of link attached to column joints (2, 5), then ultimate deformation is formed at joints (8, 9), after that yield deformation is formed at the ends of the segment outside the link in the second floor joints (11, 12), at step 5 ultimate deformation is formed in link ends at first floor. Finally, failure mechanism happens, as shown in Figure (3.19), Table (3.13) illustrates the relation between moment, and rotation. It is worthwhile to mention that no yield deformation is formed at the link in the second floor, and second floor behaves like rigid body.
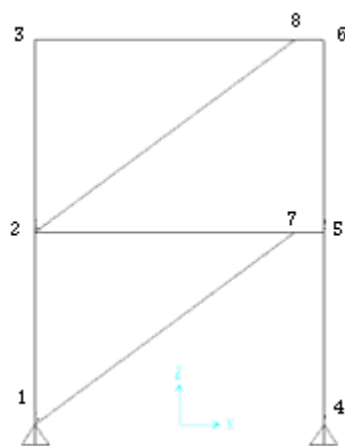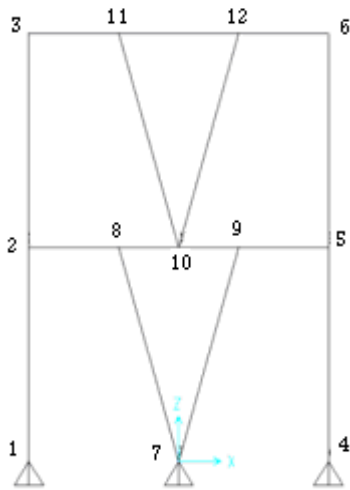
(Figure 3.19a): Joints Labels
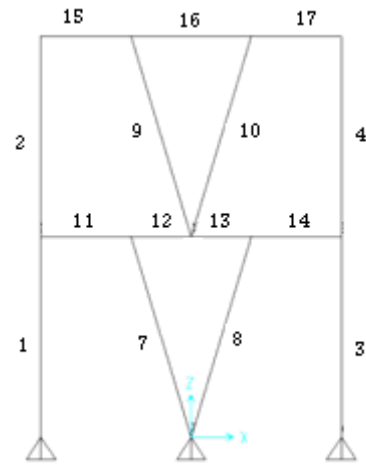


(Figure 3.19b): Elements Labels
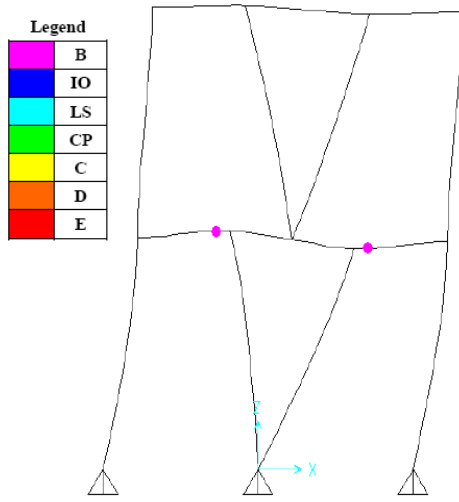


(Figure 3.19c): Step(1)Yield (B)
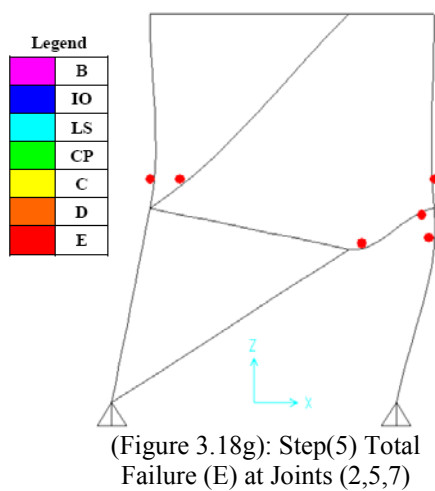at Joints (8,9)
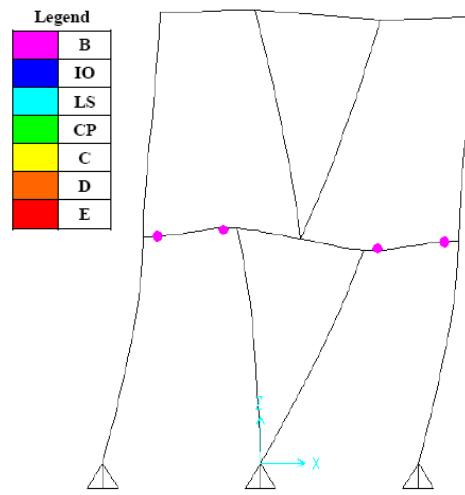


(Figure 3.19d): Step(2) Yield (B)
at Joints (2,5,8,9)
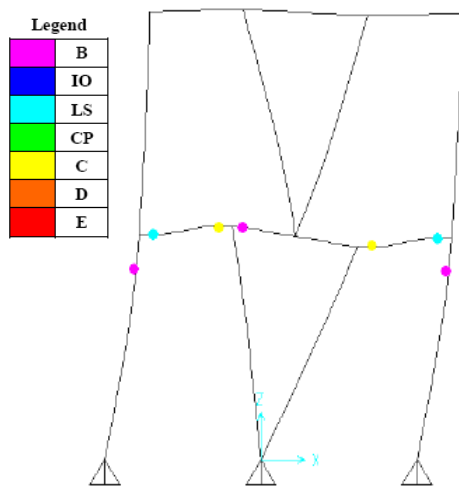


(Figure 3.19e): Step(3)
Ultimate Capacity (C) at Joints (8,9)
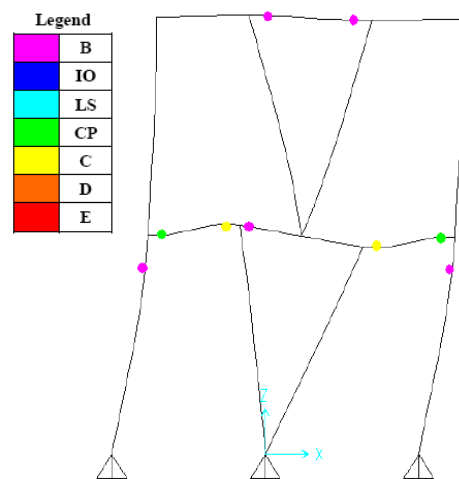


(Figure 3.19f): Step(4) Ultimate Capacity (C)
at Joints (8,9)

(Figure 3.19g): Step(5) Ultimate Capacity at Joints (2,5,8,9)

(Figure 3.19g): Step(5) Total Failure (E) at Joints (2,5,8,9,10)
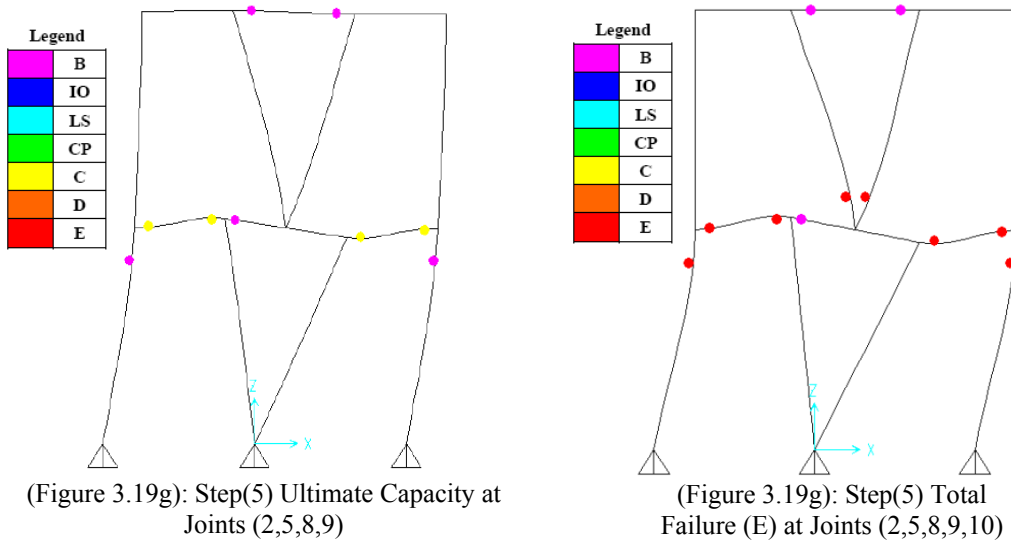
Figure (3.19): Plastic Hinge Formation for V-braced Type Long Link

Table (3.13 ) :Moment-Rotation Relationship for V-Braced Long Link 11H1

| Step | State | Rotation $R_2, \theta \%$ (rad.) | Moment Link ,M (kN-m) |
|------|-------|----------------------------------|------------------------|
| 0 | Initial | 0 | 0 |
| 1 | One End Yield J8 | 0.182 | 398 |
| 2 | Both End Yield | 0.304 | 402 |
| 3 | One End Ultimate J8 | 2.021 | 451 |
| 5 | Both End Ultimate | 3.245 | 408 |
| 6 | Failure | 239.364 | 0 |
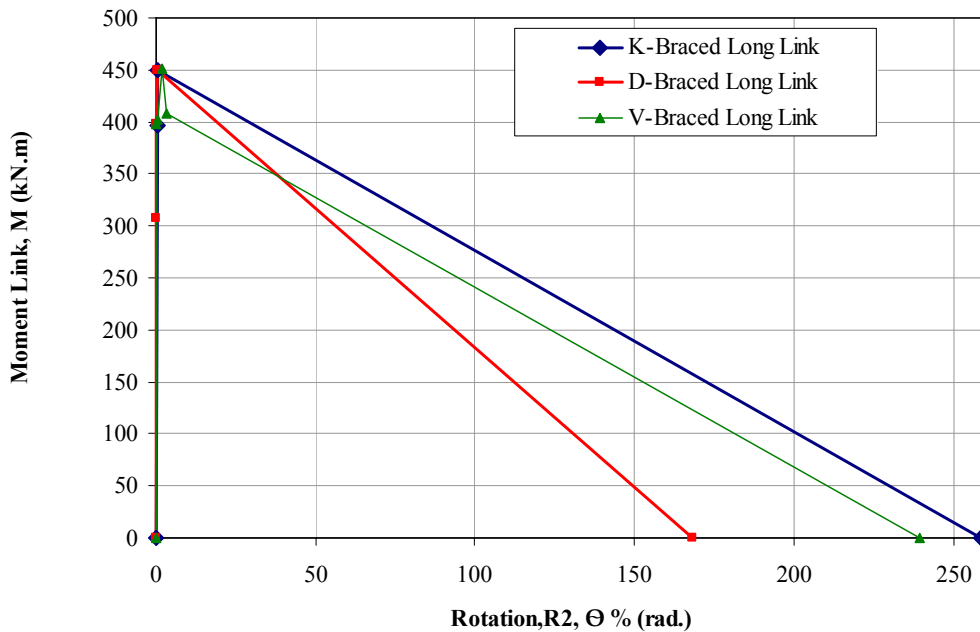


Figure (3.20): Rotation vs. Moment for Long Link (Flexural Hinge)

## 3.7. Plastic Hinge of Intermediate Link

In this type of links, both shear, and flexural yielding will be formed at the same time, as mentioned in Section 3.5, and Section 3.6, the short link accompanied by shear hinge, but for long link the hinge is flexural, analysis is performed for this link based on the exact modeling parameters, FEMA 273 from Table 5-8. At ultimate, and failure states the values for lateral displacement, and rotation based on shear hinge are greater than values based on flexural hinge, so it will be conservative to consider the hinge as a flexural one.

### 3.7.1. Plastic Hinge of K-Braced Intermediate Link

The type of hinge produced is flexural-shear hinge, as mentioned earlier it is conservative to consider the hinge as flexural. Tables (3.14) and Figures (3.21a) & (3.21b) show the relationship between shear force vs. lateral displacement for link (12), and moment vs. rotation consecutively. Finally, total failure deformation state is formed at link (12) in first floor while yield deformation state is formed at link (15) in second floor; also the ends of bracing and columns are formed failure deformation state.

Finally deformation steps are failure collapse at both ends of the link in first floor, yielding state at both ends of the link in second floor as shown in Figure (3.22).

Table (3.14): Intermediate Link (12) K-Braced Type

| state | Lateral Deformation (mm) | Rotation $R_2, \theta$ % (rad.) | Shear Force V2 (kN) | Moment Link, $M_3$ (kN.m) |
|---|---|---|---|---|
| Initial | 0 | 0 | 0 | 0 |
| Yield | 13.5 | 0.425 | 629 | 376 |
| Ultimate | 115 | 2.11 | 749 | 449 |
| Failure | 306 | 7.88 | 0 | 0 |
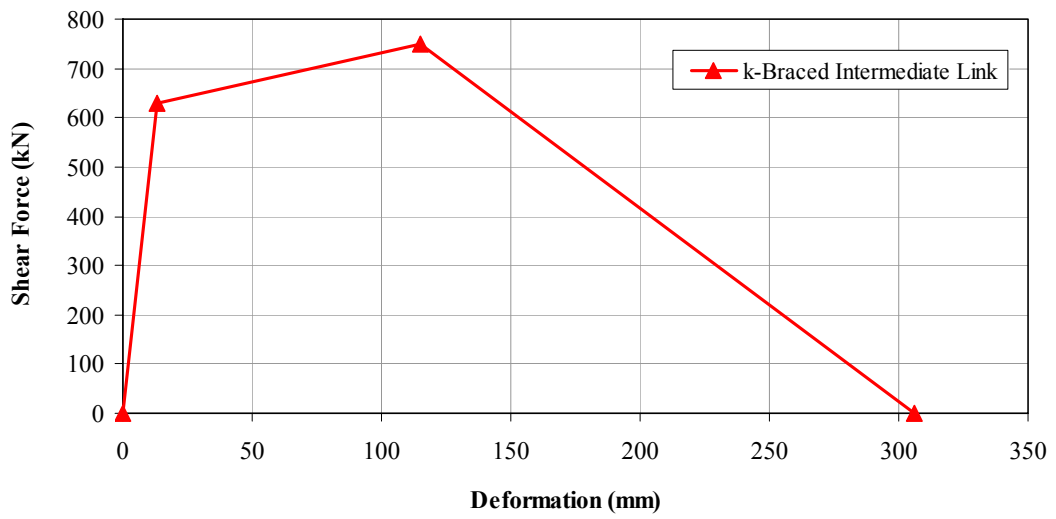
Figure (3.21a): Deformation vs. Shear Force for
K-Braced Intermediate Link (12)
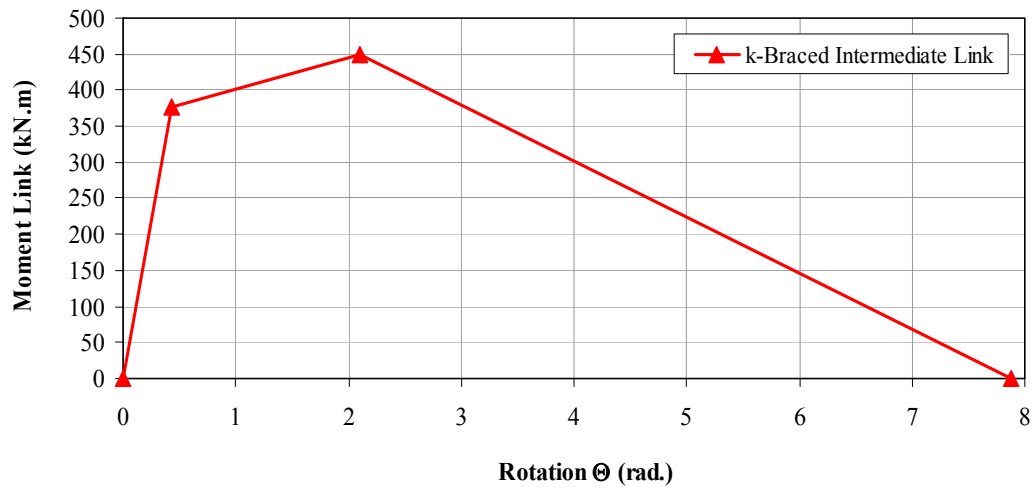


Figure (3.21b): Rotation vs. Moment for
K-Braced Intermediate Link (12)
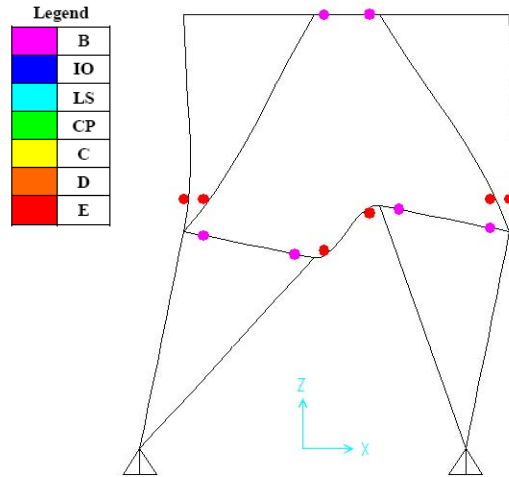
Figure (3.22): Deformed Shape at Final Step
For K-Braced Intermediate Link

### 3.7.2. Plastic Hinge of D-Braced Intermediate Link

For shear-flexural hinge type the first plastic hinge formation is at joint 5 which is the link end attached to column, ultimate deformation state is initially formed at that position, it should be kept in mind that plastic hinge is not formed at second floor story, and at the beam outside the link at first floor story, while columns and bracing have plastic hinge deformation. For shear-flexural hinge the plastic hinge formation in the link and joint mechanism occurred at joint 5, Tables (3.15), Figures (3.22a), and (3.23b) shows the relation between lateral deformation vs. shear force, and rotation vs. moment at link 10, Finally deformation steps are failure collapse as shown in Figure (3.24). It can be noted that for D-braced configuration, the deformation shape at final step is the same for long and intermediate link.

Table (3.15): Intermediate Link (10) D-Braced Type

| state | Lateral Deformation (mm) | Rotation $R2,\theta$ % (rad.) | Shear Force V2 (kN) | Moment Link, $M_3$ (kN.m) |
|---|---|---|---|---|
| Initial | 0 | 0 | 3.2 | 0 |
| Yield | 18.42 | 0.694 | 629 | 349 |
| Ultimate | 115.216 | 1.651 | 740 | 450 |
| Failure | 357 | 9.372 | 0 | 0 |

Figure (3.23a): Deformation vs. Shear Force for
D-Braced Intermediate Link



Figure (3.23b): Rotation vs. Moment for
D-Braced Intermediate Link
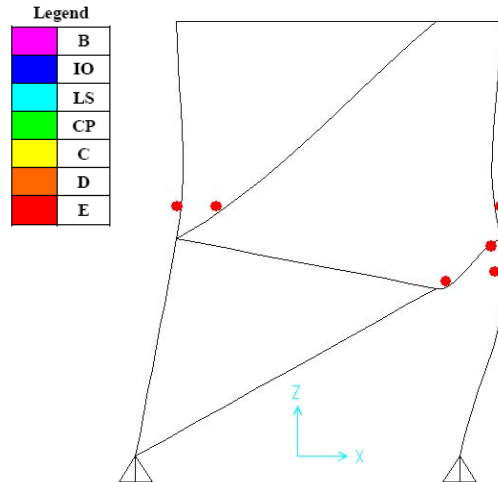
Figure (3.24): Deformed Shape at Final Step
For D-Braced Intermediate Link

### 3.7.3. Plastic Hinge of V-Braced Intermediate Link

At the beginning, yield deformation state is formed in both links (11, 14) in first floor at step 1, successive yield formation is produced in the second floor at the beam outside the links (16), at final state, it is noted that links are reached ultimate deformation state. This system is not desirable, Table (3.16), Figure (3.23a) and Figure (3.23b) show the relation between moment vs. rotation, and shear force vs. lateral deformation.

Initially the first hinge is formed in both links in the first floor, at ultimate final state plastic hinges are formed at the links (11, 14) in first floor specially at joints (8,9), in the second floor the yield state is formed only in the beam outside the links, so fuse is formed in the beam and not in the link, this system is undesirable that should be avoided,

Figure (3.26) shown the final state of analysis, the analysis for intermediate link V-braced type does not converge, and the analysis was not completed. The problem could be numerical related to assumptions made in the SAP program, but the most likely reason is that the model has a plastic hinge that failed or a mechanism has

formed, which cause the computer not to complete the analysis. The problem has been

solved by using command in the SAP2000 (Hinge Overwrite) then convergence occurs

and the analysis was computed.

Table (3.16): Intermediate Link (11) Joint 8 V-Braced Type

| State | Lateral Deformation (mm) | Rotation $R2,\theta$ % (rad.) | Shear Force $V2$ (kN) | Moment Link, $M_3$ (kN.m) |
|---|---|---|---|---|
| Initial | 0 | 0 | 0 | 0 |
| Yield | 25.5 | 0.074 | 630 | 376 |
| Ultimate | 180.5 | 3.758 | 712 | 450 |
| Failure | ---- | ---- | ---- | ---- |
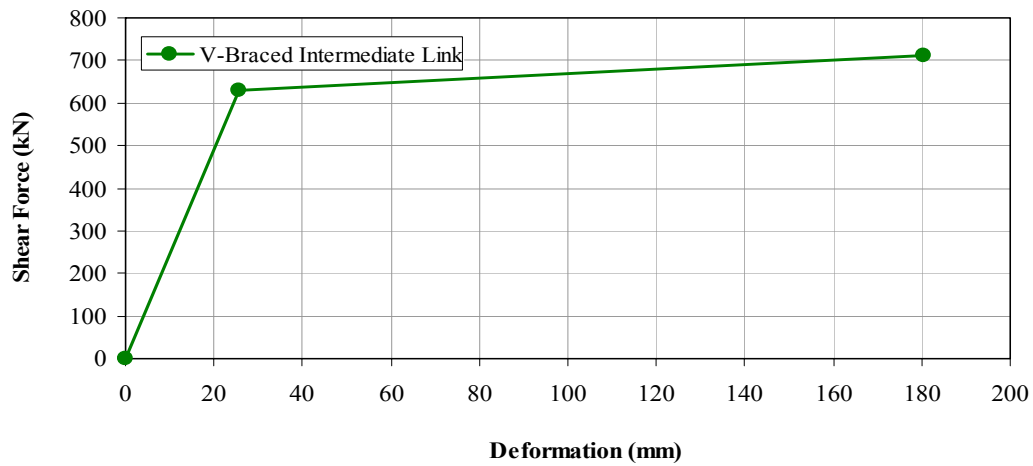


Figure (3.25a): Deformation vs. Shear Force for
V-Braced Intermediate Link



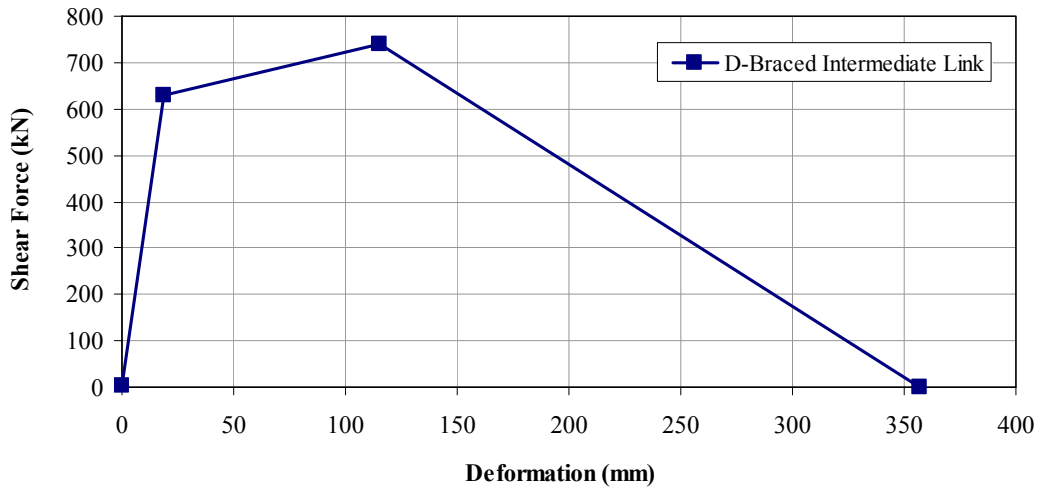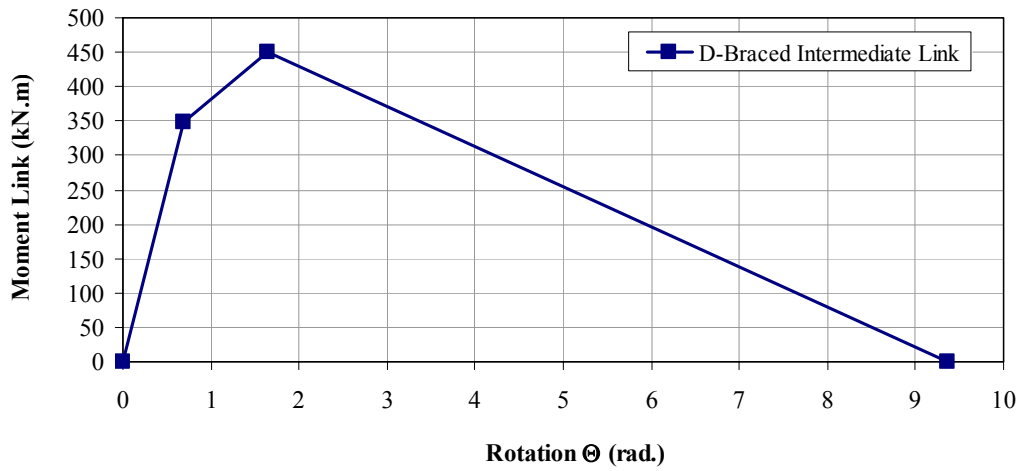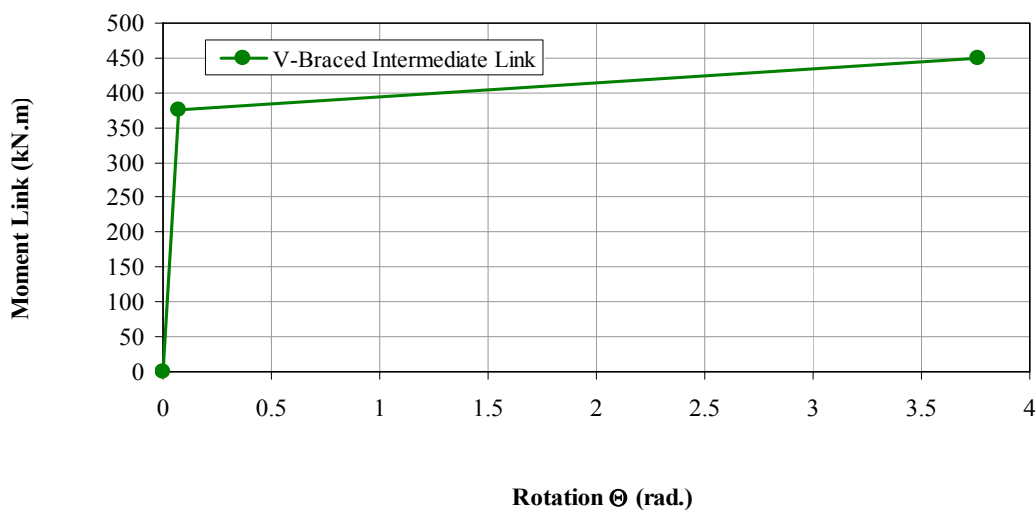Figure (3.25b): Rotation vs. Moment for V-Braced Intermediate Link
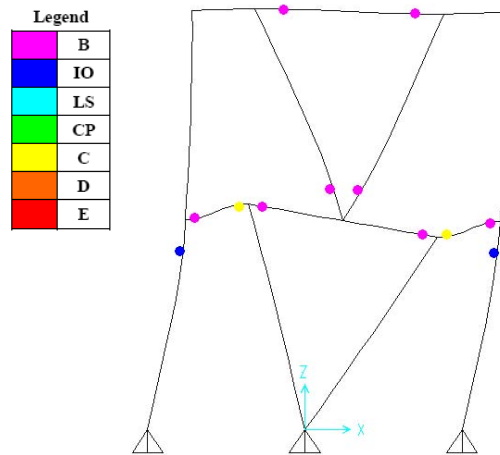
Figure (3.26): Deformed Shape at Final Step
For V-Braced Intermediate Link

### 3.7.4. Comparison of Intermediate Link between the Three Braced Types of EBF

It is deduced from Table (3.14), for K-Braced Type, shear-flexure hinge is better than moment hinge because link in second floor yield lateral deformation, otherwise for shear-moment hinge it takes 115 mm lateral deformation to produce ultimate state in link. Moreover, yield state is happened at beam outside the link at first floor. It is concluded from Table (3.15), for D-Braced Type, shear-flexure hinge is worse than moment hinge because mechanism at joint 5 occurred, while for shear-moment hinge total failure deformation occurred at first floor only. Moreover, in shear-moment hinge case it takes 357 mm to produce failure.

It is concluded from Table (3.16), for V-Braced Type, shear-flexure hinge is better than moment hinge because it takes 180 mm lateral inelastic deformation to produce failure state in link. Moreover, in shear-flexure hinge case it does not takes any deformation to produce failure.

Finally, it is concluded that shear hinge type better than moment hinge and V-Braced type is the best type of bracing at intermediate link situation.
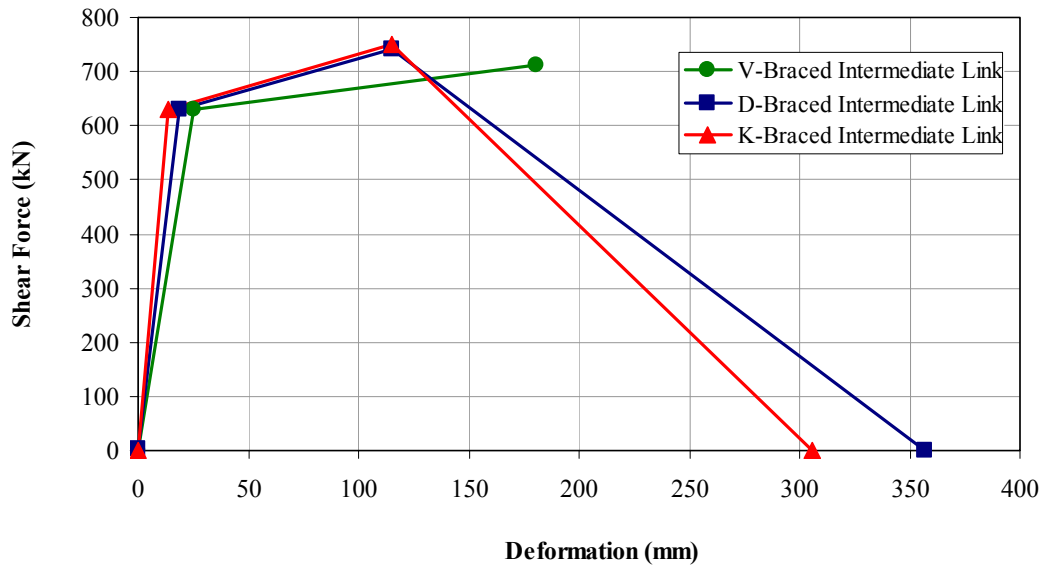
Figure (3.27a): Comparison of Intermediat Link Deformation vs. Shear Force
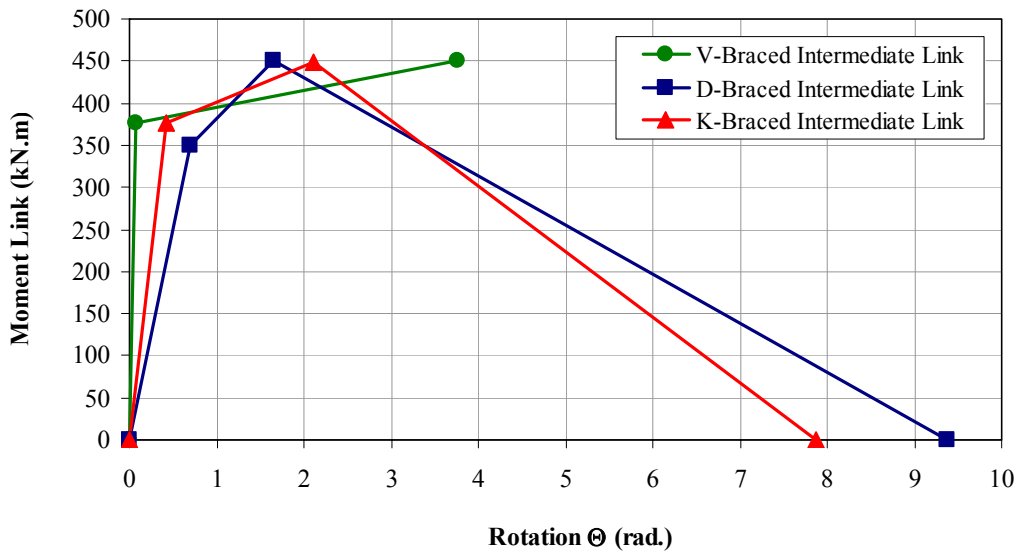


Figure (3.27b): Comparison of Intermediat Link Rotation vs. Moment Link

## 3.8. Ductile Eccentrically Braced Frames

Ductility μ is the property which defined as the ability of the structure to undergo large deformation without fracture i.e. without large reduction in strength, also ductility is defined as the ability of structure to dissipate energy, the ductility is the ratio of ultimate deformation $\Delta_u$ to yield deformation $\Delta_y$, and it is called ultimate ductility, also defined as the ratio of failure deformation to yield deformation, this ductility is called failure ductility, ductility is also expressed in terms of rotational ratio, curvature ratio, cyclic ductility ratio, and strain ratio.

$$\mu_\Delta = \frac{\Delta_u}{\Delta_y} \text{ Displacement ductility ratio}$$

$$\mu_\theta = \frac{\theta_u}{\theta_y} \text{ Rotational ductility ratio}$$

$$\mu_\kappa = \frac{\phi_u}{\phi_y} \text{ Curvature ductility ratio}$$

$$\mu_c = \frac{\Delta_y + \sum |\Delta_{pl}|}{\Delta_y} \text{ Cyclic ductility ratio}$$

$$\mu_\varepsilon = \frac{\varepsilon_u}{\varepsilon_y} \text{ Strain ductility ratio}$$

Where:

$\mu_\Delta$ is displacement ductility ratio.

$\mu_\theta$ is rotational ductility ratio.

$\mu_\Phi$ is curvature ductility ratio.

$\mu_c$ is cyclic ductility ratio.

$\mu_\varepsilon$ is strain ductility ratio.

$\Delta_y$ is yield displacement.

$\theta_y$ is yield rotation.

$\Phi_y$ is yield curvature.

$\varepsilon_y$ is yield strain.

$\Delta_u$ is ultimate displacement.

$\Delta_{pl}$ is plastic deformation.

$\theta_u$ is ultimate rotation.

$\Phi_u$ is ultimate curvature.

$\varepsilon_u$ is ultimate strain.

The ductility of material is expressed in terms of strain, the ductility is equal to the maximum attainable (ultimate) strain divided by the yield strain. The ductility supply must be greater than that demanded by the earthquake.

The ductility of cross section is expressed in term of curvature; the ductility is indicated the supplied one which should be more than the demanded ductility by earthquake.

The ductility of structural elements is expressed in term of rotation, when dealing with beam, the critical region is considered which is accompanied with significant inelastic behavior, it should be noted that the critical region coincides with the flexural plastic hinging of the beam.

The next level of rank is the structure. The overall response is given in terms of force vs. displacement. Figure (3.28d) shows a curve which is sometimes called a capacity curve or a pushover curve, the supplied ductility depends on the applied loading pattern, it should be noted that cyclic ductility ratio, $\mu_c$, is expressed as accumulation of inelastic deformation.

The ductility can be ranked as follows: strain ductility ratio > curvature ductility ratio > rotational ductility ratio > displacement ductility ratio.

It should be mentioned that curvature ductility ratio is called local ductility, and displacement ductility ratio is called global ductility which is in general less than local ductility.

In seismic design, a structural element is chosen to be the element which will be yielded during earthquake excitation, this element behaves as a fuse, which must be ductile, in moment resisting frame systems beams are the fuses, in concentrically braced frame systems braces are considered as fuses since energy dissipation is achieved through tension yielding, and compression buckling of the braces, and in eccentrically braced frame systems links are fuses because energy is dissipated through shear and/or flexural yielding in this link.

There are two types of ductility:

    a- Ductility demand which is the ductility reached during earthquake excitation.

    b- Ductility capacity which is the maximum ductility that the structure can experience without failure.
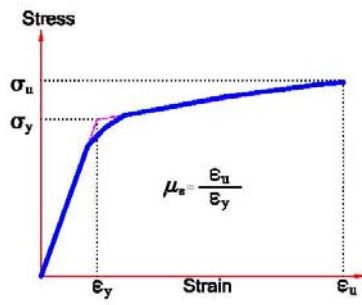
(a) Idealized Inelastic Behavior From Material

$$\mu_\varepsilon = \frac{\varepsilon_u}{\varepsilon_y}$$
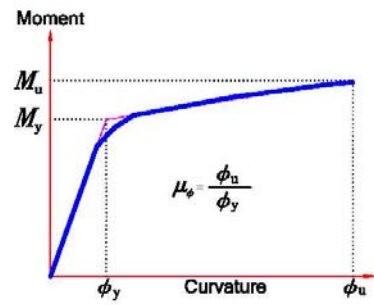
(b) Idealized Inelastic Behavior To Section

$$\mu_\phi = \frac{\phi_u}{\phi_y}$$
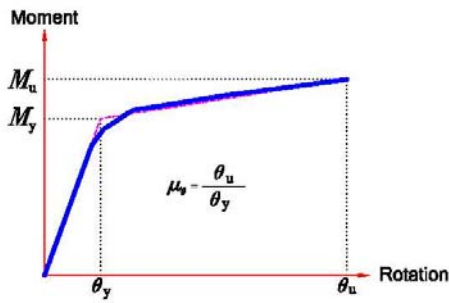
(c) Idealized Inelastic Behavior To critical region & member

$$\mu_\theta = \frac{\theta_u}{\theta_y}$$
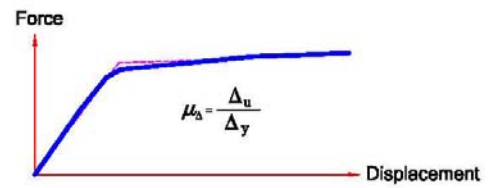
(d) Idealized Inelastic Behavior To Structure

$$\mu_\Delta = \frac{\Delta_u}{\Delta_y}$$

Figure (3.28): Inelastic Behavior of Structures

### 3.8.1. Short Link Ductility

Based on SAP2000 results, ultimate, and yield lateral deformation are obtained in order to compute displacement ductility ratio as shown below.

$$\mu_{\Delta c} = \frac{\Delta_u}{\Delta_y}$$

Where;

$\mu_{\Delta c}$ = Displacement ductility capacity ratio

- For K-Bracing short link

$$\mu_{\Delta c} = \frac{138}{6.6} = 21$$

- For D-Bracing short link

$$\mu_{\Delta c} = \frac{145}{9.3} = 15.6$$

- For V-Bracing short link

$$\mu_{\Delta c} = \frac{282}{12.34} = 23$$

Figure (3.29) shows the values of displacement ductility ratios for short link (shear yielding link) with various types of braces: K-braced, D-braced, and V-braced, the aforementioned Figure shows that the values of displacement ductility ratios for K-braced, and V-braced are close, and they are better than D-braced.

It is worthwhile to mention that the plastic hinges are formed in the links only at the first and second floors.
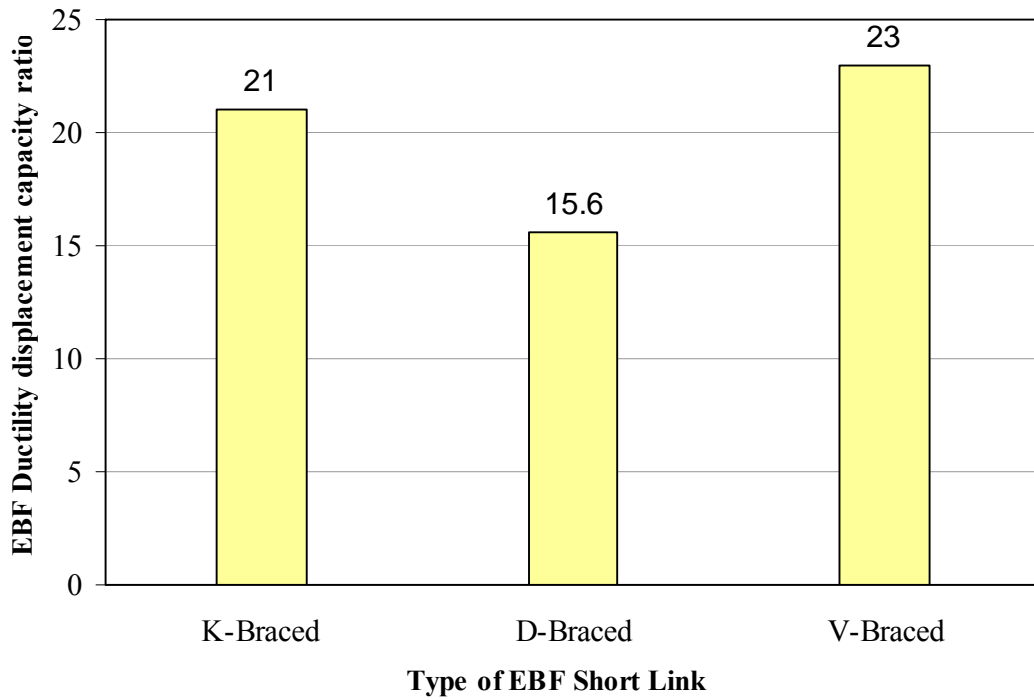
Figure (3.29): Displacement Ductility Capacity Ratios for EBF Short Link

### 3.8.2. Long Link Ductility

Based on SAP2000 results, ultimate, and yield rotation are obtained in order to compute rotation ductility ratio as shown below.

$$\mu_{\theta c} = \frac{\theta_u}{\theta_y}$$

Where:

$\mu_{\theta c}$ = Ductility rotational ratio (capacity)

- For K-Bracing long link

$$\mu_{\theta c} = \frac{0.626}{0.29} = 2.14$$

- For D-Bracing long link

$$\mu_{\theta c} = \frac{0.424}{0.214} = 1.98$$

- For V-Bracing long link

$$\mu_{\theta c} = \frac{2.021}{0.182} = 11.1$$

Figure (3.30) shows the values of rotational ductility ratios for long link (moment yielding link) with various types of braces: K-braced, D-braced, and V-braced, the aforementioned Figure shows that the value of rotational ductility ratio for V-braced is the best.

It is worthwhile to mention that the plastic hinges are formed in links, beams outside the link, braces, and columns.
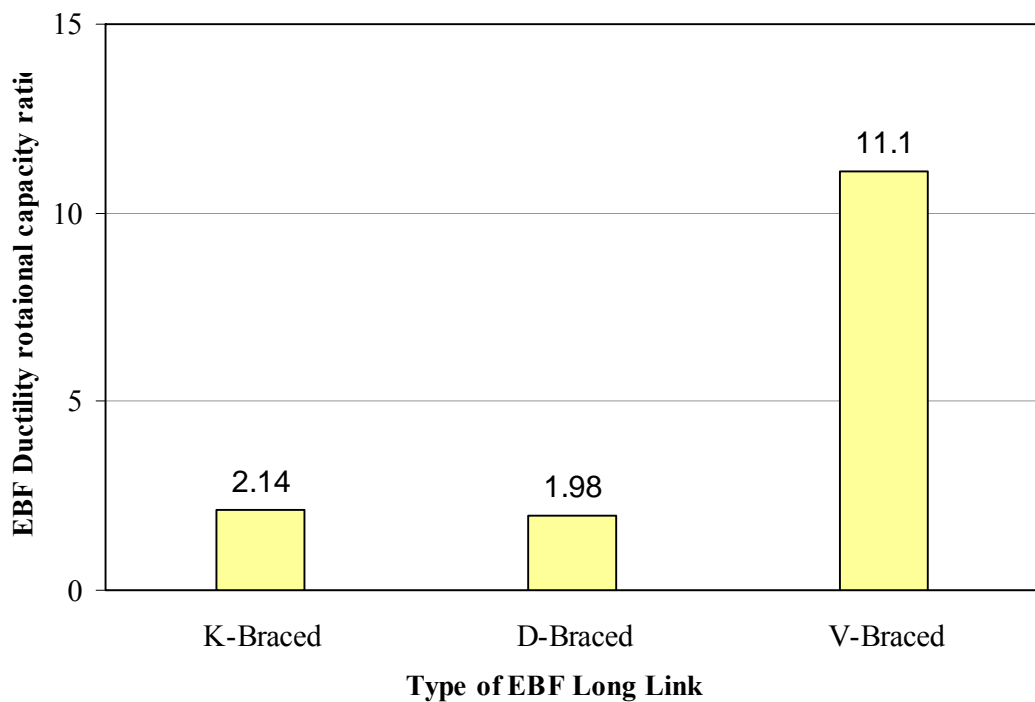


Figure (3.30): Rotational Ductility Capacity Ratios for EBF Long Link

### 3.8.3 Intermediate Link Ductility

Based on SAP2000 results, ultimate, and yield rotation are obtained in order to compute rotation ductility ratio as shown below.

$$\mu_{\theta c} = \frac{\theta_u}{\theta_y}$$

Where;

$\mu_{\theta c}$ = Rotational  ductility capacity ratio

- For K-Bracing long link

$$\mu_{\theta c} = \frac{2.106}{0.425} = 4.955$$

- For D-Bracing long link

$$\mu_{\theta c} = \frac{1.651}{0.694} = 2.38$$

- For V-Bracing long link

$$\mu_{\theta c} = \frac{3.758}{0.074} = 50.8$$

Figure (3.31) shows the values of rotational ductility ratios for  intermediate link (shear-moment yielding link) with various types of braces: K-braced, D-braced, and V-braced, the aforementioned Figure shows that the value of rotational ductility ratio for V-braced is the best.
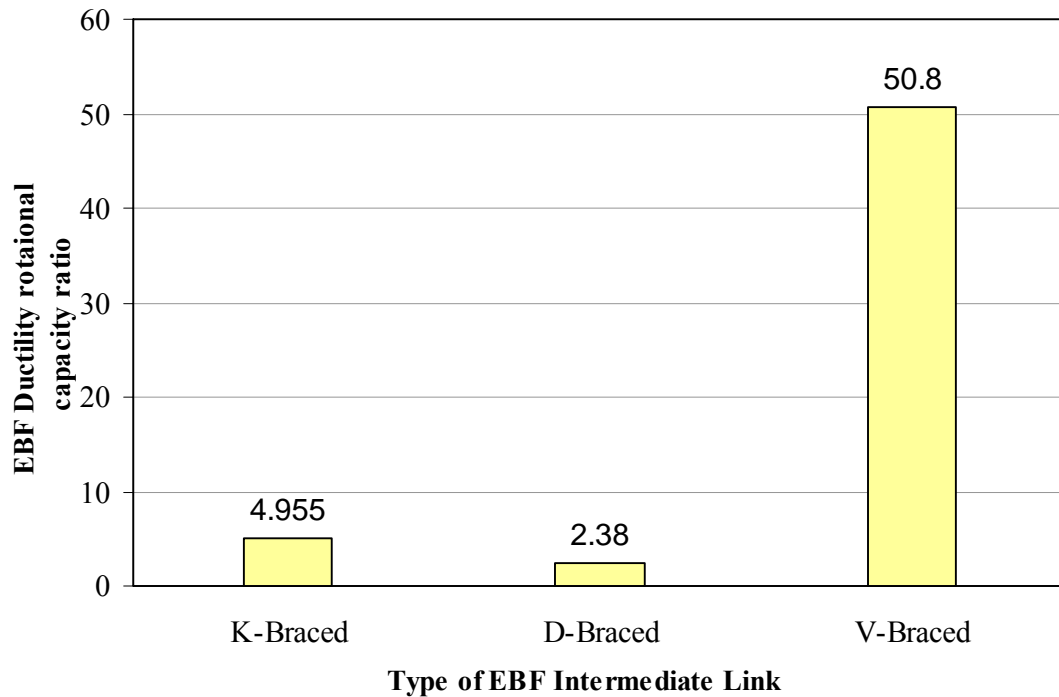
Figure (3.31): Rotational Ductility Capacity Ratios for EBF Intermediate Link

## 3.9. Link Deformation

Link deformation is normally characterized by the total link rotation angle γ (rad.). The value of link rotation angle is computed by taking the relative end deflection of the link, and dividing by the link length, this angle is between the link and the beam outside the link BOL, the total link rotation angle shall include both elastic and inelastic components of deformation of the link and the members attached to the link ends, the elastic portion of the link rotation angle is subtracted from the measured total link rotation angle γ.

Based on SAP 2000 results, it is noted that the value of the link plastic rotation angle capacity $\gamma_p$ (rad.) depends on the link length, as the link's length increase the link rotation angle capacity decrease, this is an evidence that shear yielding link is preferred

in EBFs, the reason why shear yielding links provide high levels of deformation is because a large portion of the link yields in a relatively uniform manner also long links may experience web, flange local buckling and/or lateral torsional buckling of the link which will reduce strength clearly. The results of SAP2000 are shown in Table (3.17), Figure (3.32) shows the variation of link plastic rotation capacity $\gamma_p$ (rad.) with respect to the link length e (m).

Results show that link plastic rotation angle for short link is approximately (5-7) times link plastic rotation angle for long link, this is because that for short link, web yielding occurs along the entire depth of the web and along the entire length of the link (because shear force is constant along the length of the link), but for long link, flexural yielding occurs only at the link ends due to high moment gradient at the link ends.

Applying simple plastic theory (geometry of rigid–plastic mechanism of EBFs), the kinematics of the plastic mechanism require that:

$$\gamma_p = \frac{L}{e}\theta_p \text{ For K-braced EBF}$$
$$\gamma_p = \frac{L}{e}\theta_p \text{ For D-braced EBF}$$
$$\gamma_p = \frac{L}{2e}\theta_p \text{ For V-braced EBF}$$

The above equations show the relationship between link plastic rotation angle $\gamma_p$ and frame plastic interstory drift angle $\theta_p$, $\gamma_p$ is obtained by multiplying $\theta_p$ by (L/e) for K-braced, D-braced EBFs, or (L/2e) for V-braced EBF. L is the span length, and e is the link length.

Table (3.17): Link Plastic Rotation Angle for Three Types of Eccentrically Braced Frames

| Braced Type | Link plastic rotation angle ($\gamma_p$) (rad.) | | |
| --- | --- | --- | --- |
| | Short Link (0.6m) | Intermediate Link (1.2m) | Long Link (1.8m) |
| K-Braced EBF | 0.3723 | 0.21215 | 0.052 |
| D-Braced EBF | 0.4148 | 0.23695 | 0.0591 |
| V-Braced EBF | 0.38435 | 0.23045 | 0.07655 |
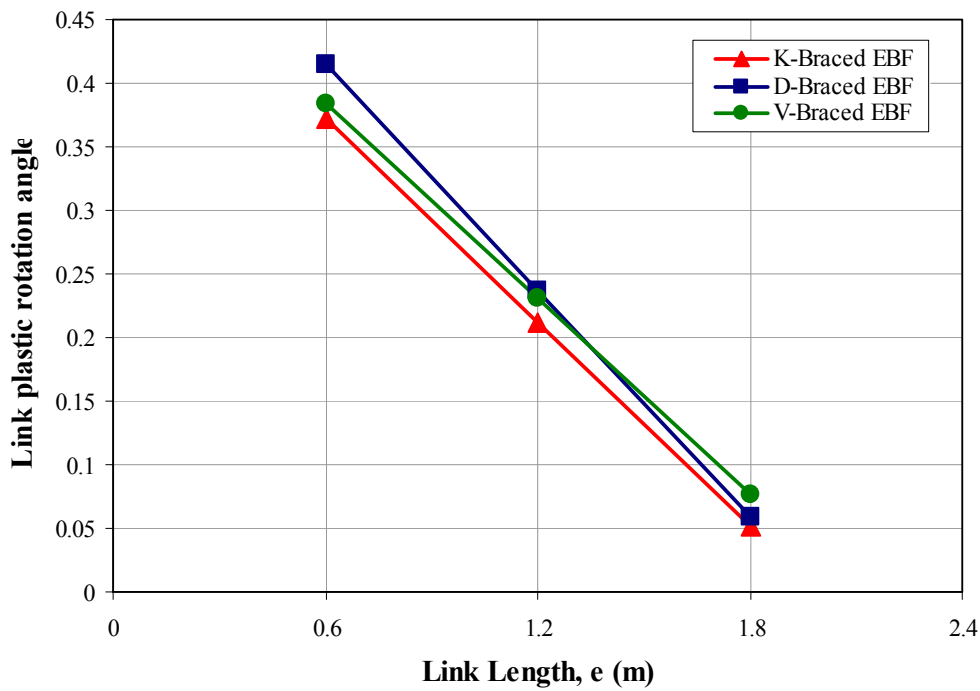


Figure (3.32): Variation of Link Angle with Link Length

# CHAPTER FOUR

# CONCLUSIONS AND RECOMMENDATIONS

## 4.1. Summary

This study aims to help structural engineers in order to design seismic resisting steel structures that have large inelastic deformation due to earthquake. As shown earlier, the study concerns about EBFs which can be described as a combination of moment resisting frame which gives good ductility, and concentrically braced frame which gives strength, and stiffness. Researches and studies for EBFs started at mid-1970s, to be up to date with the new architectural requirements for example EBFs produce spaces for doors, windows, and heating, ventilating, and air conditioning (HVAC) utilities, unlike the concentrically braced frames which cause obstruction for different utilities.

The EBF configurations covered in this study are the common types which are:

(1) K-Braced EBF.

(2) D-Braced EBF.

(3) V-Braced EBF.

Each EBF configuration is studied for three cases according to the description of link's length: short link (shear yielding), long link (flexural yielding), and intermediate link (combined shear and flexural yielding).

Analysis has been performed using SAP2000 software (static and dynamic finite element analysis of structure, version 12), by modeling 2D frames with different type of braces. Each model has been subjected to gravity load and seismic load (lateral displacement).

The analysis used is nonlinear static procedure analysis (pushover analysis) which is a popular tool for seismic performance evaluation of existing and new

structures. The nonlinear static procedure is intended to provide a simplified approach the nonlinear response behavior of a structure at different levels of lateral displacements, ranging from initial elastic response through development of a failure mechanism.

Response behavior is gauged by measurement of the strength of the structure, at various increments of lateral displacement. With the increase in the magnitude of the loading, weak links and failure modes of the structure are found.

The FEMA-273 document developed modeling parameters and analysis procedures for pushover analysis. These documents define force-deformation criteria for plastic hinges used in pushover analysis. As shown in Figure (1.4), the points labeled A, B, C, D, E, and F are used to define the force deformation behavior of the hinge and three points labeled IO, LS and CP are used to define the acceptance criteria for the hinge. The values assigned to each of these points vary depending on the type of member as well as many other parameters defined in the FEMA-273 document as shown in the Figure (1.4). The SAP2000 static pushover analysis capabilities, which are fully integrated into the program, allow quick and easy implementation of the pushover procedures prescribed in the FEMA-273 document for both two and three dimensional buildings.

## 4.2. Conclusions

On the bases of this study the following conclusions may be drawn:

1- By comparing the elastic drift results for both short and long link systems, it is found that the drift values for short link is less than long link so short link is three times stiffer than long link.

2- K-braced configuration is found as the best type of braces based on elastic stiffness. The  next one is V-braced configuration .

3- Seismic design philosophy is to choose frame elements (fuses) that will yield in an earthquake, this fuse must be ductile and designed as the weak member. In short link EBFs it is found that the failure will be at the link which will have excessive inelastic deformation. The energy is dissipated through shear and / or flexural yielding in this link, braces, columns, portions of the beam outside the link, and all related connections remain elastic as the link deforms and reaches its expected strength. Short link V-braced EBF is found to have the largest value of plastic deformation capacity.

4- Long link EBFs behave like moment resisting frames since the failure not only in the link, but also at locations outside the link, it is worthwhile to mention that soft story phenomenon is likely to be formed at long link EBFs. K-braced EBF is found to have the largest value of plastic deformation capacity.

5- Intermediate link for V-braced configuration is found to be the best type with other.

6- Long links attached to columns is not recommended to be used in seismic-resistant EBFs. In the case D-braced EBF type formation of joint mechanism occurred at the joint attaching link to column.

7- An EBF generally possesses excellent ductility. Studying short link EBF, the ductility of K-braced and V-braced are close together, and both of them are better than D-braced EBF.

8- Short link (shear yielding link) is preferred for best structural performance of an EBF.

9- The study shows that short link (shear yielding link) for the three brace configurations achieves a plastic rotation capacity $\gamma_p$ which is approximately equals to 0.4 radian.

10- Flexural yielding link (long link) exhibits small plastic rotation capacity $\gamma_p$ which ranges between 0.05-0.07 radian, the aforementioned is applicable for the three brace configurations, the section used above is W16x36 (A572-50).

11- Shear yielding link develops plastic rotation capacity $\gamma_p$ larger than the one produced by flexural yielding link; this is clear evidence why shear yielding link is preferred in EBFs.

12- Link plastic rotation angle capacity $\gamma_p$ of an intermediate link (shear-flexural yielding link) is determined by linear interpolation between shear yielding link, and flexural yielding link.

13- It can be seen that links ductility supply is normally characterized by the link plastic rotation angle capacity $\gamma_p$.

14- The short link is subjected to yielding along its entire length, and it occurs at the web only. On the other hand for long link, it is subjected to yielding at the ends of the member.

15- Results indicate that a properly stiffened short link can strain harden and develop a shear strength which is approximately 1.5 $V_p$ = 944 kN, knowing that $V_p$ equals to 590kN, the end moment of a link that has yielded in shear can

continue to increase due to strain hardening and ,therefore, flexural hinges can develop. From static equilibrium of the link, shear and flexural yielding will occur simultaneously $e = \dfrac{2M_p}{V_p}$

For a shear link, at strain hardening, the link ultimately achieves shear strength of 1.5 $V_p$, therefore, the link's length that guarantees shear yielding for link is: $e = \dfrac{1.6M_p}{V_p}$

16- It can be noted that flexural hinges dominate the link response, and link will yield in flexure when e is larger than: $\dfrac{2.6M_p}{V_p}$

17- Damage due to seismic force in short link EBF system is formed only in links, so the disruption is limited in link's location, this is correct for the three brace configurations studied. On the other hand, damage due to seismic force in long link EBF system is not only formed in link, but also outside the link (column, brace…etc.).

## 4.3. Recommendations

The following recommendations can be offered:

1- Shear yielding links are recommended to be used in EBFs .

2- K-braced configuration which has link at mid-span of beam is considered to be the best type based on stiffness, and strength, and it is recommended in practice.

3- For ductility K-braced, and V-braced configurations are considered to be the best types .

# REFERENCES

AISC. (2000). **Load and Resistance Factor Design Specification for Steel Hollow Structural Sections**, American Institute of Steel Construction, Chicago, Illinois.

AISC. (2001). **Load and Resistance Factor Design Specification for Structural Steel Buildings,** American Institute of Steel Construction, Chicago, Illinois.

AISC. (2005). **Seismic Provisions for Structural Steel Buildings**, American Institute of Steel Construction, Chicago, Illinois.

Akiyama, H., (1985). **Earthquake-Resistant Limit-State Design of Buildings**, University of Tokyo Press, Japan

Armouti, Nazzal S., (2004). **Earthquake Engineering, Theory and Implementation.** First Edition, Jordan.

ASCE. (2000). **Prestandard and Commentary for the Seismic Rehabilitation of Building FEMA 356 Report**, prepared by the American Society of Civil Engineers, Published by Federal Emergency Management Agency, Washington, D. C.

Becker, R., and Ishler, M., (1996). **Seismic Design Practice For Eccentrically Braced Frames—Based on the 1994 UBC**, Steel Tips, American Institute of Steel Construction, Chicago, Illinois.

Building Seismic Safety Council. (1997). **NEHRP Guidelines for the Seismic Rehabilitation of Buildings (FEMA Publication 273)**, Washington, D.C.

Bruneau, M., Uang, C. -M., and Whittaker, A. (1998), **Ductile Design of Steel Structures**, New York,  McG raw-Hill.

Chen, W.V., and Sohal, I., (1995). **Plastic Design and Second-Order Analysis of Steel Frames, Spring-Verlag**, New York.

CSI, Structural Analysis Program, SAP2000 Non-Linear Version 12, Computer and Structure, Inc., Berkeley, 2008.

Engelhardt, M. D., and Popov, E. P., (1989). **Behavior of Long Links in Eccentrically Braced Frames**, Report No. UCB/EERC-89/01, Pacific Earthquake Engineering Research Center, University of California at Berkeley.

Engelhardt, M. D. , and Popov, E. P., (1992). **Experimental Performance of Long Links in Eccentrically Braced Frames**, Journal of Structural Engineering, ASCE, 118 (11), 3067-3088.

Engelhardt, M. D., and Popov, E. P., (1989). **On Design of Eccentrically Braced Frames**, Earthquake Spectra, Vol. 5, No. 3, 495-511.

Farzad Naeim, (2001). **The Seismic Design Handbook**. Second Edition, USA. Kluwer Academic Publishers.

Foutch, D. A., (1989). **Seismic Behavior of Eccentrically Braced Steel Building**, Journal of Structural Engineering, ASCE, 115 (8), 1857-1876.

Furukawa, S., Goel, S.C., and Chao, S.H., (2008). **Seismic Evaluation of Eccentrically Braced Steel Frames Designed by Performance-Based Plastic Design Method,** the Fourteenth World Conference on Earthquake Engineering, Beijing, China.

Hines, E.M., (2008). **Eccentric Braced Frame Design for Moderate Seismic Regions**, Tufts University, Medford, MA.

Hjelmstad, K. D., and Popov, E. P., (1983). **Seismic Behavior of Active Beam Links in Eccentrically Braced Frames,** Report No. UCB/EERC-83/15, Earthquake Engineering Research Center, University of California at Berkeley.

Kasai, K., and Popov, E. P., (1986). **A Study of Seismically Resistant Eccentrically Braced Steel Frame Systems,** Report No. UCB/EERC-86/01, Earthquake Engineering Research Center, University of California at Berkeley

Kasai, K. and Popov, E. P., (1986). **General Behavior of WF Steel Shear link Beams**, Journal of Structural engineering, ASCE, 112 (2), 362-382.

Köber, H., Dima, S., (2005). **The Behavior of Eccentrically Braced Frames with Short Links**, Technical University of Civil Engineering, Bucharest

Lindsey, S.D., and Goverdhan, A.V., (2003). **Eccentric Braced Frames: Suggested Design Ptocedures for Wind and Low Seismic Force**, American Institute of Steel Construction.

Malley J. O., and Popov, E. P., (1983). **Design Considerations for Shear Links in Eccentrically Braced Frames**, Report No. UCB/EERC-83/24, Earthquake Engineering Research Center, University of California at Berkeley.

Malley J. O., and Popov, E. P., (1983). **Shear Links in Eccentrically Braced Frames**, Journal of Structural Engineering, ASCE, 110 (9), 2275-2295.

NEHRP. (2001). **Commentary on Recommended Provisions for the Development of Seismic Regulations for New Buildings (FEMA 369)**, Federal Emergency Management Agency, Washington, D. C.

NEHRP. (2001). **Recommended Provisions for the Development of Seismic Regulations for New Buildings (FEMA 368)**, Federal Emergency Management Agency, Washington, D. C

Okazaki, T., Arce, G., Ryu, H. C., and Engelhardt, M. D., (2004). **Recent Research on Link Performance in Steel Eccentrically Braced Frames**, 13th World Conference on Earthquake Engineering, Vancouver, B. C., Canada, August 1-6, Paper No. 302

Popov, E.P., (1980). **An Update on Eccentric Seismic Bracing**, Engineering Journal, American Institute of Steel Construction, California.

Popov, E. P., Kasai, K., and Engelhardt, M. D., (1987). **Advances in Design of Eccentrically Braced Frames, Earthquake Spectra**, Vol. 3, No. 1, 43-55.

Popov, E. P., Ricles, J. M., and Kasai, K., (1992). **Methodology for optimum EBF Link Design Proceedings**, Tenth World Conference of Earthquake Engineering, Vol. 7, Balkema, Rotterdam, 3988-3983.

Richards, P. W. , and Uang, C. M., (2003). **Development of Testing Protocol for Short Links in Eccentrically Braced Frames**, Report No. SSRP-2003/08, University of California, San Diego, La Jolla, CA.

Ricles, J. M., and Popov, E. P., (1994). **Inelastic Link Element for EBF Seismic Analysis**, Journal of Structural Engineering, ASCE, 120 (2), 441-463.

Roeder, C.W., and Popov, E. P., (1978). **Eccentrically Braced Steel Frames for Earthquakes,** Journal of structural Division, ASCE, Vol. 104, No. ST3.


Tehranized, M., Taghikhani, T., Kioumarsi, M., and Hajnajafi, L., (2007). **Comparative Study on Seismic Behavior of Special Concentric Braced Frames with Eccentric Braced Frames**, Amirkabir University, Tehran.

# تأثير مواقع الروابط على تصرف الإطارات لامركزية التكتيف

إعداد
عامر صاحب ارحيم

المشرف
الدكتور نزال العرموطي

ملخص

تهدف هذه الدراسة لتحسين مهارات المهندس الإنشائي لتصميم الهياكل الفولاذية المقاومة لأفعال الزلازل والتي تتعرض لتشوهات لدنة (غير مرنة) . إن نظام الهياكل الفولاذية لامركزية التكتيف ـهي اهتمام هذه الدراسةـ عبارة عن مزيج من نظام مقاومة العزوم والذي يمتاز بالممطولية الجيدة و نظام هياكل مركزية التكتيف ذات المتانة والجساءة العالية.

الأبحاث والدراسات في نظام الهياكل الفولاذية لامركزية التكتيف بدأت في منتصف السبعينيات من القرن الماضي لتواكب متطلبات معمارية عصرية ومنها أن هذا النظام يوفر فضاءات مناسبة للأبواب، نوافذ، مجاري الهواء (تدفئة وتبريد)، مفرغات الهواء على العكس من الهياكل الفولاذية مركزية التكتيف ، التي تسبب إعاقة لأنواع مختلفة من الخدمات.

بحثت هذه الدراسة ثلاثة أنواع من الهياكل الفولاذية اللامركزية التكتيف وهي:
1- نوع K : وفي هذا النوع يكون موقع الرابط في منتصف الجسر.
2- نوع D : وفي هذا النوع يكون موقع الرابط مجاورا للعمود.
3- نوع V : وفي هذا النوع يكون موقع الرابط على جانبي التكتيف.

الأنواع إعلاه تختلف فيما بينها بمواقع الروابط، ويعتبر الرابط جزء من الجسر عند كل تكتيف، وهو العضو الإنشائي المبدد للطاقة و هو أضعف الأعضاء الإنشائية، ويعتبر هذا الرابط شبيه بالمصهر في الدوائر الكهربائية ، حيث أنه سوف يعاني من تشوهات لدنة كبيرة قد تصل إلى الفشل و تبقى باقي الأعضاء الإنشائية ضمن المجال المرن.

كل نوع من أنواع التكتيف اللامركزي أعلاه درس ثلاث مرات بناء على طول الرابط: الرابط القصير (رابط خضوع القص)، الرابط الطويل (رابط خضوع الثني)، الرابط المتوسط (رابط خضوع قص وثني)، وتمت مقارنتهم من حيث ما يلي:
1- متطلبات المتانة.
2- متطلبات الممطولية.
3- متطلبات الجساءة.
4- زاوية الدوران اللدنة (تشوهات الرابط).

تم عمل التحليل الإنشائي لكل حالة بوساطة SAP2000 من خلال تصميم نموذج ثنائي الأبعاد بارتفاع كلي 8 متر وارتفاع طابقي 4 متر والفضاء 6 متر وكان طول الرابط القصير 0.6 متر والرابط المتوسط 1.2 متر والرابط الطويل 1.8 متر وكل نموذج تصميمي تعرض لأحمال ميتة وأحمال جانبية والتي هي عبارة عن إزاحة مقدارها 1 متر .

أظهرت نتائج هذه الدراسة أن الرابط القصير هو أفضل الأنواع في تصاميم الهياكل الفولاذية لامركزية التكتيف لحدوث إجهاد الخضوع في الرابط فقط ، علماً أن الخضوع يكون في كامل عصب الرابط على جميع طوله أثناء تسليط الحمولات الجانبية، علاوة على ذلك إن نوع التكتيف K والنوع V هما الأفضل من حيث متطلبات الممطولية و زاوية الدوران اللدنة السعوية.